Cellular regulation of the hemITAM-coupled platelet receptor C-type lectin-like receptor 2 (CLEC-2): *In vitro* and *in vivo* studies in mice

…

Zelluläre Regulation des hemITAM-gekoppelten Thrombozyten-rezeptors *C-type lectin-like receptor 2* (CLEC-2): *In vitro* und *in vivo* Studien in Mäusen

Doctoral thesis for a doctoral degree
at the Graduate School of Life Sciences,
Julius-Maximilians-Universität Würzburg,
Section Biomedicine

submitted by

Viola Lorenz

from Rodewisch

Würzburg, 2015

Submitted on:

Members of the *Promotionskomitee*:

Chairperson:	Prof. Dr. Manfred Gessler
Primary Supervisor:	Prof. Dr. Bernhard Nieswandt
Supervisor (Second):	PD Dr. Heike Hermanns
Supervisor (Third):	Prof. Dr. Christoph Kleinschnitz

Date of Public Defense:

Date of Receipt of Certificates:

For Harald

TABLE OF CONTENTS

Summary

Platelet aggregation at sites of vascular injury is essential to limit posttraumatic blood loss, but may also cause acute ischemic disease states such as myocardial infarction or stroke. Stable thrombus formation requires a series of molecular events involving platelet receptors and intracellular signal transduction, which contribute to adhesion, activation and aggregation of platelets. In this thesis, the cellular regulation of platelet surface receptors and their involvement in thrombus formation was investigated using genetically modified mice.

In the first part of the study, the functional relevance of the immunoreceptor tyrosine-based activation motif (ITAM)-coupled collagen receptor GPVI and of the recently identified hemITAM-bearing C-type lectin-like receptor 2 (CLEC-2) for *in vivo* thrombus formation was analyzed. Megakaryocyte/ platelet-specific CLEC-2 knock out mice displayed a defective lymphatic development and were protected from occlusive arterial thrombus formation. These phenotypes were more pronounced in mice with a GPVI/CLEC-2 double deficiency. Hemostasis was not compromised in CLEC-2 or GPVI single-deficient animals, as they showed only mildly prolonged tail bleeding times. Combined depletion of both receptors resulted in markedly prolonged bleeding times revealing an unexpected redundant function of the two receptors in hemostasis as well as thrombosis. These findings might have important implications for the development of anti-CLEC-2/ anti-GPVI agents as therapeutics.

In the second part, mechanisms underlying the cellular regulation of CLEC-2 were studied. Previous studies have shown that injection of the anti-CLEC-2 antibody INU1 results in complete immunodepletion of platelet CLEC-2 in mice, which is preceded by a severe transient thrombocytopenia thereby limiting its potential therapeutic use. It is demonstrated that INU1-induced CLEC-2 immunodepletion occurs through Src family kinase (SFK)-dependent receptor internalization *in vitro* and *in vivo*, presumably followed by intracellular degradation. In mice with spleen tyrosine kinase (Syk) deficiency, INU1-induced CLEC-2 internalization/ degradation was fully preserved, whereas the associated thrombocytopenia was largely prevented. These results show that CLEC-2 can be downregulated from the platelet surface through internalization *in vitro* and *in vivo* and that this can be mechanistically uncoupled from the associated antibody-induced thrombocytopenia.

Since INU1 IgG induced a pronounced thrombocytopenia, the *in vivo* effects of monovalent INU1 F(ab) fragments were analyzed. Very unexpectedly, injection of the F(ab) fragments resulted in widespread thrombus formation leading to persistent neurological deficits of the animals. This intravascular thrombus formation is the result of CLEC-2-dependent platelet activation and aggregation. The mechanism underlying the thrombus formation is still unknown and depends potentially on binding of a yet unidentified ligand to F(ab)-opsonized CLEC-2 on platelets.

Zusammenfassung

Die Aggregation von Thrombozyten ist ein essentielle Prozess, um Blutungen nach einer Gefäßverletzung zu stoppen. Sie kann aber auch zu akuten thrombotischen Erkrankungen, wie Herzinfarkt und Schlafanfall, führen. Die Bildung eines stabilen Thrombus ist ein dynamischer Prozess, der ein definiertes Zusammenspiel von thrombozytären Rezeptoren und intrazellulären Signalen benötigt, die zur Adhäsion, Aktivierung und Aggregation der Thrombozyten beitragen. In der hier vorliegenden Dissertation wurde zellulär Regulation von thrombozytären Oberflächenrezeptoren und ihre Beteiligung an der Thromben-Bildung mittels genetisch veränderter Mäuse untersucht.

Im ersten Teil der Arbeit wurde die funktionelle Relevanz des *immunoreceptor tyrosine-based activation motif* (ITAM)-gekoppelten Kollagenrezeptors GPVI und des vor kurzem entdeckten hemITAM-gekoppelten *C-type lectin-like receptor 2* (CLEC-2) für die *in vivo* Thromben-Bildung charakterisiert. Mäuse mit einer Megakaryozyten/ Thrombozyten-spezifischen CLEC-2-Defizienz weisen Defekte in der Entwicklung ihrer lymphatischen Gefäße auf und sind vor arteriellen Gefäßverschlüssen geschützt. Dieser Phänotyp war in Mäusen mit einer Defizient GPVI und CLEC-2 verstärkt. GPVI oder CLEC-2-defiziente Mäuse zeigen eine normale Hämostase, da ihre Schwanzblutungszeiten nur minimal verlängert waren. Die gleichzeitige Defizienz beider Rezeptoren verlängerte die Blutungszeiten der Tiere allerdings erheblich. Das spricht dafür, dass beiden Rezeptoren eine unerwartete redundante Funktion sowohl in der Hämostase als auch während der pathologischen Thromben-Bildung haben. Diese Ergebnisse könnten für die Entwicklung neuer therapeutischen Wirkstoffen, die gegen GPVI und/ oder CLEC-2 gerichtet sind, bedeutsam sein.

Im zweiten Teil der Arbeit wurde die zelluläre Regulation von CLEC-2 untersucht. Frühere Studien haben gezeigt, dass die Behandlung von Mäusen mit dem gegen CLEC-2 gerichteten Antikörper INU1 zu einem spezifischen Verlust des Rezeptors in zirkulierenden Thrombozyten führt. Dieser Prozess, der „Immunodepletion“ genannt wird, ist von einer Thrombozytopenie begleitet, die das therapeutische Potential eines solchen Ansatzes reduziert. Im Verlauf der Arbeit konnte gezeigt werden, dass die INU1-abhängige Immunodepletion *in vitro* und *in vivo* mittels *src family kinase* (SFK)-abängiger Internalisierung geschieht. Der Internalisierung ist vermutlich ein intrazellulärer Abbau nachgeschaltet. In Mäusen mit einer *spleen tyrosine kinase* (Syk) Defizienz war die INU1-abhängige Thrombozytopenie zum größten Teil verhindert, aber die Herabregulation durch Internalisierung von CLEC-2 blieb erhalten. Diese Ergebnisse zeigen, dass CLEC-2 *in vitro* und *in vivo* durch Internalisierung von der Thrombozyten-Oberfläche herabreguliert werden

kann. Darüber hinaus kann dies von der Antikörper-vermittelten Thrombozytopenie mechanistisch entkoppelt werden.

Da die Injektion von INU1 IgG eine starke Thrombozytopenie in der Tieren verursacht, sollen die *in vivo* Effekte von monovalenten INU1 F(ab) Fragmenten getestet werden. Unerwarteter weise führte die Injektion dieser F(ab) Fragmente zu einer systemischen Thromben-Bildung, die unter anderem neurologische Defizite in den Tieren auslösten. Diese intravaskuläre Thromben-Bildung ist ein Ergebnis von CLEC-2-abhängier Thrombozyten Aktivierung und Aggregation. Der Mechanismus, der dieser Thromben-Bildung zugrunde liegt, ist bisher noch nicht aufgeklärt. Möglicherweise wird er durch die Bindung eines unbekannten Liganden an das F(ab)-gebunde CLEC-2 auf Thrombozyten ausgelöst.

1 INTRODUCTION

1.1 Platelets

In the hematopoietic system, the anuclear and discoid-shaped platelets are the smallest cells with a size of 3-4 µm in humans and 1-2 µm in mice. They originate from their giant precursors cells, megakaryocytes (MKs), residing in the bone marrow (BM). A current model suggests that MKs extend long cytoplasmic protrusions, so-called proplatelets, into sinusoidal blood vessels, where the tip of these structures is shed and becomes further fragmented into platelets by shear forces.[1,2] The number of platelets in the blood is astonishingly high, in the range of 250,000/µl in humans and 1,000,000/µl in mice. Human platelets circulate in the blood for 7-10 days, whereas the life span of murine platelets is restricted to approx. 5 days. Aged platelets are constantly cleared by the hepatosplenic reticuloendothelial system and most of the produced platelets encounter this fate. Since platelets lack a nucleus, their protein *de novo* synthesis is limited. However, platelets contain several organelles and structures like mitochondria, the open canalicular and dense tubular system, glycogen stores and granules, which store different proteins.

Platelets play an essential role in hemostasis, as they survey the vascular integrity while circulating through the blood stream. At sites of vascular wall damage, platelets rapidly adhere to the exposed components of the extracellular matrix (ECM). This leads to subsequent platelet activation, secondary mediators release and local production of thrombin, promoting the recruitment and activation of further platelets, which results in aggregation and thrombus formation. This process is essential to seal vascular injuries and to prevent subsequent blood loss. Under pathological conditions, e.g. at sites of atherosclerotic plaque rupture, platelet aggregation may lead to uncontrolled thrombus formation, causing arterial occlusion or embolism and thus may cause severe disease states such as myocardial infarction or stroke. These pathologies are the leading causes of death and morbidity in industrialized societies.[3] As a consequence, platelet inhibition is the primary therapeutic option in the prophylaxis and treatment of ischemic cardio- and cerebrovascular diseases.

Beyond their function in hemostasis and thrombosis, platelets also play important roles in embryonic development, wound healing, inflammatory processes, angiogenesis and tumor metastasis.[4-6]

1.1.1 Platelet activation and thrombus formation

Platelet activation and subsequent thrombus formation at sites of vascular injury is a multistep process that is initially triggered by exposure of the ECM at the wound site. The ECM contains or binds a number of adhesive macromolecules, such as laminins, collagens and von Willebrand factor (vWF). The subsequent process of platelet aggregation and thrombus formation can be divided into three major steps: (i) tethering and adhesion of platelets, (ii) platelet activation and finally (iii) platelet aggregation and thrombus growth (Figure 1).

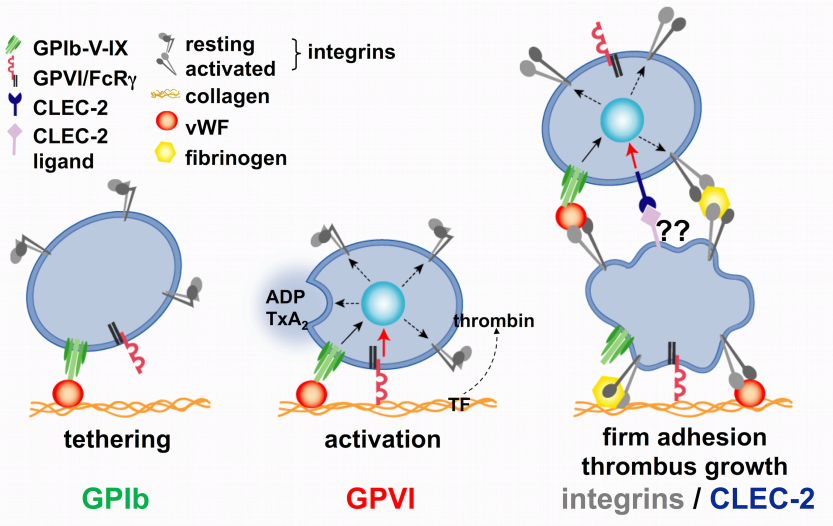

Figure 1. Platelet adhesion and thrombus formation at the ECM. Platelet tethering on the ECM is mediated by the GPIbα-vWF interaction and thereby enables GPVI to bind to exposed collagen. The GPVI-collagen interaction results in release of secondary mediators such as ADP and TxA_2 and the shift of platelet integrins to the activated high-affinity state, thereby mediating full platelet activation. In parallel, tissue factor (TF) locally triggers thrombin formation contributing to platelet activation. Taken from: Nieswandt, Pleines, Bender. *J Thromb Haemost* 2011[7]

First, the initial contact of platelets to the ECM is facilitated by the platelet glycoprotein (GP) Ib-V-IX complex interacting with collagen-bound vWF. Binding of GPIbα tethers platelets to the damage vessel wall under high shear conditions,[8] such as found in arterioles or stenosed arteries. These interactions are only transient and do not mediate firm adhesion, but rather leads to rapid deceleration and “rolling” of circulating platelets. Thereby the interaction of collagen with the immunoglobulin-like GPVI, the major platelet collagen receptor, is enabled as the second step of thrombus formation.[9-11] The GPVI-collagen interaction induces intracellular signaling that result in integrin activation (see below) and the release of the “second wave mediators” thromboxane A_2 (TxA_2) and adenosine diphosphate (ADP).[11] Together with locally produced thrombin, these mediators contribute to platelet activation by binding to G protein-coupled receptors (GPCRs) (G_q, $G_{12/13}$, G_i) and subsequently inducing full platelet activation.[12]

In a third step, firm adhesion of the platelets to the ECM is mediated by conversion of integrins from a low-affinity to a high-affinity (active) state through the intracellular signaling. This “inside-out”-signaling allows the interaction of the activated integrins with their ligands.[13,14] High-affinity β1 integrins bind to different ligands: α2β1 (also termed GPIa/IIa) binds to collagen, α5β1 to fibronectin and α6β1 to laminin. The major platelet integrin αIIbβ3 (GPIIb/IIIa) binds to fibrinogen and to collagen-bound vWF on the ECM.[15] Upon firm adhesion of the platelets, thrombus growth is induced by recruitment and activation of further platelets from the blood stream via release of ADP and TxA_2. Subsequently, clustering of platelets occurs via plasma fibrinogen and αIIbβ3 bound vWF leading to the formation of a stable thrombus.

However, it is speculated that besides secondary mediators, further yet unidentified receptor-ligand interactions on the platelet surface could play a role in thrombus formation and stabilization of the growing plug.[16] Previously, it was shown that the immunodepletion of platelet C-type lectin-like receptor 2 (CLEC-2) using antibodies results in reduced thrombus stability and enhanced embolization, but the CLEC-2 ligand in this process remains to be identified.[17]

1.1.2 Signaling events during platelet activation

Platelets express a variety of receptors on the plasma membrane, that mainly induce two major signaling pathways during platelet activation, both of which culminate in the activation of phospholipase (PL) C isoforms (Figure 2).[18] This leads to a subsequent elevation of intracellular calcium levels ($[Ca^{2+}]_i$) which is a central step in platelet activation and a prerequisite for granule release, integrin activation and procoagulant activity.[19] Platelets possess three different types of granules: α-granules, dense granules and lysosomes. The α-granules contain adhesive molecules like fibrinogen, vWF and thrombospondin as well as growth and coagulation factors. P-selectin expression on the platelet surface upon α-granule release is a major degranulation marker and therefore widely used to assess the activation state of platelets *in vitro*. Dense granules store small molecules like ADP, adenosine triphosphate (ATP), serotonin and TxA_2, which are the most important secondary mediators for thrombus formation. Upon platelet activation and a subsequent increase in $[Ca^{2+}]_i$, these granules are first centralized and then secreted.

Soluble agonists such as ADP, TxA_2, epinephrine and serotonin as well as locally produced thrombin stimulate GPCRs (G_q, $G_{12/13}$, G_i) (Figure 2). The G proteins induce multiple signaling events, like stimulation of Rho-GTPases (via $G_{12/13}$), phosphoinositide-3-kinase (PI3K)/Akt signaling (via G_i) and activation of PLCβ (via G_q).[12] These signaling events result in cytoskeletal rearrangements, platelet shape change and cell spreading.

The second major signaling pathway is initiated by the GPVI-Fc receptor γ-chain (FcRγ-chain) complex or by CLEC-2 and requires the phosphorylation of critical tyrosine residues in the immunoreceptor tyrosine-based activation motif (ITAM) or hemi-ITAM (hemITAM) respectively, which is similar to signaling cascades used by immunoreceptors. Signal transduction occurs via Src family kinases (SFK), the spleen tyrosine kinase (Syk), as well as via downstream adapter and effector proteins that activate PLCγ2. The details of this signaling pathway are discussed in the next chapter.

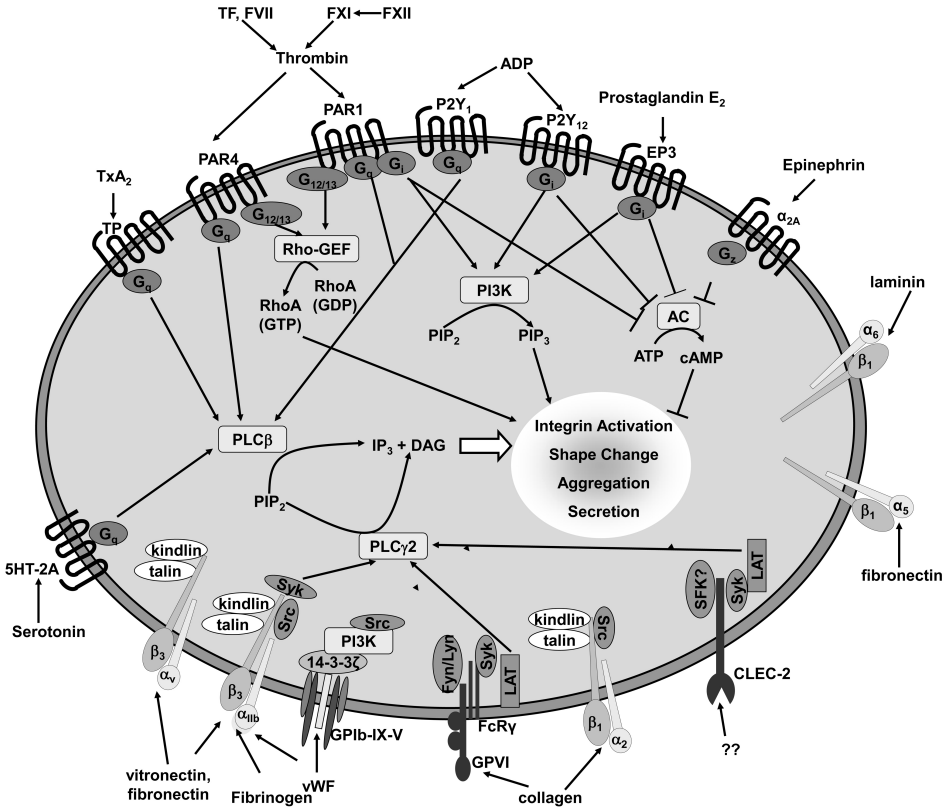

Figure 1. Major signaling pathways in platelets. Soluble agonists activate GPCRs involving G_q, $G_{12/13}$, G_i leading to activation of PLCβ. Cross-linking of the platelet activating receptors GPVI or CLEC-2 by ligand engagement results in activation of PLCγ2. (PIP_2: phosphatidylinositol-4,5-biphosphate, IP_3: inositol-1,4,5-trisphosphate, DAG: diacylglycerol, TF: tissue factor, TP: TxA_2 receptor, PAR: protease-activated receptor, RhoGEF: Rho-specific guanine nucleotide exchange factor, AC: adenylyl cyclase) Taken from: Stegner, Nieswandt. *J Mol Med* 2011[18]

In GPCR as well as in (hem)ITAM signaling, the activation of PLC isoforms leads to the hydrolysis of the membrane phospholipid phosphatidylinositol-4,5-biphosphate (PIP_2) to inositol-1,4,5-trisphosphate (IP_3) and diacylglycerol (DAG). IP_3 triggers Ca^{2+}-mobilization from intracellular stores. The decrease in the Ca^{2+}-store content subsequently opens Ca^{2+}-channels in the plasma membrane, inducing a process termed store-operated Ca^{2+}-entry (SOCE). DAG activates protein kinase C (PKC) and induces moderate receptor-operated Ca^{2+}-entry (ROCE) via transient receptor potential channel (TRPC) 6. Elevations in $[Ca^{2+}]_i$ are a central step during platelet activation and a prerequisite for proper cellular responses including firm adhesion, granule secretion and aggregation.

1.2 The C-type lectin-like receptor 2 (CLEC-2)

1.2.1 Chromosomal localization, protein structure and expression

CLEC-2 is a ~32 kDa type II transmembrane protein encoded by the *Clec1b* gene.[20] Human and mouse *Clec1b* genes are mapped on chromosome 12 and 6, respectively. [20,21] The gene is located within the natural killer gene complex (NKC), forming a separate superfamily together with Dectin-1 and lectin-type oxidized low-density lipoprotein receptor-1 (LOX-1).[22] Human CLEC-2 was first described by Colonna *et al.* and a database search reveled a mouse homologue of CLEC-2 with approx. 60% identity over the whole sequence (Figure 3).[20] CLEC-2 was originally identified as a transcript in immune cells such as monocytes, dendritic cells and granulocytes.[20,22] Later it was found, to be expressed at low levels in liver sinusoidal endothelial cells, Kupffer cells, peripheral blood mononuclear cells and at high levels only in MKs and platelets, in both humans and mice.[20,23-25] On platelets, it serves as receptor for the powerful platelet activating snake venom rhodocytin (RC, also termed aggretin), which can be isolated from the Malayan pit viper *Calloselasma rhodostoma*.[25]

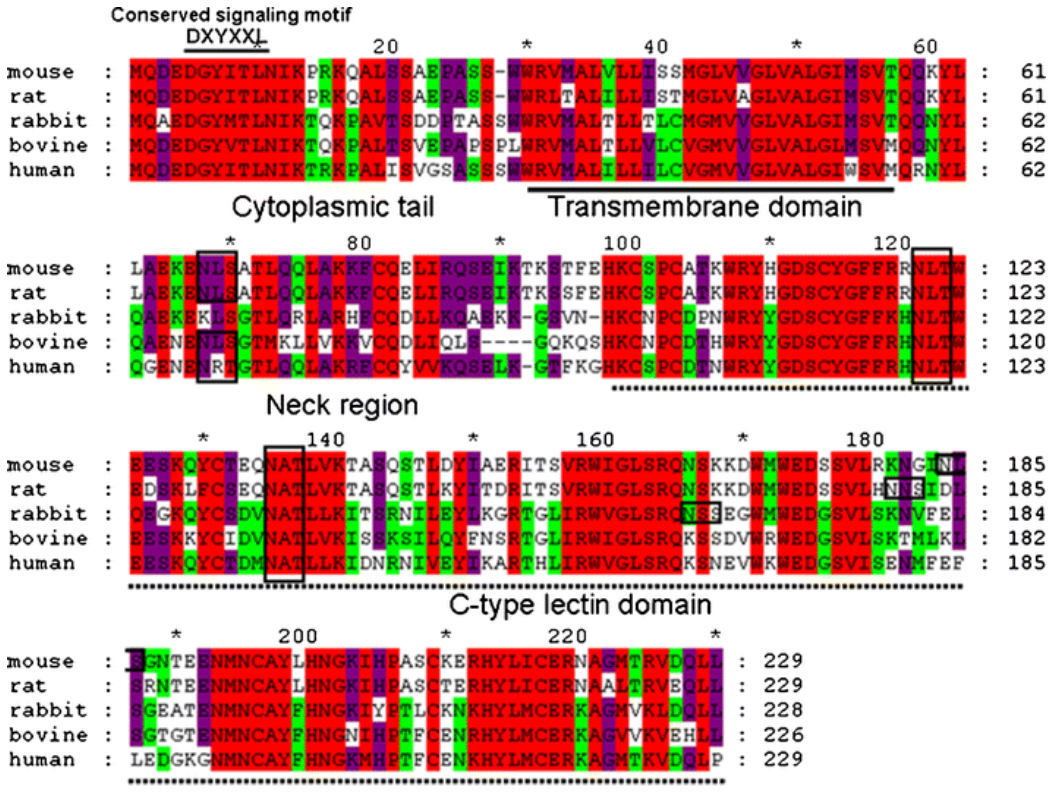

Figure 3. Comparison of amino acid sequence of CLEC-2 of different species (mouse, rat, rabbit, bovine and human). The cytoplasmic tail contains the conserved ITAM signaling motif (YXXL). The red shading represents 100% conservation, the purple shading represents 80% and the green 60%. Different predicted N-glycosylation sites are located within CLEC-2, indicated by black boxes. Taken from Wang *et al. Glycoconj J* 2012[26]

CLEC-2 belongs to the superfamily of C-type lectin receptors (CLRs), which fulfill diverse functions, including cell adhesion, tissue remodeling, platelet activation, endocytosis and innate immunity.[27,28] This superfamily can be divided into 17 groups based on their phylogeny and domain organization.[29] C-type lectins were originally considered to be Ca^{2+}-dependent carbohydrate-binding proteins, containing a conserved carbohydrate recognition domain (CRD).[27,30] Meanwhile, it is known that some of these proteins, like CLEC-2, contain a C-type lectin-like domain (CTLD), which is homologous to a CRD, but lacks the sequence responsible for Ca^{2+}- and carbohydrate binding.[29,31,32]

CLEC-2 is a type II transmembrane protein, thus it has an extracellular carboxyl-terminal domain and an intracellular NH_2-terminal domain. Human as well as murine CLEC-2 consists of 229 amino acids (aa) with a molecular mass of approx. 27 kDa and an apparent molecular mass of 32-33 kDa under reducing conditions (Figure 3).[20,25] It has a single extracellular CTLD connected by a neck region to a single transmembrane domain of 26 aa and a cytoplasmic tail of 31 aa containing one half of an ITAM, a so-called hemITAM.[20,25] The tyrosine residue present in the hemITAM becomes phosphorylated upon receptor activation and the signal is further transduced into the cytoplasm. Within the CTLD, six conserved cysteine residues are present, which are likely to generate three intrachain disulfide bonds that are typical for C-type lectins.[33] Furthermore, there are three to four predicted N-glycosylation sites on CLEC-2 (Figure 3). However, only two sites (N120, N134) are conserved within different species. Glycosylation at both sites is necessary for translocation of CLEC-2 to the cell surface.[26] In 2007, Watson and colleagues solved the crystal structure of the extracellular domain of CLEC-2 (Figure 4).[34] The key structure, which is responsible for ligand binding, is a hyper-variable semi-helical loop region consisting of 3-10 helices (Figure 4). Major ligand-induced conformational changes are unlikely as the overall fold is compact and robust. However, binding of a ligand to the hyper-variable loop could induce rotation around the axis of the helical element.[34,35]

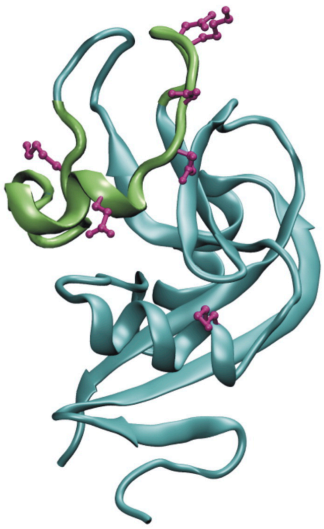

Figure 4. Structural features of CLEC-2. The structure of the extracellular domain of CLEC-2. The platelet membrane would be at the bottom of the figure. Upon ligand binding, the long loop region (green) has the potential to rotate. The pink-labeled residues play a role in ligand binding as was shown by site-directed mutagenesis. Taken from: O'Callaghan. *Curr Opin Pharmacol* 2009[35]

1.2.2 CLEC-2-induced intracellular signaling

The snake venom RC is a tetramer and binds the long loop region of the extracellular domain of CLEC-2. Structural analysis suggests that one tetramer can bind multiple copies of CLEC-2, thereby clustering the receptor on the cell surface.[25,35] Upon ligand engagement of CLEC-2, the cytoplasmic tyrosine residues within the hemITAM are phosphorylated by SFK and Syk (Figure 5).[25,36] It was shown that CLEC-2 is active as a non-disulfide-linked homodimer on the platelet surface, which enables the binding of the tandem Src homology 2 (SH2) domains of Syk.[37] This leads to tyrosine phosphorylation and recruitment of adapter proteins, Tec family tyrosine kinases and various effector proteins including the linker of activation of T-cells (LAT), SH2 domain containing leukocyte protein of 76 kDa (SLP-76), Gads, Rac1 and PLCγ2.[25,38] Several of these proteins are critical for activation, such as Syk and PLCγ2, whereas the lack of others can be overcome at high agonist concentrations, e.g. LAT and Gads.[25] Pollitt and colleagues showed that CLEC-2 signaling takes place in lipid rafts and that the receptor translocates upon activation before phosphorylation of the hemITAM occurs.[39] Furthermore, CLEC-2-dependent platelet activation is discussed to be dependent on actin polymerization, the reinforcement by the release of secondary mediators, such as ADP and TxA_2, as well as on Rac1 activation.[39]

To prevent unwanted platelet activation, constitutive signaling via CLEC-2 is inhibited by G6b-B and to a minor extent by platelet endothelial cell adhesion molecule-1 (PECAM-1), both containing immunoreceptor tyrosine-based inhibitory motifs (ITIMs) in their cytoplasmic domains.[40,41]

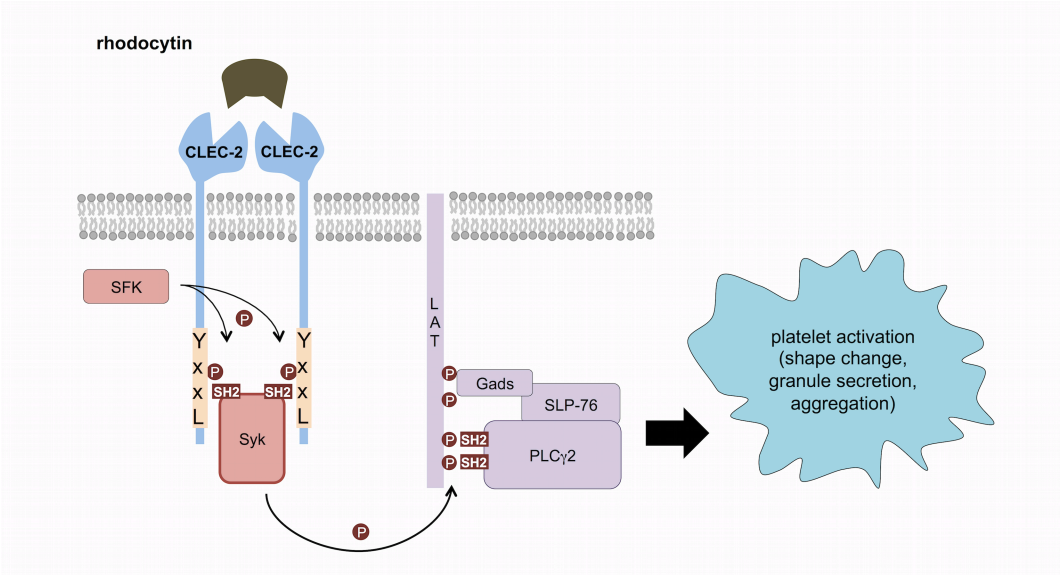

Figure 5. CLEC-2 signaling in platelets. Ligand engagement (e.g. rhodocytin) causes phosphorylation (P) of a tyrosine residue (Y) within the hemITAM by SFK and Syk. This initiates a downstream signaling cascade involving the adaptor/ effector proteins LAT, Gads, SLP-76 and PLCγ2. Eventually, this culminates in platelet activation characterized by shape change, granule secretion and finally platelet aggregate formation. Modified from Watson *et al. J Thromb Haemost* 2010[42]

1.2.3 Function of CLEC-2 in physiological and pathophysiological processes

CLEC-2 is a unique platelet receptor, which contributes not only to thrombus formation and stabilization, but is critical for developmental processes, tumor metastasis and prevention of inflammatory bleeding, making it a potential pharmacological target to modulate these processes.

CLEC-2 was first identified in 2006[25] in platelets and three independent publications demonstrated that the constitutive knock out results in embryonic or perinatal lethality of mice.[43-45] It became clear that other strategies are necessary to effectively delete the receptor in platelets. To this end, our group generated a monoclonal rat anti-mouse CLEC-2 antibody, INU1.[17] This antibody depletes the receptor from circulating platelets resulting in a "knock out-like phenotype".[17] Using this approach, we demonstrated that CLEC-2 plays an important role in thrombus formation and stabilization *in vitro* and *in vivo*. CLEC-2-deficiency protects mice from occlusive arterial thrombus formation.[17] CLEC-2-depleted mice have a variable prolongation of bleeding times indicating a moderate hemostatic defect.[17] Parallel to our study, mice conditionally deficient for CLEC-2 in MKs and platelets (*Clec1b*$^{fl/fl\ PF4cre}$) were generated. The analysis of these animals with regard to thrombosis and hemostasis is part of this thesis and is addressed later.

Besides this, the MK/ platelets-specific CLEC-2 knock out mouse was generated to investigate the unexpected role of CLEC-2 during embryonic development. These mice are viable despite having a defect in the separation of the lymphatic from the blood vasculature, resulting in blood-filled lymphatic vessels and perivascular edema formation[46] (see also Figure 6 A,B). Recent studies revealed that the interaction of CLEC-2 on platelets with its physiological ligand podoplanin is critical for lymphangiogenesis.[46] Podoplanin is a ubiquitous transmembrane glycoprotein, most notably expressed on lymphatic endothelial cells (LEC), type 1 lung alveolar cells, kidney podocytes and lymph node stromal cells, but which is absent on blood vascular endothelial cells and platelets.[35,42,47,48] Hence, platelets come into contact with podoplanin expressed on LECs during embryonic development, when lymph sacs form from the cardinal vein and sprout centrifugally to form mature lymphatic networks.[49] Uhrin and colleagues showed that platelets can be activated and form aggregates at connections of paired lymph sacs with their parental anterior cardinal veins.[49] These results, which were obtained using podoplanin knock out mice, were connected to earlier publications describing "non-separating" phenotypes in mice deficient for proteins involved in the CLEC-2 signaling pathway, namely Syk, SLP-76[50-52] and PLCγ2.[53] Later, Osada and colleagues showed that not platelet aggregates, but rather the released granule contents from podoplanin-activated CLEC-2-positive platelets are important for blood/ lymphatic vessel separation.[54] They showed in *in vitro* studies that granule contents from

GPVI-stimulated (poly(PHG)) platelets significantly inhibit LEC migration, proliferation and tube formation.[54] However, Finney and colleagues could not confirm this result using granule releases after platelet stimulation with RC. They hypothesized that direct contact of platelets to podoplanin on LEC results in podoplanin crosslinking and altered constitutive signaling, which leads to inhibition of LEC migration.[46]

Further studies showed that CLEC-2 is not only required for lymphatic vessel development during embryogenesis, but also for maintaining the lymphatic vessel integrity in adult mice. Irradiated mice that were reconstituted with *Clec1b*$^{-/-}$ fetal liver cells develop blood-filled mesenteric lymphatic vessels and Peyer's patches 7 weeks after transplantation (Figure 6 C,D).[46] At the lymphovenous (LV) junction, lymph drains into the blood stream and a LV valve (LVV) prevents retrograde blood flow into the lower-pressure lymphatic system.[55] Circulating platelets come into contact with LECs at the LV junctions and initiate podoplanin-CLEC-2 signaling events.[56] This results in platelet activation and formation of fibrin-rich thrombi.[56] This special kind of intravascular hemostasis functions together with the LVV to safeguard the lymphatic vascular network throughout life.[56]

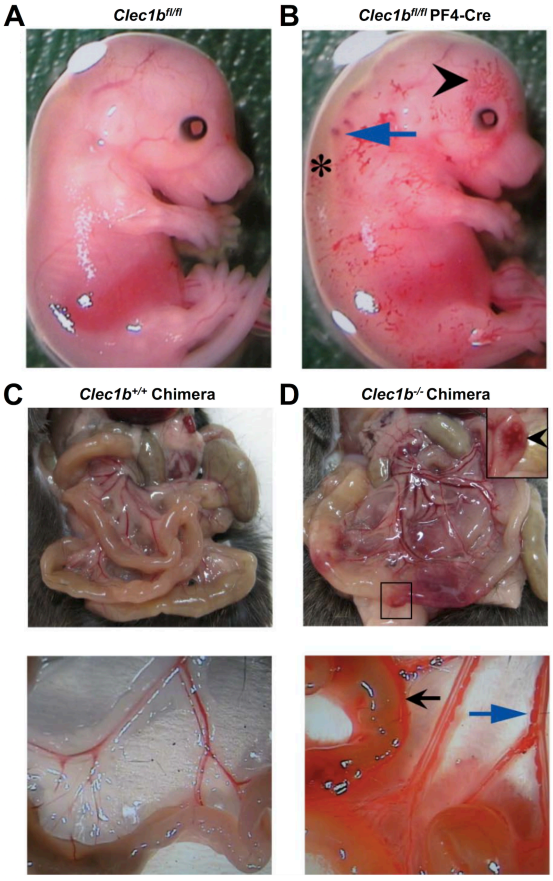

Figure 6. MK/ platelet-specific deletion of CLEC-2 results in defective lymphatic development. (A,B) *Clec1b*$^{fl/fl\ PF4\text{-}Cre}$ embryos at E14.5 show edema formation (asterisk), hemorrhages (blue arrow) and blood-filled lymphatic vessels in the skin (black arrowhead), which is not seen in control littermates. (C,D) Fetal liver cells from *Clec1b*$^{-/-}$ mice were injected into irradiated 6-weeks old C57BL/6 mice. 7 weeks post transplantation the mesentery and intestines were surrounded by blood fluid upon opening the abdominal cavity (black arrow, bottom panel). Bloody Peyer's patches (arrowhead, top panel) and blood-filled lymphatic vessels (blue arrow, bottom panel) were visible. Modified from: Finney *et al. Blood* 2012[46]

Additionally, the MK/ platelets-specific CLEC-2 knock out mice develop spontaneous bleeding in their mucosal lymph nodes (LN).[57] Studies in podoplanin and CLEC-2-deficient animals revealed that both are required to maintain the vascular integrity in LN. Within LN,

podoplanin is expressed on LECs and on fibroblastic reticular cells (FRCs), which surround high endothelial venules (HEVs). HEVs are specialized blood vessels, which permit transmigration of circulating lymphocytes, while maintaining vascular integrity.[58-62] CLEC-2-positive platelets interact with podoplanin-positive FRCs at the abluminal side of HEVs. The platelets become activated and release sphingosine-1-phosphate (S1P) in the perivenular space, promoting VE-cadherin expression on HEVs, thereby preserving the barrier function.[57] This cross-talk is critical for HEV integrity during immune responses and in situations of increased lymphocyte trafficking, such as chronic inflammation.[57]

Recent studies demonstrated that platelets are essential to maintain vascular integrity during inflammation.[63] Especially, platelet CLEC-2 as well as components of the CLEC-2 signaling pathway were shown to be involved in preventing inflammation-induced hemorrhages in skin and lung, albeit the underlying mechanism is still unclear.[64] Potentially, podoplanin-CLEC-2 mediated local S1P release from platelets may protect vascular integrity in inflamed tissues as it was observed for the HEV integrity in LNs.

Besides the importance of CLEC-2 during embryonic development and for maintaining vascular integrity, other functions of CLEC-2 have been postulated. CLEC-2 has been shown to enhance the infectivity of human immunodeficiency virus type 1 (HIV-1) produced in HEK293T cells.[23] This effect was not mediated by a direct interaction of CLEC-2 and the envelope protein, implying that a protein from the HEK293T cell was captured during viral budding.[23] Thereafter, two studies demonstrated that podoplanin is expressed on HEK293T cells and gets incorporated into virions released from these cells.[65,66] Binding of podoplanin to CLEC-2 could be an important mechanism in viral dissemination as viruses can be passively transported by platelets within the blood stream.[65,66]

Early studies demonstrated that podoplanin, which is present on the majority of tumor cells, activates platelets through CLEC-2, thereby inducing platelet aggregation, which promotes tumor metastasis.[47,67] Platelet aggregates coat tumor cells within the blood, enabling the tumor cells to evade the immune system and mediate their adherence to the vascular endothelium.[68-71] Furthermore, activated platelets release growth and angiogenic factors facilitating tumor cell extravasation and growth at metastatic sites.[68-70]

Despite its central function in multiple physiological and pathophysiological processes, the cellular regulation of CLEC-2 in platelets is still largely unknown. This may, however, be of major importance for the development of pharmaceuticals that modulate CLEC-2 function under disease conditions.

1.3 The major collagen receptor glycoprotein (GP) VI

The major collagen receptor GPVI is a 62 kDa type I transmembrane protein. It belongs to the immunoglobulin (Ig) superfamily and is closely related to the natural killer cell receptor and FcαR.[72] The expression of GPVI is restricted to platelets and MKs in humans and mice,[73] making it a potentially specific target for anti-thrombotic therapy.[74]

1.3.1 Signal transduction of GPVI

The extracellular domain of GPVI consists of two IgG domains bearing the collagen-binding site, followed by a mucin-rich stalk containing O-glycosylation sites, a transmembrane domain and a cytoplasmic tail.[11,75] The cytoplasmic tail has only 27 aa including a basic and a prolin-rich region for the constitutive binding of calmodulin[11,76] and SFK (Fyn and Lyn),[77] respectively. The intracellular domain is non-covalently associated with the FcRγ-chain representing the signaling subunit of GPVI.[11,78] The FcRγ-chain is expressed as a disulphide-linked homodimer, each monomer containing two tyrosine residues in the conserved ITAM.[11,13,79,80]

Subendothelial fibrillar collagens are the most potent thrombogenic substrates at the lesion site triggering platelet adhesion, activation and ultimately aggregation. Whereas different receptors can indirectly interact with collagen via vWF,[8] only two platelet receptors can directly bind to collagen: α2β1 and GPVI.[81] While the integrin α2β1 has a major role in adhesion and platelet anchoring, only GPVI has been established to induce signaling and platelet activation upon collagen binding.[81] GPVI specifically recognizes the glycine-proline-hydroxyproline (GPO) repeats within the collagen.[11] Platelet activation via GPVI can also be induced by the collagen-related peptide (CRP), consisting of GPO repeats and the snake-venom toxin convulxin (CVX), which is capable of clustering four GPVI proteins.[82,83]

Upon crosslinking of GPVI by ligand binding, the SFKs Fyn and Lyn come into contact with the FcRγ-chain and mediate tyrosine phosphorylation of the ITAM (Figure 7).[78,80,84] The phosphorylated ITAM serves as a binding site for the SH2 domains of the tyrosine kinase Syk[85,86] which becomes autophosphorylated and thereby initiates a complex downstream signaling cascade via the phosphorylation of adaptor proteins LAT,[87] SLP-76[88] and of effector enzymes, such as PI3K, PLCγ2 and small GTPases.[89] This triggers DAG- and IP_3-production, leading to activation of PKC and an elevation of $[Ca^{2+}]_i$. Elevated $[Ca^{2+}]_i$ enables platelet activation, degranulation and aggregation of the cells.[11,42]

To prevent basal signaling through GPVI, ITIM-containing receptors, such as PECAM-1, carcinoembryonic antigen cell adhesion molecule-1 (CECAM-1) or G6b-B have been shown to act as negative regulators of GPVI signaling.[42] Furthermore, platelet reactivity can be

downregulated through A disintegrin and metalloprotease (ADAM)10 and ADAM17, which can cleave the extracellular domain of GPVI, generating a 55 kDa soluble GPVI fragment and a 10 kDa transmembrane remnant fragment, but the *in vivo* significance of this is not clear.[90]

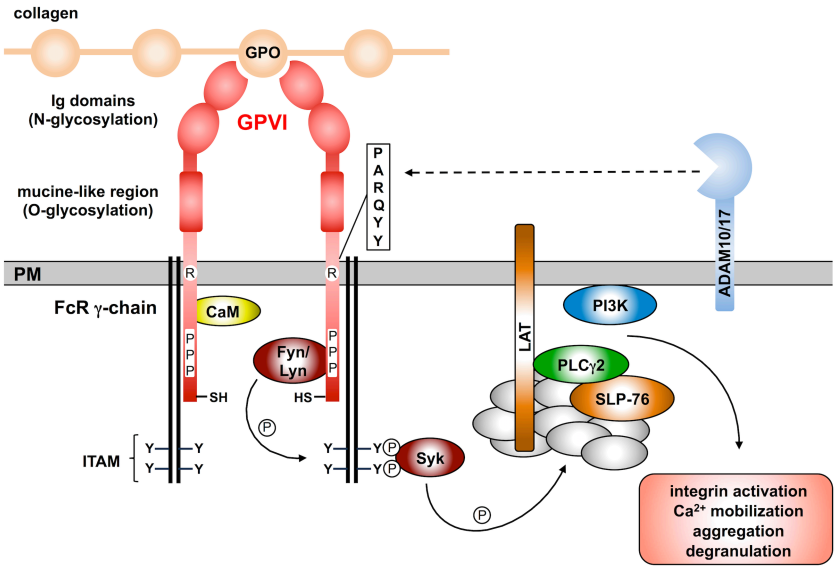

Figure 7. Signaling of the GPVI/ FcRγ-chain complex in platelets. Crosslinking of GPVI dimers occurs through binding of the extracellular Ig domains to the GPO repeats within collagen. This causes Fyn/Lyn-mediated phosphorylation of the ITAMs in the FcRγ-chain initiating in turn a Syk-dependent signaling cascade. This initiates the formation of the LAT signalosome, which compromises multiple adapter and effector proteins such as PI3K and PLCγ2. Finally, this results in platelet integrin activation, Ca^{2+} mobilization, degranulation and aggregation. ADAM10/17-mediated GPVI ectodomain shedding also occurs in response to GPVI stimulation and may represent a mechanism to downregulate platelet reactivity. The cleavage site for ADAM10 is depicted, whereas the exact site for ADAM17 is so far not known. Abbreviation: PM, plasma membrane. Taken from: Dütting *et al.*, *Trends Pharmacol Sci* 2012[75]

1.3.2 GPVI receptor regulation by monoclonal antibodies

Earlier studies from our group demonstrated that *in vivo* administration of monoclonal rat anti-GPVI αntibodies (termed JAQ1, 2, 3) leads to "immunodepletion" or downregulation of the GPVI receptor in circulating platelets resulting in a "knock out-like" phenotype in mice.[74,91] Using different genetically modified mouse strains, it was shown that two distinct pathways exist to regulate the prevalence of GPVI on the surface: ectodomain shedding by metalloproteinases and internalization/ intracellular clearance (Figure 8).[74,92] Interestingly, both processes are absent in mice carrying a point mutation in the FcRγ-associated ITAM showing that signaling through the receptor is essential.[92] GPVI internalization and subsequent intracellular clearance was observed in mice lacking LAT or PLCγ2, revealing the existence of a so far uncharacterized signaling pathway downstream of GPVI.[92] However, ectodomain shedding was abolished in these animals, demonstrating that this process depends on classical GPVI signaling.[92] Two proteinases of the ADAM family are involved in

the extracellular cleavage of platelet receptors: ADAM10 and ADAM17. The latter is the principal sheddase for GPIbα,[93] whereas cleavage of GPV or GPVI can occur through either ADAM10 or ADAM17, depending on the shedding-inducing stimulus.[90,94] Furthermore, injection of JAQ1 into mice lacking both ADAM10 and ADAM17 in platelets provided evidence that a third protease may exist in platelets that cleaves GPVI *in vivo* as shedding is unaltered in these animals.[94]

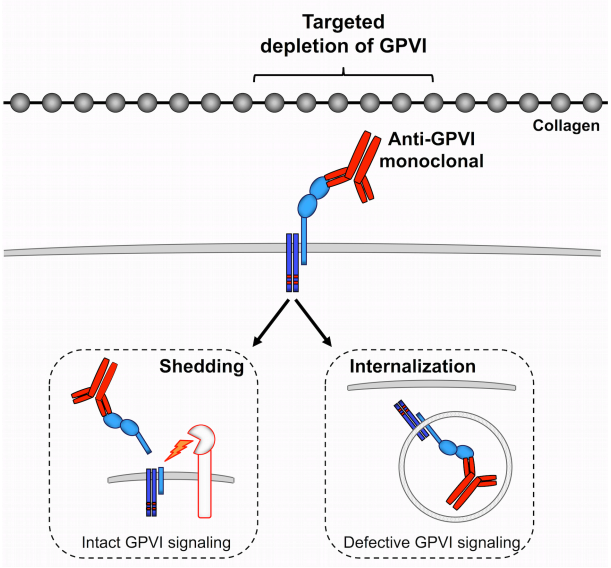

Figure 8. GPVI receptor regulation by JAQ1 *in vivo*. JAQ1 injection results in downregulation of GPVI from the platelet surface by two different ways. In platelets with intact GPVI signaling JAQ1 triggers metalloproteinase-dependent ectodomain shedding. If signaling downstream of the ITAM is defective, GPVI is internalized and intracellular cleared. Modified from: Stegner *et al.*, *Arterioscler Thromb Vasc Biol* 2014[95]

However, *in vitro* incubation of platelets with JAQ1 does only block GPVI without any further effects specifically without platelet activation or receptor downregulation.[96] Therefore, to study platelet GPVI receptor regulation *in vitro*, platelets were treated with established shedding inducing agents. The calmodulin inhibitor W7 induces the disruption of calmodulin from receptors, thereby facilitating GPVI ectodomain shedding through ADAM10.[94,97] Furthermore, GPVI shedding can be triggered *in vitro* by carbonyl cyanide m-chlorophenylhydrazone (CCCP) that induces mitochondrial injury by uncoupling oxidative phosphorylation and thereby triggers receptor shedding mainly by ADAM17.[98]

1.3.3 Comparison of CLEC-2 and GPVI signaling in murine platelets

While the hemITAM-bearing receptor CLEC-2 and the ITAM-bearing GPVI/FcRγ-chain complex differ in their structure, they share some similarities in their signaling pathways (Figure 9 A).[42] Both pathways involve sequential activation of SFK and Syk, leading to a downstream tyrosine phosphorylation cascade and to the recruitment of several adaptor and effector proteins (Figure 5, 7). Ligand-induced cross linking of GPVI leads to phosphorylation of two conserved tyrosines in the ITAM of the FcRγ-chain through SFKs Lyn and Fyn.[78,80,84] The phosphorylated tyrosines serve as a binding site for the tandem SH2 domain containing Syk, which then becomes autophosphorylated. In contrast, CLEC-2 mediates powerful

platelet activation through SFK and Syk, while Syk is regulated through a novel dimerization mechanism via the single hemITAM in the intracellular domain.[25,36] CLEC-2 is present as a dimer on resting platelets and it is discussed that Syk binds to two phosphorylated hemITAMs in two CLEC-2 receptors (Figure 9 A).[37,38,99] Despite this novel mechanism of Syk regulation, downstream signaling events are similar for both receptors. Syk regulates a complex signaling pathway that involves the recruitment of adapter proteins, Tec family tyrosine kinases and various effector proteins such as PLCγ2.[25,99] In both cases, some of these proteins are critical for the signaling, such as Syk and PLCγ2, whereas the lack of others like LAT and Gads can be compensated at high agonist concentrations.[25,100] The only notable difference with regard to downstream signaling is the absolute requirement for SLP-76 in GPVI signaling, while stimulation of CLEC-2 with a high agonist concentration can still induce a weak activation in the absence of this adapter protein.[25,99]

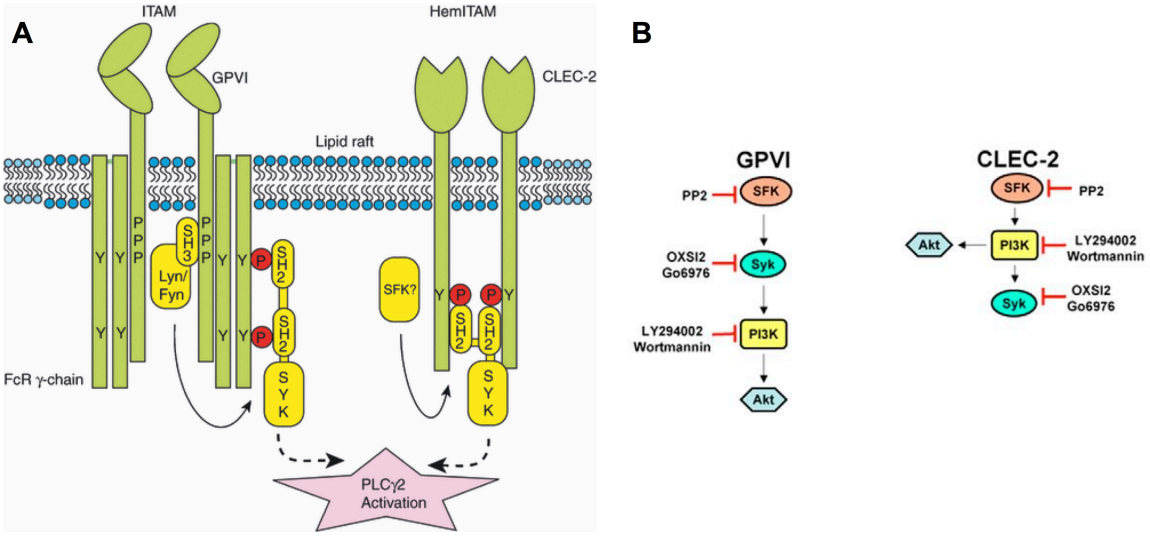

Figure 9. Comparison of the signaling pathways downstream of the ITAM-bearing GPVI-FcRγ-chain complex and the hemITAM-bearing receptor CLEC-2. (A) Ligand induced activation results in phosphorylation (P, red) of the tyrosine residues (Y) within the ITAM motif of the FcRγ-chain through the SFK Lyn and Fyn. The phosphorylated residues serve as a binding site for Syk, which is essential for signaling and downstream phosphorylation of effector proteins, including PLCγ2. CLEC-2 is present as a dimer and upon activation, the hemITAM is phosphorylated leading to Syk recruitment and further downstream signaling. Taken from: Watson SP *et al.*, *J Thromb Haemost*, 2010[42] (B) This model represents the different roles of SFK and Syk in PI3K activation upon stimulation of GPVI and CLEC-2, respectively. (PP2: SFK inhibitor; OXS12/GO6975: Syk inhibitors; LY294002, Wortmannin: PI3K inhibitors) Taken from: Manne *et al., J Biol Chem* 2015[101]

Although signaling downstream of Syk is fairly similar between CLEC-2 and GPVI, there is increasing evidence that the proximal events in their signaling cascade are distinct. Syk inhibition abolishes RC-induced phosphorylation of the hemITAM of CLEC-2 although phosphorylation of the GPVI/FcRγ-chain ITAM is fully preserved.[102] A recent study identified a novel signaling mechanism in CLEC-2-mediated Syk activation using different inhibitors for SFK, Syk and PI3K. It has been shown that inhibition of PI3K abolishes Syk phosphorylation and platelet activation downstream of CLEC-2, but not GPVI (Figure 9 B).[101] The contribution

of SFK in CLEC-2 signaling is not yet completely understood. In contrast, in GPVI signaling it has been clearly demonstrated that the GPVI-bound SFKs Lyn and Fyn phosphorylate the ITAM in the FcRγ-chain upon ligand-induced cross-linking.[78,80,84] Further studies are required to establish the exact proximal events in CLEC-2 signaling.

1.4 Modulation of platelet surface receptors by experimental antibodies

Monoclonal antibodies (mAbs) are widely used in the treatment of various diseases, such as tumors, autoimmune disorders, cardiovascular diseases, chronic inflammation and infections.[103] The specificity of mAbs has made them valuable therapeutic agents. However, murine mAbs have some limitations including short serum half-life, immune reactions,[104] loss of efficacy and function, which may lead to drug resistance development.[105] Therefore, most of the currently used therapeutic antibodies are human mAbs. Research focuses now on the development of new expression systems e.g. chicken eggs[106] or transgenic plants, as therapeutic proteins derived from plants are safer than proteins of animal origin.[107,108]

Due to their nature mAbs can accomplish their therapeutic effects through different mechanisms: binding, blocking or signaling.[109] Binding of the mAbs may disrupt the function of cells and their interaction with other cells resulting in cell death or apoptosis.[109] The physical binding of mAbs can block receptors on the cell surface, preventing ligand-induced signal transduction.[109] Furthermore, mAbs can also mimic ligand binding and thereby induce signaling and interaction with the immune system through complement-dependent cytotoxicity, antibody-dependent cellular phagocytosis or antibody-dependent cellular cytotoxicity.[109]

Ischemic cardio- and cerebrovascular diseases are primarily treated with anti-platelet agents.[110] However, all available anti-platelet and anti-coagulant agents have unwanted effects such as an increasing bleeding risk, especially when used in combination drug regimens.[110,111] The humanized mAb F(ab) fragment abciximab (trade name “ReoPro”) is used as a platelet inhibitor in clinical settings. It binds non-specifically to the platelet integrin αIIbβ3, thereby blocking its function. However, pharmacological blocking of αIIbβ3 leads to an increased risk of bleeding.[110,112]

A new and promising strategy is the antibody-mediated “immunodepletion” of platelet surface receptors. This approach has so far only been described for the platelet collagen receptor GPVI in the murine model.[74] GPVI downregulation can be induced *in vivo* by injection of the mAbs JAQ1, 2 or 3, resulting in long-term anti-thrombotic protection in models of pulmonary thromboembolism, arterial thrombosis and ischemic stroke without provoking bleeding complications.[74,113-115] Interestingly, while this potential strategy was elaborately analyzed in mice, antibody-induced loss of GPVI was also found in platelets of two patients who had

developed anti-GPVI autoantibodies,[116,117] as well as in human platelets circulating in non-obese diabetic/ severe combined immunodeficient mice.[118] Due to these intriguing findings, GPVI has extensively been discussed as a potential valuable new anti-thrombotic target in several studies.[74,91,94,119]

Importantly, recent studies demonstrated that also CLEC-2 could be temporarily depleted from the platelet surface.[17] The mechanisms underlying this process were studied in this thesis.

1.5 Aim of the study

Platelets are key players in hemostasis as well as in thrombotic events. Thus, progress in understanding the function of platelet receptors is required in order to identify potential new targets for antithrombotic therapy.

The surface receptors CLEC-2 and GPVI are the only (hem)ITAM receptors present on murine platelets. They share similarities in their intracellular signaling pathways. While GPVI-deficient animals have been extensively studied, consequences of CLEC-2 deficiency were largely unknown at the beginning of this study. The aim of this thesis is (I) to analyze MK/ platelets-specific CLEC-2 knock out mice with regards to their development as well as their platelet function and signaling. Furthermore, this study intends (II) to clarify whether GPVI and CLEC-2 have redundant functions in murine models of thrombosis and hemostasis. Therefore, genetically double-deficient animals are generated and analyzed.

Despite its central function in multiple physiological and pathophysiological processes, not much is known about the cellular regulation of CLEC-2 in platelets. This may, however, be of major importance for the development of pharmaceuticals that modulate CLEC-2 function under disease conditions. The aim of this study is (III) to elucidate the mechanism underlying the targeted CLEC-2 downregulation. To immunodeplete CLEC-2 from circulating platelets, different genetically modified mice are injected with the anti-CLEC-2 antibody INU1 and the regulation of CLEC-2 is examined.

Intact antibodies of the IgG subclass can have unwanted effects, therefore antibody F(ab) fragments are considered to be better pharmacological agents. Hence, F(ab) fragments of INU1 are prepared by enzymatic digestion of the intact IgG and (IV) their effects are analyzed in different genetically modified mice *in vivo*.

2 MATERIALS AND METHODS

2.1 Materials

2.1.1 Reagents and chemicals

Acetic acid	Roth (Karlsruhe, Germany)
Adenosine diphosphate (ADP)	Sigma (Deisenhofen, Germany)
3-amino-9-ehylcarbazole (AEC) solution	EUROPA (Cambridge, UK)
Agarose	Roth (Karlsruhe, Germany)
Alexa Fluor 488	Invitrogen (Karlsruhe, Germany)
Ammonium peroxodisulphate (APS)	Roth (Karlsruhe, Germany)
Apyrase (grade III)	Sigma (Deisenhofen, Germany)
Aquatex	Merck Millipore (Darmstadt, Germany)
Atipamezole	Pfizer (Karlsruhe, Germany)
8-azaguanine (50x)	Sigma (Deisenhofen, Germany)
Beta-mercaptoethanol	Roth (Karlsruhe, Germany)
benzyl alcohol	Sigma (Deisenhofen, Germany)
benzyl benzoate	Sigma (Deisenhofen, Germany)
Bovine serum albumin (BSA)	AppliChem (Darmstadt, Germany)
Calcium chloride	Roth (Karlsruhe, Germany)
Clopidogrel (Plavix®)	Sanofi-Aventis (Paris, France)
Convulxin	Alexis Biochemicals (San Diego, USA)
Dasatinib	Selleckchem (München, Germany)
Disodiumhydrogenphosphate	Roth (Karlsruhe, Germany)
dNTP mix	Fermentas (St.Leon-Rot, Germany)
Dry milk, fat-free	AppliChem (Darmstadt, Germany)
Dylight488	Pierce (Rockford, IL, USA)
EDTA	AppliChem (Darmstadt, Germany)
Enhanced chemiluminescence (ECL)	PerkinElmer LAS (Boston, USA)
Eosin	Roth (Karlsruhe, Germany)
Ethanol	Roth (Karlsruhe, Germany)
Eukitt mounting medium	Sigma (Deisenhofen, Germany)
Fentanyl	Janssen-Cilag GmbH (Neuss, Germany)
Fibrillar type I collagen (Horm)	Nycomed (München, Germany)
Flumazenil	Delta Select GmbH (Dreieich, Germany)
Fluorescein-isothiocyanate (FITC)	Molecular Probes (Oregon, USA)
Fluoroshield™ (with/ w/o DAPI)	Sigma (Deisenhofen, Germany)
Freund's Adjuvant	Sigma (Deisenhofen, Germany)
GeneRuler 1kb DNA Ladder	Fermentas (St. Leon-Rot, Germany)
Glucose	Roth (Karlsruhe, Germany)
Glutaraldehyde	Roth (Karlsruhe, Germany)
Glycerol	Roth (Karlsruhe, Germany)
Hematoxylin	Sigma (Deisenhofen, Germany)
HEPES	Roth (Karlsruhe, Germany)
n-Hexane	Sigma (Deisenhofen, Germany)
High molecular weight heparin	Sigma (Deisenhofen, Germany)
Human fibrinogen	Sigma (Deisenhofen, Germany)

Human vWF	CSL Behring (Marburg, Germany)
Igepal CA-630	Sigma (Deisenhofen, Germany)
Indomethacin	Sigma (Deisenhofen, Germany)
Integrilin	GlaxoSmithKline (Germany)
Isopropanol	Roth (Karlsruhe, Germany)
Loading Dye Solution, 6x	Fermentas (St. Leon-Rot, Germany)
Magnesium chloride	Roth (Karlsruhe, Germany)
Magnesium sulfate	Roth (Karlsruhe, Germany)
Medetomidine (Dormitor)	Pfizer (Karlsruhe, Germany)
Midazolam (Dormicum)	Roche Pharma AG (Grenzach-Wyhlen, Germany)
Midori Green Advanced DNA stain	Nippon Genetics Europe (Düren, Germany)
MOPS	AppliChem (Darmstadt, Germany)
Naloxon	Delta Select GmbH (Dreieich, Germany)
4-12% NuPage Bis-Tris gradient gels	Invitrogen (Karlsruhe, Germany)
NuPage LDS Sample buffer (4x)	Invitrogen (Karlsruhe, Germany)
osmic acid solution 2%	Merck (Darmstadt, Germany)
PageRuler Prestained Protein Ladder	Fermentas (St. Leon-Rot, Germany)
Paraformaldehyde (PFA)	Roth (Karlsruhe, Germany)
Phalloidin-Alexa647	Sigma (Deisenhofen, Germany)
Phenol/chloroform/isoamylalcohol	AppliChem (Darmstadt, Germany)
Poly-L-lysine solution	Sigma (Deisenhofen, Germany)
PP2	VWR (Darmstadt, Germany)
Prostacyclin (PGI_2)	Calbiochem (Bad Soden, Germany)
Protein G-Sepharose	GE Healthcare (Uppsala, Sweden)
Protease Inhibitor Cocktail (100x)	Sigma-Aldrich (Schnelldorf, Germany)
Proteinase K	Germentas (St. Leon-Rot, Germany)
Phycoerythrin (PE)	EUROPA (Cambridge, UK)
Refludan (heparin)	Schering (Berlin, Deutschland)
Rotiphorese Gel 30 (PAA)	Roth (Karlsruhe, Germany)
Sodium chloride	AppliChem (Darmstadt, Germany)
Sodium cacodylate	Roth (Karlsruhe, Germany)
Sodium citrate	AppliChem (Darmstadt, Germany)
Sodiumdihydrogenphosphate	Roth (Karlsruhe, Germany)
Sodium hydroxide	AppliChem (Darmstadt, Germany)
TEMED	Roth (Karlsruhe, Germany)
3,3,5,5-tetramethylbenzidine (TMB)	EUROPA (Cambridge, UK)
Thrombin	Roche Diagnostics (Mannheim, Germany)
TRIS ultra	Roth (Karlsruhe, Germany)
U46619	Alexis Biochemicals (San Diego, USA)

Collagen-related peptide (CRP) was synthesized by the Baylor College (Houston, Texas, USA). Rhodocytin was a generous gift from J. Eble (University Hospital Frankfurt, Germany). All enzymes were purchased from Fermentas (St. Leon-Rot, Germany) or obtained from Invitrogen (Karlsruhe, Germany). All other chemicals were obtained from Sigma (Deisenhofen, Germany) or Roth (Karlsruhe, Germany).

2.1.2 Cell culture materials

BSA, low endotoxin	PAA Laboratories (Cölbe, Germany)
Cell strainer, 100 µm	BD Falcon (Bedford, USA)
Concentrator tube, exclusion size 10 kDa	VivaScience (Hannover, Germany)
DL-Dithiothreitol	Sigma (Deisenhofen, Germany)
DMEM + GlutaMAX-I	Gibco (Karlsruhe, Germany)
D-PBS	Gibco (Karlsruhe, Germany)
Dimethyl sulfoxide (DMSO)	AppliChem (Darmstadt, Germany)
Foetal Bovine Serum (FCS)	Gibco (Karlsruhe, Germany)
HAT (hypoxanthine-aminopterin-thymidine, 50x)	Roche Diagnostics (Mannheim, Germany)
IMDM + GlutaMAX-I	Gibco (Karlsruhe, Germany)
Iodacetamide	Merck (Darmstadt, Germany)
Penicillin-Streptomycin	Gibco (Karlsruhe, Germany)
Pepsin, immobilized	Merck (Darmstadt, Germany)
Polyethylene glycol 1500 (PEG 1500)	Roche Diagnostics (Mannheim, Germany)
RPMI	Gibco (Karlsruhe, Germany)
Steritop Bottle Top Filter 0.22 µm	Millipore (Massachusetts, USA)
Superdex 200 (SD) column	Amersham Biosciences (Freiburg, Germany)
Thrombopoetin (TPO)	Invitrogen (Karlsruhe, Germany)
Tissue culture dishes (100x20 mm)	Greiner (Frickenhausen, Germany)
Tissue culture flasks	Greiner (Frickenhausen, Germany)
Trypsin-EDTA	Gibco (Karlsruhe, Germany)
Well plates (6-well, 24-well or 96-well)	Greiner (Frickenhausen, Germany)

2.1.3 Antibodies

2.1.3.1 Purchased primary and secondary antibodies

Mouse anti-phosphotyrosine 4G10	Upstate (California, USA)
Rabbit anti-human vWF Ig	DAKO (Hamburg, Germany)
Goat anti-rat/Cy3	Biolegend (London, United Kingdom)
Rabbit anti-rat Ig-FITC	DAKO (Hamburg, Germany)
Rabbit anti-mouse CLEC-2	Dianova (Hamburg, Germany)
Rat anti-mouse IgG-HRP	DAKO (Hamburg, Germany)
Rat anti-mouse Ly-6G	Biolegend (London, United Kingdom)

2.1.3.2 Monoclonal antibodies (mAbs)

Monoclonal antibodies (mAbs) generated and modified in our laboratory:

antibody	isotype	antigen	described in
DOM1	IgG1	GPV	[120]
DOM2	IgG1	GPV	[120]
INU1	IgG1κ	CLEC-2	[17]
INU2	not determined	CLEC-2	unpublished
JAQ1	IgG2a	GPVI	[74]
JON/A	IgG2b	GPIIb/IIIa	[121]
JON1	IgG2a	GPIIb/IIIa	[120]
JON6 (14A3)	IgG2b	GPIIb/IIIa	unpublished
MWReg 30	IgG1	α2 integrin	unpublished
p0p4	IgG2b	GPIbα	[120]
p0p/B	(p0p4-F(ab))	GPIbα	[120]
p0p6	IgG2b	GPIX	[120]
ULF1	IgG2a	CD9	[120]
WUG1.9	IgG1	P-selectin	unpublished
12C6	IgG2b	α2 integrin	unpublished

2.1.4 Animals

Specific-pathogen-free male mice (NMRI, C57Bl/6J) and rats (WISTAR) at 4 to 10 weeks of age were obtained from Janvier (Le Genest-Saint-Isle, France).

Gp6$^{-/-}$ mice were generated by Markus Bender in the laboratory as described previously.[122] *Clec1b*$^{fl/fl}$ mice[46] were kindly provided by Steve P. Watson (University of Birmingham, Birmingham, UK). The *Syk*$^{fl/fl}$ mice[123] were kindly provided by Friedemann Kiefer (Max-Planck-Institute for Molecular Biomedicine, Münster, Germany). The *Tln1*$^{fl/fl}$ mice[124] were kindly provided by David Critchley (Max Planch Institute of Biochemistry, Martinsried, Germany). To generate MK/ platelet-specific knock out mice, the floxed mice were intercrossed with mice carrying the Cre-recombinase under control of the platelet factor 4 (PF4) promoter.[125] *Fcer1g*$^{-/-}$ (further referred to as *FcRγ*$^{-/-}$)[126] were generated in our group. The hemITAM knock in mice carry an inactivating point mutation in the hemITAM (Y7A) and were generated in our group. As the constitutive knock in results in embryonic or perinatal lethality, fetal-liver chimeric mice were generated. Recipient C57Bl/6 mice at 6 weeks of age were lethally irradiated with 10 Gray. The livers of 13.5 to 14.5 day-old mouse embryos were isolated from time-mated female mice, a single cell suspension was prepared and cell number was counted in a Neubauer chamber. Four million cells diluted in 150 µl DMDM were intravenously injected into one recipient mouse. Animals received 2 g/l neomycine in water for 6 weeks. *Syk*$^{ZAP\ KIN}$,[127] *Lat*$^{-/-}$,[87] *Grb-2*$^{fl/fl}$,[128] *SLAP*$^{-/-}$/*SLAP2*$^{-/-}$,[129] *CD41-YFP* ^{KIN},[130] *Gp5*$^{-/-}$,[131]

vWF$^{-/-}$,[132] *F12*$^{-/-}$,[133] *Nbeal2*$^{-/-}$,[134] and Munc13-4 knock out (*Unc13d*$^{-/-}$)[135] mice have been published previously.

When indicated, heparin (Refludan® 50 µg/g body weight) was injected intravenously directly before the experiment.[136] When indicated, clopidogrel (Plavix® 75 mg/kg body weight) was administered twice orally by gavage feeding 48 h and 24 h prior to the experiment.[137]

All animal studies were approved by the district government of Lower Franconia (Bezirksregierung Unterfranken).

2.1.5 Cell lines

The mouse myeloma cell line Sp2/0-Ag14 was kindly provided by D. Männel (University Hospital Regensburg, Germany). These cells were maintained in the presence of 8-azaguanine, a purine analogue that is metabolized by hypoxanthine-guanine phosphoribosyltransferase (HGPRT). The resulting metabolite gets incorporated into DNA resulting in an abort of DNA synthesis. Thus, HGPRT-positive cells died, while HGPRT-negative cells survived and could be used for the generation of hybridoma cells (see 2.2.1.2).

2.1.6 Buffers and media

All buffers were prepared and diluted using *aqua ad injectabilia* from Delta Select (Pfullingen, Germany) or double-distilled water (ddH_2O).

Blocking solution (immunoblotting)

BSA or fat-free dry milk in PBS or washing buffer	5%

Cacodylate buffer (electron microscopy), pH 7.2

sodium cacodylate	50 mM

Clearing solution (BABB,LSFM)

1 part benzyl alcohol
2 parts benzyl benzoate

Coating buffer (ELISA), pH 9.0

$NaHCO_3$	50 mM

Coomassie staining solution

Acetic acid	10%
Methanol	40%
Coomassie Brilliant blue	1 g/l

Coomassie destaining solution

Acetic acid	10%
Methanol	40%

Coupling buffer 2x, pH 9.0

$NaHCO_3$	14 g/l
Na_2CO_3	8.5 g/l

DMEM growth medium

DMEM	
FCS	10%
Penicillin-Streptomycin	1%

DMEM selection medium

DMEM	
FCS	10%
Penicillin-Streptomycin	1%
Geneticin (G-418)	700 µg/ml

Elution buffer (affinity chromatography)

Glycine (pH 2.8)	0.1 M
add H_2O	

Fixation buffer I (electron microscopy)

sodium cacodylate, pH 7.2	0.1 M
glutaraldehyde	2.5%
formaldehyde	2%

Fixation buffer II (electron microscopy)

sodium cacodylate, pH 7.2	50 mM
osmium tetroxid	2%

IP buffer

TRIS HCl, pH 8.0	15 mM
NaCl	155 mM
EDTA	1 mM
NaN_3	0.005%

Laemmli buffer (SDS-PAGE)

TRIS	40 mM
Glycine	0.95 M
SDS	0.5%

Lysis buffer (DNA isolation)

TRIS base	100 mM
EDTA	5 mM
NaCl	200 mM
SDS	0.2%
add Proteinase K (20 mg/ml)	100 µg/ml

Lysis buffer (tyrosine phosphorylation), pH 7.5

NaCl	300 mM
Tris	20 mM
EGTA	2 mM
EDTA	2 mM
Na_3VO_4	2 mM
Igepal CA-630	2%
protease inhibitor cocktail (100x)	2%

MK Medium

IMDM	
FCS	10%
Penicillin-Streptomycin	1%
thrombopoetin	50 ng/ml

Neutralization buffer (affinity chromatography)

TRIS base (pH 9.0)	1.0 M

Permeabilization buffer

PFA	4%
Igepal CA-630	0.1%
in PHEM (pH 7.2)	

PHEM, pH 6.9

PIPES	60 mM
HEPES	25 mM
EGTA	10 mM
$MgSO_4$	2 mM

Phosphate buffer (PB), pH 7.14

Na_2HPO_4	0.1 M

Phosphate buffered saline (PBS), pH 7.14

NaCl	137 mM (0.9%)
KCl	2.7 mM
KH_2PO_4	1.5 mM
Na_2HPO_4	8 mM

Separating gel buffer

TRIS/HCl, pH 8.8	1.5 M

Sodium citrate buffer

$Na_6C_6H_5O_7$/HCl pH 4.0	0.1 mol/l

Sørensen buffer

solution A: KH_2PO_4	0.1 M
solution B: Na_2HPO_4	0.1 M

→ final solution: mix solution A : solution B (2:3) for pH 6.98

Stacking gel buffer

TRIS/HCl, pH 6.8	0.5 M

Stripping buffer

Tris/HCl, pH 6.8	62.5 mM
SDS	2%
β-mercaptoethanol	100 mM

Superdex 200 (SD) column buffer (pH 7.2)

NaCl	0.15 M
Na_2HPO_4	0.05 M

50x TAE	
TRIS base	0.2 M
Acetic acid	5.7%
EDTA (0.5 M, pH 8)	10%
TE buffer, pH 8	
TRIS base	10 mM
EDTA	1 mM
Transfer buffer	
Tris Ultra	50 mM
Glycine	40 mM
Methanol	20%
Tris-buffered saline (TBS), pH 7.3	
NaCl	137 mM (0.9%)
Tris/HCl	20 mM
Tyrode-HEPES buffer, pH 7.3	
NaCl	137 mM (0.9%)
KCl	2.7 mM
$NaHCO_3$	12 mM
NaH_2PO_4	0.43 mM
$CaCl_2$	1 mM
$MgCl_2$	1 mM
HEPES	5 mM
BSA	0.35%
Glucose	0.1%
Washing buffer	
Tween 20 in PBS	0.1%

2.2 Methods

2.2.1 Production and modification of monoclonal antibodies

2.2.1.1 Immunization of rats

To generate rat anti-CLEC-2 antibodies, three female WISTAR rats, 6 weeks of age, were immunized with either of the following antigens: platelets (0.5×10^9 washed mouse platelets in resting state, washed in sterile PBS) or immunoprecipitate from wild-type platelet lysates using INU1 (lysate from 0.5×10^9 washed mouse platelets, pull-down with 5 µg/ml INU1 and 25 µl protein G-Sepharose per rat). In a third attempt, purified mCLEC-2 Fc-fusion protein[17] (100 µg per rat for the initial, 50 µg per rat for all following immunizations) was used. Each antigen was dissolved in Freund's adjuvant. For the initial immunization, antigens were solubilized in Freund's adjuvant complete and injected subcutaneously in three bolus injections of 150 µl per rat. All following immunizations were performed in Freund's adjuvant

incomplete. Rats were repeatedly (3-5 times, intervals of 21 days) subcutaneously immunized with the immunogens.

2.2.1.2 Generation of hybridoma cells

The rat spleen was removed under sterile conditions and filtered through a 100 µm cell strainer to obtain a single cell suspension. For the fusion of mouse myeloma and rat splenic cells, spleen cells were washed twice in RPMI/pen-strep medium (160 *x g*, 5 min, RT), mixed with mouse myeloma cells (Ag14, 10^8 cells per fusion) and washed twice with RPMI/pen-strep by centrifugation at 900 rpm for 5 min. Supernatant was removed carefully and 1 ml of polyethylene glycol 1500 (37°C) was added drop-wise over a time period of 2 min. This was followed by a slow addition of 10 ml RPMI/pen-strep medium (37°C) over a time period of 10 min. Cells were then seeded into 15 96-well plates and fed with medium containing hypoxanthine-aminopterin-thymidine (HAT) to select only the fused hybrid cells which solely survive in this medium until screening.

2.2.1.3 Screening of hybridoma clones by ELISA

To detect hybridoma clones producing mAbs directed against the respective antigen (mCLEC-2), hybridoma supernatant was tested by Enzyme-linked immunosorbent assay (ELISA). Therefore, ELISA plates were coated o/n at 4°C with the mCLEC-2 Fc-fusion protein (5 µg/ml in coating buffer). After blocking with 5% BSA in H_2O for 1 h at 37°C, the hybridoma supernatant was added and left to incubate for 1 h at 37°C. ELISA plates were washed 3 times with washing buffer and left to incubate with the secondary antibody anti-rat HRP (1:3,000) in washing buffer for 1h. After extensive washing, the ELISA was developed using TMB substrate. False-positive clones producing mAbs directed against the Fc-part of the fusion protein were detected using a second ELISA in parallel with an unspecific Fc-fusion protein generated in our laboratory.

2.2.1.4 Preparation of F(ab)2- and F(ab)-fragments via size chromatography

To generate F(ab)2-fragments from full length antibodies, concentrated and dialyzed IgG (4.0 mg/ml) in 0.1 mol/l sodium citrate buffer was incubated with immobilized pepsin in the ratio of 5:1 and left to incubate for 4 h at 37°C under shaking conditions. For size chromatography, samples were dialyzed against Superdex 200 column buffer and pH was adjusted to pH 7.2. Then, the digested solution was added to a Superdex 200 column with a flow rate of 2.0 ml/min (~25 cm/h). Fractions were collected and tested on SDS-PAGE (15%) for sufficient digestion and purity. The F(ab)2 fractions were concentrated by centrifugation using a concentrator tube (VivaSpin®, exclusion size 10 kDa), sterile filtrated and stored at -20°C until use or further digestion to F(ab)-fragments.

For generation of F(ab)-fragments, F(ab)2-fragments (1 mg/ml) were dialyzed against TRIS/HCl (50 mmol/l, pH 8.0) o/n at 4°C. To digest the F(ab)2 fragments, 10 mmol/l DL-dithiothreitol (DTT) was added and samples were incubated for 30 min at 37°C followed by incubation with 20 mmol/l iodoacetamide for 30 min at 37°C. The digested F(ab)-fragments were added to a Superdex 200 column with a flow rate of 2.0 ml/min (~25 cm/h) and fractions were collected and tested on SDS-PAGE (15%) for sufficient digestion and purity. The F(ab) fractions were concentrated by centrifugation, sterile filtrated and stored at -20°C until use.

2.2.1.5 Alexa Fluor 488 /Fluorescein (FITC) labeling

Affinity purified antibodies were labeled with Alexa Fluor 488/FITC in a fluorophore/protein-ratio of approx. 3:1. The purified antibody (4 mg) was dialyzed against coupling buffer o/n at 4°C. Alexa Fluor 488 NHS-ester was dissolved in anhydrous DMSO to a final concentration of 1 mg/ml. This solution was added to the antibody and left to incubate at for 2 h RT. The reaction was stopped by adding 100 µl of 1 M NH_4Cl. Alexa Fluor 488-labeled antibody was separated from the uncoupled fluorophore by gel filtration on a PD-10 column.

2.2.2 Mouse genotyping

2.2.2.1 Mouse genotyping using flow cytometry

FcR$\gamma^{-/-}$ mice were genotyped using flow cytometry. To determine the surface expression level of GPVI, mice were bled from the retro-orbital plexus to 50 µl in 300 µl heparin. 50 µl of the 1:20 diluted whole mouse blood were incubated with the FITC-conjugated anti-GPVI antibody JAQ1 in saturating concentrations for 15 min at RT and analyzed on a FACSCalibur (Becton Dickinson, Heidelberg, Germany).

2.2.2.2 Isolation of genomic DNA from mouse tissue

Mouse ear punching samples were dissolved in 500 µl DNA lysis buffer by o/n incubation at 56°C under shaking conditions (900 rpm). 500 µl phenol/chloroform was added and, after vigorous shaking, samples were centrifuged at 10,000 rpm for 10 min at RT. Approx. 450 µl supernatant were taken und transferred into a new tube containing 500 µl isopropanol. After vigorous shaking, samples were centrifuged at 14,000 rpm for 10 min at 4°C. The DNA pellet was then washed with 500 µl 70% ethanol and centrifuged again at 14,000 rpm for 10 min at 4°C. The DNA pellet was left to dry and finally resuspended in 70 µl TE-buffer. 1-2 µl DNA solution was used for a PCR reaction.

2.2.2.3 Mouse genotyping by PCR

Detection of the *Clec1b* floxed allele by PCR

Primers:

Clec1b_fw 5’ TTT CTG CCT CTC TGC CTT GC 3’

Clec1b_rev 5’ CGT CAT GAA CAG AAA ACT GAC G 3’

Pipetting scheme		PCR program		
genomic DNA	2 µl			
Taq-buffer (10x)	2 µl	95°C	5:00 min	
$MgCl_2$ (25mM)	1.2 µl	95°C	0:30 min	35x
dNTPs (10 mM)	0.4 µl	60°C	0:30 min	
Clec1b_fw	0.1 µl	72°C	1:00 min	
Clec1b_rev	0.1 µl	72°C	10:00 min	
Taq-Polymerase (5 U/µl)	0.125 µl	4°C	∞	
H_2O	14.075 µl			

Resulting band sizes:

wt: 172 bp

floxed allel: 333 bp

Detection of the *Syk* floxed allele by PCR

Primers:

Syk_flox_F 5’ GGT GCC TAC AGG TCT ACA GC 3’

Syk_flox_R 5’ AAC CTG GTA ATT TCA TAA CGC C 3’

Pipetting scheme		PCR program		
genomic DNA	1 µl			
Taq-buffer (10x)	2.5 µl	96°C	3:00 min	
$MgCl_2$ (25mM)	2.5 µl	94°C	0:30 min	35x
dNTPs (10 mM)	1 µl	56°C	0:30 min	
Syk_flox_F	1 µl	72°C	1:00 min	
Syk_flox_R	1 µl	72°C	10:00 min	
Taq-Polymerase (5 U/µl)	0.25 µl	4°C	∞	
H_2O	15.75 µl			

Resulting band sizes:

wt: 198 bp

floxed allel: 285 bp

Detection of the *Tln1* floxed allele by PCR

Primers:

Tln1_fw 5’ AAG CAG GAA CAA AAG TAG GTC TCC 3’

Tln1_rev 5’ GCA TCG TCT TCA CCA CAT TCC 3’

Pipetting scheme		PCR program		
genomic DNA	1 µl			
Taq-buffer (10x)	2.5 µl	95°C	4:00 min	
$MgCl_2$ (25mM)	2.5 µl	95°C	0:30 min	35x
dNTPs (10 mM)	1 µl	58°C	0:30 min	
Tln1_fw	0.5 µl	72°C	0:30 min	
Tln1_rev	0.5 µl	72°C	5:00 min	
Taq-Polymerase (5 U/µl)	0.5 µl	4°C	∞	
H_2O	16.5 µl			

Resulting band sizes:

wt: 657 bp

floxed allel: 779 bp

Detection of the *PF4-Cre* transgene by PCR

Primers:

PF4-Cre_fw 5’ CCC ATA CAG CAC ACC TTT 3’

PF4-Cre_rev 5’ TGC ACA GTC AGC AGG TT 3’

Pipetting scheme		PCR program		
genomic DNA	1 µl			
Taq-buffer (10x)	2.5 µl	95°C	5:00 min	
$MgCl_2$ (25mM)	2.5 µl	95°C	0:30 min	35x
dNTPs (10 mM)	1 µl	58°C	0:30 min	
PF4-Cre_fw (1:10)	1 µl	72°C	0:45 min	
PF4-Cre_rev (1:10)	1 µl	72°C	5:00 min	
Taq-Polymerase (5 U/µl)	0.25 µl	4°C	∞	
H_2O	15.75 µl			

Resulting band sizes:

wt: no PCR product

PF4-cre: 450 bp

Agarose gel electrophoresis

Agarose (final concentration 1.5%) was dissolved in 1x TAE buffer and heated in a microwave. When the temperature had decreased to approx. 60°C, 5 µl Midori green per 100 µl were added and the fluid was poured into a tray with a comb. After solidification of the gel, the tray was positioned in an electrophoresis chamber containing 1x TAE butter. PCR products were mixed with 6x sample loading buffer and loaded into the gel slots. For size-separation, DNA samples were run for approx. 30 min at 120-160 V.

2.2.3 Biochemistry

2.2.3.1 Western blotting

For Western blot analysis, washed platelets (2 x 10^6/ µl) were solubilized in lysis buffer (20 min on ice) and subsequently centrifuged at 14,000 rpm for 10 min at 4 °C. The supernatant is mixed with 4x NuPAGE LDS sample buffer (and β-mercaptoethanol for reducing conditions) and incubated for 5 min at 96°C. Samples were separated by sodium dodecyl sulfate polyacrylamide gel electrophoresis (SDS-PAGE; 12%) with a molecular weight marker and transferred onto a polyvinylidene difluoride membrane. To prevent non-specific antibody binding, membranes were blocked in 5% fat-free milk or 5% BSA dissolved in washing buffer for 2 h at RT or o/n at 4°C. Membranes were incubated with the required primary antibody (5 µg/ml) o/n with gentle shaking at 4°C. Afterwards, membranes were washed three times with washing buffer for 15 min at RT. Next, membranes were incubated with the appropriate HRP-labeled secondary antibodies for 1 h at RT. After three washing steps, proteins were visualized using ECL solution.

2.2.3.2 Immunoprecipitation

For immunoprecipitation of individual proteins, platelet lysates were precleared with Protein G Sepharose for 1 h at 4°C under rotating conditions. The respective antibody and prewashed Protein G Sepharose were added to the supernatant of the precleared platelet lysate and rotated for 2 h or o/n at 4°C. The sepharose pellet was washed in a 1:1 mixture of 2x lysis buffer and Ca^{2+}-free Tyrode's buffer, containing 0.2% IGEPAL and protease inhibitors. Finally, 4x NuPage LDS sample buffer was added and samples were incubated for 5 min at 96°C. Precipitated proteins were either used for immunization of rats or subjected to Western blotting.

2.2.3.3 Tyrosine phosphorylation assay

To study tyrosine phosphorylation, 0.7x10^6 platelets/µl were activated with rhodocytin or INU1 antibody under constant stirring conditions (1,000 rpm) at 37°C. Stimulation was stopped by the addition of an equal volume ice-cold lysis buffer after the indicated time points. For whole-cell tyrosine-phosphorylation, 4x NuPage LDS sample buffer and β-mercaptoethanol were added. Samples were incubated at 70°C for 10 min and separated by SDS-PAGE on 4-12% NuPage Bis-Tris gradient gels followed by transfer onto a PVDF membrane. Membranes were blocked for 1 h at RT in 5% BSA in washing buffer and then incubated with the primary anti-phosphotyrosine antibody 4G10 o/n at 4°C. Membranes were then washed 4x 15 min in washing buffer before incubation with secondary HRP-conjugated anti-mouse IgG antibody in washing buffer (1:2,000). Following extensive washing, proteins were visualized using ECL solution.

2.2.4 *In vitro* analysis of platelet function

2.2.4.1 Platelet preparation and washing

Mice were bled under isoflurane anesthesia from the retro-orbital plexus. 700 µl blood were collected in a reaction tube containing 300 µl heparin in TBS (20 U/ml, pH 7.3). Blood was centrifuged at 800 rpm for 5 min at RT. Supernatant and buffy coat were transferred into a new tube and centrifuged at 800 rpm for 6 min at RT to obtain platelet rich plasma (PRP). To prepare washed platelets, PRP was centrifuged at 2,800 rpm for 5 min at RT and the pellet was resuspended in 1 ml Ca^{2+}-free Tyrode's buffer containing apyrase (0.02 U/ml) and PGI_2 (0.1 µg/ml). After 10 min incubation at 37°C, the sample was centrifuged at 2,800 rpm for 5 min. After a second washing step, the platelet pellet was resuspended in the appropriate volume of Tyrode's buffer containing apyrase (0.02 U/ml) to obtain the desired platelet count (500,000 platelets/µl) and left to incubate for at least 30 min at 37°C before analysis.

2.2.4.2 Analysis of blood cells counts

To determine blood cell counts, 50 µl blood were drawn from the retro-orbital plexus of anesthetized mice using heparinized microcapillaries and collected into a tube containing 300 µl heparin in TBS (20 U/ml, pH 7.3). Blood cell counts and parameters were determined using a Sysmex KX-21N automated hematology analyzer (Sysmex Corporation, Kobe, Japan).

2.2.4.3 Flow cytometry

To determine platelet counts, 50 µl blood were collected from the retro-orbital plexus in heparin-containing tubes, diluted 1:20 with Ca^{2+}-free Tyrode's buffer and stained with anti-GPV-FITC and anti-αIIbβ3 PE (JON1-PE) antibodies for 15 min at RT. The reaction was stopped by addition of 500 µl PBS and samples were analyzed directly on a FACSCalibur instrument (BD Bioscience, Heidelberg, Germany).

For determination of basal glycoprotein expression levels, platelets ($1x10^6$) were stained with saturating amounts of fluorophore-conjugated antibodies for 10 min at RT. After stopping the reaction with 500 µl PBS, the samples were analyzed on a FACSCalibur.

As a positive control for maximal INU1-binding, washed platelets were incubated with the indicated antibody for 15 min at RT, washed with PBS and then stained with an anti-rat IgG-FITC antibody for 15 min at RT. All samples were analyzed on a FACSCalibur.

For platelet activation studies, washed blood was activated with agonists at the indicated concentrations for 15 min at RT in the presence of saturating amounts of fluorophore-conjugated monoclonal antibodies (phycoerythrin (PE)-coupled JON/A and FITC-coupled

anti-P-selectin antibody). After stopping the reaction with 500 µl PBS, the samples were analyzed on a FACSCalibur. For all stainings the following settings were used:

Detectors/Amps:

Parameter	Detector	Voltage
P1	FSC	E01
P2	SSC	380
P3	Fl1	650
P4	Fl2	580
P5	Fl3	150

Threshold:

Value	Parameter
253	FSC-H
52	SSC-H
52	Fl1-H
52	Fl2-H
52	Fl3-H

Compensation:

Fl1	2.4% of Fl2
Fl2	7.0% of Fl1
Fl2	0% of Fl3
Fl3	0% of Fl2

2.2.4.4 Aggregometry

To determine platelet aggregation, light transmission was measured using washed platelets in Tyrode's buffer without Ca^{2+} adjusted to a concentration of $0.5x10^6$ platelets/µl. Alternatively, heparinized PRP was diluted into Tyrode-HEPES buffer containing 2 mM Ca^{2+}. Agonists were added at the indicated concentrations to the continuously stirring (1,000 rpm) platelet suspension. Light transmission was recorded on a Fibrintimer 4-channel aggregometer (APACT Laborgeräte und Analysensysteme) for 10 min and expressed in arbitrary units with buffer representing 100% transmission. For platelet activation using thrombin, washed platelets were diluted in Tyrode's buffer containing 2 mM Ca^{2+}, for all other agonists platelets were diluted in the same buffer in the presence of 70 µg/ml human fibrinogen.

2.2.4.5 Immunofluorescence staining

Washed platelets ($0.3x10^6$ platelets/ µl) were left untreated or were incubated for 15 min at 37°C either with DMSO, PP2 or PP3 (25 µM). CLEC-2 internalization was induced by incubation with 20 µg/ml fluorescently-labeled INU1 antibody (INU1-Alexa Fluor488, referred to as INU1-F488) for 15 min at 37°C. Non-immune rat IgG antibodies (Emfret Analytics) served as a control. Next, 100 µl of platelets were fixed on poly-L-lysine (PLL, Sigma-Aldrich)-coated coverslips for 30 min, and, when indicated, permeabilized in PHEM buffer supplemented with 4% paraformaldehyde (PFA) and 1% IGEPAL® CA-630. Unspecific binding sites were blocked using 5% BSA and 0.1% goat serum in PBS and samples were subsequently stained with an anti-rat IgG-Cy3 antibody under permeabilizing or non-permeabilizing conditions. Slides were then incubated with phalloidin-Atto647N (referred to as PhalF647) diluted in permeabilizing buffer and mounted with Fluoroshield (Sigma-Aldrich). Samples were visualized using a Leica TCS SP5 confocal microscope.

2.2.4.6 Platelet adhesionto vWF under flow condition

To study platelet binding to vWF under flow conditions, coverslips were coated with human anti-human vWF (1:500, DAKO) antibody at 37°C o/n, washed with PBS, incubated with 100 µl murine plasma obtained from control mice and blocked for 1 h with 1% BSA in H_2O. Blood (700 µl) was collected into 300 µl heparin (20 U/ml in TBS, pH 7.3). Whole blood was diluted 2:1 in Tyrode's buffer containing Ca^{2+} and filled into a 1 ml syringe. Transparent flow chambers with a slit depth of 50 µm, equipped with the coated coverslips, were connected to a syringe that was filled with diluted whole blood. Perfusion was performed using a pulse-free pump under high shear stress equivalent to a wall shear rate of 1,700 s^{-1} (4 min). Adhesion of platelets to bound vWF started 90 sec after perfusion of the slide. Thereafter, coverslips were washed by a 4 min perfusion with Tyrode's buffer at the same shear rate and phase-contrast images were recorded from at least five different microscopic fields (40x objective). Image analysis was performed off-line using MetaVue® software (40x objective).

2.2.4.7 Platelet spreading on vWF

Glass coverslips were coated with a polyclonal rabbit anti-human vWF antibody (1:500, DAKO) for 2 h at 37°C or o/n at 4°C under humid conditions. The coverslips were blocked with 1% BSA in PBS for 1 h at RT. Subsequently the slides were incubated with heparin-plasma for 2 h at RT. Washed platelets at $0.3x10^6$ platelets/µl were diluted 1:2.3 in Tyrode's with Ca^{2+}, incubated with integrilin (40 µg/ml) and botrocetin (5 µg/ml) and were allowed to adhere on the prepared coverslips for 5, 15 or 30 min at RT. Samples were fixed with 4% PFA for 15 min and image analysis was performed off-line using MetaVue® software (100x objective).

2.2.4.8 Platelet spreading on fibrinogen

Glass coverslips were coated with 100 µg human fibrinogen (diluted in PBS) o/n at 4°C under humid conditions. Subsequently, they were blocked with 2% BSA for 2 h at RT. The coverslips were rinsed with Tyrodes's buffer and washed platelets at $0.3x10^6$ platelets/µl were diluted 1:2.3 in Tyrode's with Ca^{2+} were added and incubated at RT for the indicated time periods. Samples were fixed with 4% PFA for 15 min and platelet were visualized with a Zeiss Axiovert 200 inverted microscope (100x objective) using differential interference contrast (DIC) microscopy. Representative images were taken and evaluated according to different platelet spreading stages.

2.2.4.9 Clot retraction

For clot retraction studies, platelets were adjusted to a concentration of $3x10^6$ platelets/µl in platelet poor plasma (PPP). 250 µl of the platelet suspension was mixed with 1.5 µl erythrocyte suspension (to contrast the clot), obtained during platelet isolation from whole

blood, and 20 mM $CaCl_2$. Clotting was induced by addition of high thrombin concentrations (3 U/ml). Subsequent clot retraction was monitored at 37°C under non-stirring conditions and recorded with a digital camera over time.

2.2.4.10 Determination of aPTT and PT

To determine the activated partial thromboplastin time (aPTT) and prothrombin time (PT), mouse plasma was obtained from citrated whole blood by centrifugation at 2,800 rpm for 5 min at RT. The assays were performed in the central laboratory at the University hospital of Würzburg in collaboration with Dr. med. Karin Sauer.

2.2.4.11 Light sheet fluorescence microscopy (LSFM)

Male NMRi mice were anesthetized by intraperitoneal injection of medetomidine 0.5 µg/g, midazolam 5 µg/g and fentanyl 0.05 µg/g body weight and injected with 50 µg of INU1 F(ab). Platelets were antibody stained with an anti-GPIX Alexa Fluor 647 antibody (0.4 µg per gram body weight). After 15 min upon INU1 F(ab) injection, the mice were transcardially perfused with ice-cold PBS to wash out the blood and ice-cold 4% PFA (pH 7.2) to fix the tissues. The brains were harvested and stored in 4% PFA for at least 30 min. The samples were then washed in PBS, followed by dehydration in a graded ethanol series (30%, 50%, 70%, 80%, 90% and 100% for 2 h each) at room temperature. After the samples were rinsed in 100% n-hexane for 2 h, the n-hexane was replaced stepwise by a clearing solution consisting of 1 part benzyl alcohol in 2 parts benzyl benzoate (BABB). Air exposure was strictly avoided at this step. Tissue specimens became optically transparent and suitable for the LSFM imaging after incubation in the clearing solution for at least 2 h at room temperature.

After sample fixation and clearing, the specimen was affixed with Pattex acrylamide glue to a home-built glass rod and placed in a homebuilt cover glass chamber filled with clearing solution. Images were acquired with a commercial inverted microscope (Axiovert 200, Zeiss) equipped with a 5x objective. The sample was illuminated from one side by various laser sources: 405-nm diode laser (56ICS025, CVI Melles Griot), 473-nm DPSS laser (MBL-473 100 mW, CNI), 532-nm DPSS laser (MGL-W532 500 mW, CNI), and 639-nm diode laser (Cube 640-40, Coherent). The fluorescence emission light was filtered using a motorized filter wheel (Standa) according to the excitation wavelength: Alexa Fluor 488 (Invitrogen) 488 nm HQ525/50. Multicolor stacks were acquired by imaging each plane sequentially by each wavelength and emission filter combination. Stacks were taken in increments of 5 µm. Resulting multicolor stacks were processed with ImageJ (NIH). Subsequently, individual images and videos were prepared using the 3D image processing software Volocity (PerkinElmer).

2.2.5 *In vivo* analysis of platelet function

2.2.5.1 Determination of platelet life span

Mice were intravenously injected with a Dylight-488 conjugated anti-GPIX antibody (0.5 µg/g body weight). 1 h after injection (day 0) as well as on the 5 consecutive days, 50 µl blood were collected and the percentage of GPIX-positive platelets was determined by flow cytometry.

2.2.5.2 Determination of platelet count recovery

Mice were intravenously injected with an anti-GPIbα antibody (2 µg/g body weight) to induce immune thrombocytopenia. Platelet counts were measured at 1, 72, 96, 120, 144, 168 and 240 h after injection by flow cytometry.

2.2.5.3 Detection of INU1 plasma levels after injection

Mice were injected with 100 µg biotinylated INU1. After 1, 24, 72 and 120 h 100 µl blood was collected and plasma was obtained by centrifugation at 2,800 rpm for 5 min at RT. To detect free INU1 in these plasma samples ELISA was performed. Nunc MaxiSorp™ plates were coated with 50 µl of 10 µg/ml anti-rat IgG antibodies o/n. The plates were washed three times with PBS-Tween (PBS-T) and blocked with 10% fat-free milk in PBS for 1 h at RT. After one washing step, 50 µl of the obtained plasma were transferred to the wells and incubated for 2 h at RT under slight agitation. After five washing steps, plates were incubated with horseradish peroxidase-conjugated streptavidin (1:3,000 in 1% fat-free milk in PBS-T, 50 µl/ well) for 45 min at RT. After five washing steps, plates were developed using 3,3,5,5-tetramethylbenzidine (TMB). The reaction was stopped by addition of 2 M H_2SO_4 (50 µl/ well) and absorbance at 450 nm and 620 nm (background) was measured with a Multiscan Ascent Plate Reader (Thermo Scientific, Braunschweig, Germany).

2.2.5.4 Intravital microscopy of thrombus formation in $FeCl_3$-injured mesenteric arterioles

Mice (4-5 weeks of age) were anesthetized and the mesentery was exteriorized through a midline abdominal incision. Arterioles (35-60 µm diameter) were visualized with a Zeiss Axiovert 200 inverted microscope (10x objective) equipped with a 100-W HBO fluorescent lamp source and a CoolSNAP-EZ camera (Visitron, Munich, Germany). Injury was induced by topic application of a 3 mm^2 filter paper saturated with $FeCl_3$ (20%). Adhesion and aggregation of fluorescently labeled platelets (Dylight-488 conjugated anti-GPIX IgG derivative) in arterioles was monitored for 40 min or until the complete occlusion occurred (blood flow stopped for >1 min). Digital images were recorded and analyzed off-line using MetaVue® software.

2.2.5.5 Tail-bleeding time assay

Mice were anesthetized by intraperitoneal injection of medetomidine 0.5 µg/g, midazolam 5 µg/g and fentanyl 0.05 µg/g body weight and a 1 mm segment of the tail tip was ablated with a scalpel. Tail bleeding was monitored by gently absorbing the drop of blood with a filter paper in 20 s intervals without interfering with the wound site. When no blood was observed on the paper, bleeding was determined to have ceased. The experiment was manually stopped after 20 min by cauterization.
Alternatively, tail bleeding times were determined in 37°C warm saline (0.9% NaCl). Upon amputation, the tail tip was placed in a plastic tube containing 4 ml saline, bleeding was observed and determined to have ceased when stopped for >1 min. Lost blood volume was determined via weight against a saline filled reference tube and increased weight of the tube was multiplied by the density of blood.

2.2.5.6 Whole-body imaging of mice using a *in vivo* imaging system (IVIS)

Mice were injected with 8 µg anti-GPIX-Alexa750 antibody to label circulating platelets. After 4 hours, mice were anesthetized with medetomidine 0.5 µg/g, midazolam 5 µg/g and fentanyl 0.05 µg/g body weight and the abdominal and thoracic region was shaved with an electric clipper. Subsequently, mice were injected with the indicated antibodies and *in vivo* imaging was performed using an *in vivo* imaging system (IVIS Spectrum, Perking Elmer) at 800 nm (emission filter).

2.2.5.7 Two Photon-intravital microscopy (2P-IVM) of the brain

Mice were anesthetized and a 1 cm incision was made along the midline to expose the frontoparietal skull. The bone was thinned using a Dremel's rotatory tool and afterwards the skin incision was sewed. After 24 h of resting, the mouse was anesthetized and a jugular vein catheter was laid to inject antibodies during the imaging. Subsequently, the mouse was placed on a customized metal stage equipped with a stereotactic holder to immobilize its head. Brain vasculature was visualized by injection of tetramethylrhodamine dextran (8 µg/g body weight, 2MDa). Platelets were antibody stained (0.4 µg per gram body weight) with anti-GPIX Alexa Fluor 488. Images were acquired with a fluorescence microscope equipped with a 20x water objective with a numerical aperture of 0.95 and a TriM Scope II multiphoton system (LaVision BioTec), controlled by ImSpector Pro-V380 software (LaVision BioTec). Emission was detected with HQ535/50-nm and ET605/70-nm filters. A tunable broad-band Ti:Sa laser (Chameleon, Coherent) was used at 760 nm to capture Alexa Fluor488 and rhodamine dextran fluorescence. ImageJ software (NIH) was used to generate movies.

2.2.6 Megakaryocyte (MK) analysis

2.2.6.1 Differentiation of fetal liver cell-derived MKs

The livers of 13.5 to 14.5 day-old mouse embryos were isolated from time-mated female mice and a single cell suspension was cultured for 72 h in IMDM medium containing 10% fetal calf serum, 1% penicillin/streptomycin and 50 ng/ml recombinant thrombopoietin. The mature MKs were enriched on day 3 of culturing using a BSA density gradient (3% and 1.5% BSA in PBS). These MKs were treated with INU1-F488 for the indicated time points. Subsequently, they were spun onto glass slides, fixed and stained with an anti-rat IgG-Cy3 antibody under permeabilizing or non-permeabilizing conditions. After intensive washing the samples were stained with PhalF647 diluted in permeabilizing buffer. Nuclei were stained with DAPI. Samples were visualized using a Leica TCS SP5 confocal microscope.

2.2.7 Transmission electron microscopy (TEM)

2.2.7.1 TEM of platelets in suspension

PRP was fixed by addition of an equal amount of cacodylate buffer containing 5% glutaraldehyde (GLA) for 10 min at 37°C without stirring. For complete fixation, samples were incubated for 1 h at RT and afterwards at 4°C until further processing. Next, samples were washed three times for 5 min by addition of 1 ml cacodylate buffer and subsequently centrifugation for 5 min at 1,500 g (37°C). A 2% low melting agarose solution in cacodylate buffer was prepared and kept at 45°C. After the final washing step, platelets were resuspended carefully in 1 ml agarose solution and immediately centrifuged for 5 min at 14,000 rpm (37°C). All, except 100 µl agarose solution, was discarded and samples were incubated on ice for 10 min. The hardened agarose pellets were cut out of the tubes and then cut into approx. 1 mm^2 pieces and stored in cacodylate buffer. Samples were fixed in cacodylate buffer containing 1% OsO4 for 45 min - 1 h at RT, washed twice with ddH_2O and incubated for 60 min at 4°C in 2% uranylacetate in ddH2O. After three washing steps with ddH2O, samples were dehydrated in 70% (4x5 min), 95% (3x15 min) and 100% (3x15 min) ethanol. Next, samples were incubated first in 100% propylenoxyde (2x10 min) and then in a 1:1 mixture propylenoxyde/epon (1x60 min) under rotating conditions. After two further incubations in epon at RT (first step: over night, second step: 2-3 h), samples were embedded in gelatine capsules and left to dry at 60°C for 48 h. 50 nm thin sections were cut using an ultra microtom (Leica Ultracut UCT), contrasted and analyzed. Sections were visualized with an EM900 electron microscope (Zeiss, Oberkochen, Germany). Negatives were digitalized by scanning and processed with Adobe Photoshop.

2.2.7.2 TEM of brain sections

Mice were injected with INU1 F(ab) (50 µg), anesthetized and perfused for 3 min with PBS followed by 8 min with fixation buffer (2% GLA, 1% PFA in phosphate buffer (PB)). Subsequently, skulls containing the brains were dissected, immersed in fixation buffer and incubated o/n at RT. Afterwards, the skulls containing the brains were washed in PB and transferred in SØrensen buffer (pH 6.98) containing 5% EDTA and incubated o/n at RT. The buffer was replaced on five consecutive days. Thereafter, the organs were processed for TEM as described above. Sections were inspected with an LEO912AB electron microscope (LEO, Oberkochen, Germany) at the Institute of Anatomy and Cell Biology, University of Würzburg, Germany.

2.2.8 Histology

2.2.8.1 Preparation of paraffin sections

Tissues from adult mice were dissected, washed in PBS and fixed o/n in PBS containing 4% PFA. Afterwards, organs were washed three times with PBS, dehydrated and embedded in paraffin. Organs were cut using a Microm Cool Cut microtome (Thermo Scientific, Braunschweig, Germany) to prepare 5 µm thin sections.

2.2.8.2 Hematoxylin/ eosin staining of paraffin sections

Sections were deparaffinated by two incubations in xylol (3 min each). Rehydration was carried out using decreasing ethanol concentrations (100, 96, 90, 80 and 70%) with two incubation steps in each solution and final 2 min incubation in deionized water. Next, sections were stained for 30 s with hematoxylin, followed by a 10 min washing step using running tab water and were stained for 2 min with 0.05% Eosin G. The sections were washed shortly and dehydration was carried out using the same ethanol concentrations and incubation times as described above in reversed order. Finally, sections were incubated twice in xylol each for 3 min, dried and mounted using Eukitt mounting medium. Samples were analyzed using a Leica DHI 4000B inverse microscope equipped with a Leica digital camera.

2.2.8.3 GPIb-staining of paraffin sections

Sections of paraffin-embedded samples were incubated for 10 min at 97°C in EDTA buffer (1 mM EDTA, pH 8.0) for antigen retrieval. After blocking of endogenous HRP using 3% H_2O_2 in PBS and unspecific epitopes with 5% BSA and non-immunogenic rat IgG, sections were probed with HRP-conjugated antibodies directed against GPIbα at 4°C o/n. Detection was performed with 3-amino-9-ehylcarbazole (AEC) substrate, nuclei were counterstained

with hematoxylin and sections were mounted with Aquatex. The sections were analyzed using a Leica DHI 400B inverse microscope equipped with a Leica digital camera.

2.2.8.4 Immunofluorescence staining of the bone marrow

Male mice were injected with INU1 (100 µg) and femora were removed, fixed with 4% PFA and 5 mM sucrose, transferred into 10% sucrose in PBS and dehydrated using a graded sucrose series. Subsequently, the samples were embedded in Cryo-Gel and frozen. 7 µm thick cryosections were generated using a CryoJane tape transfer system (Leica Biosystems). Unspecific binding sites were blocked with 5% BSA and 0.1% goat serum in PBS and samples were subsequently stained with an anti-rat IgG-Cy3 antibody. After intensive washing, the sections were probed with an anti-GPIb-AlexaF488 antibody (referred to as GPIb-F488) to specifically label platelets and MKs and an anti-CD105-AlexaF647 antibody (referred to as CD105-F647) to stain the endothelium. Nuclei were stained with DAPI. Samples were visualized using a Leica TCS SP5 confocal microscope.

2.2.9 Data analysis

The results presented in this thesis are mean ± SD from at least three independent experiments per group, if not otherwise stated. Differences between the groups were statistically analyzed using the Mann-Whitney-U-test. *p*-values <0.05 were considered as statistically significant (*), $p < 0.01$ = ** and $p < 0.001$ = ***.

3 RESULTS

3.1 CLEC-2-deficient animals are protected from occlusive arterial thrombus formation

3.1.1 MK/ platelet CLEC-2 is essential for lymphatic development

Since constitutive CLEC-2-deficient mice die perinatally, *Clec-2*$^{fl/fl,\ PF4\text{-}Cre}$ (further referred to as *Clec2*$^{-/-}$) mice, specifically lacking CLEC-2 in MKs and platelets, were used for all analyses.[46] As previously described, *Clec2*$^{-/-}$ mice were born at normal Mendelian ratios, although embryos showed edema formation and a defective lymphatic development (Figure 6 B).[46] Adult mice displayed a defective blood-lymph vessel separation, which came evident by blood-filled lymphatic vessels in the mesentery (Figure 10 A). To monitor the health status of these animals and scan for possible signs of inflammatory diseases, blood cell counts were analyzed. The white blood cell count, which may indicate infections, was unaltered in the CLEC-2-deficient animals as compared to wild type (*Wt)* controls (Figure 10 B). Similarly, blood loss could result in changes in red blood cell numbers, the amount of hemoglobin or of the hematocrit, which represents the total volume percentage of all corpuscular components in the blood. However, all determined parameters were within the normal range in *Clec2*$^{-/-}$ mice indicating that the alterations in the lymphatic system did not have a major impact on blood cell distribution (Figure 10 B).

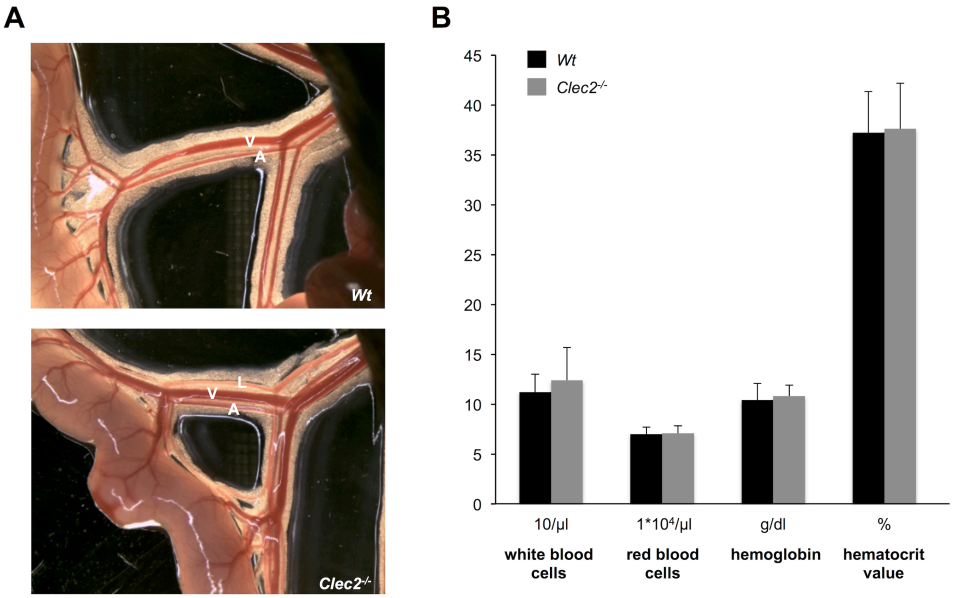

Figure 10. Analysis of MK/platelet-specific CLEC-2-deficient mice. (A) Representative images of the intestine are shown. L= lymphatic vessel, A= arteriole, V= vein. (B) To analyze blood cell counts, mice were bled and the blood cell counts and parameters were determined using a Sysmex KX-21N automated hematology analyzer. (*n* = 4, representative of at least three independent measurements)

3.1.2 *Clec2*$^{-/-}$ mice exhibit a mild thrombocytopenia

Since the blood-lymphatic vessel separation defect in *Clec2*$^{-/-}$ mice might influence the hemostatic system, platelet counts were determined. CLEC-2-deficient mice showed a mild reduction of the platelet count to approx. 70% of control mice (Figure 11 A) confirming previous results.[46] A reduction of the platelet count could have several possible reasons. For example, continuous and rapid clearance of non-functional, structurally altered or hyperactive platelets can lead to a sustained thrombocytopenia. Hence, the platelet life span of *Clec2*$^{-/-}$ and *Wt* platelets was determined *in vivo*. Circulating platelets were labeled by injection of a fluorescence-tagged anti-GPIX antibody and the labeled platelet population was monitored over time using flow cytometry. Directly after antibody injection, approx. 90% of the circulating platelets were labeled in both *Wt* and CLEC-2-deficient animals (Figure 11 B). The amount of labeled platelets decreased over time with comparable kinetics in both *Wt* and *Clec2*$^{-/-}$ mice, suggesting that the platelet turnover was unaltered in mice lacking CLEC-2.

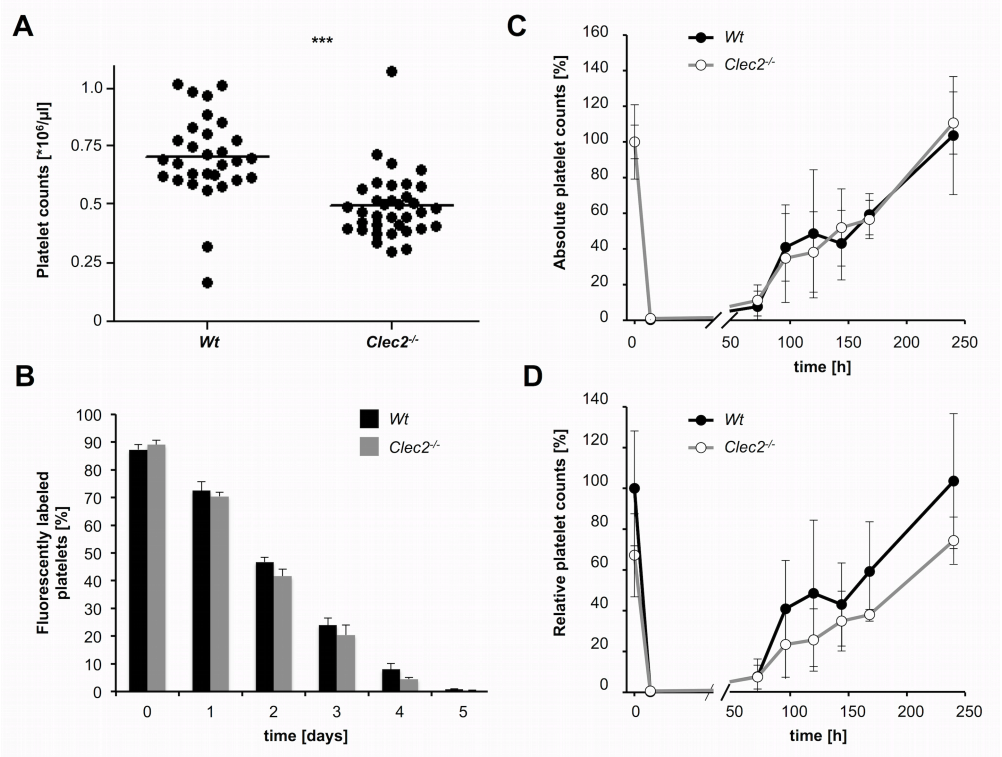

Figure 11. Platelet analysis of *Clec2*$^{-/-}$ mice. (A) Platelet count was determined by flow cytometric analysis. ***, P < 0.001. (B) Circulating platelets were labeled with a fluorescent anti-GPIX antibody and the labeled platelets in *Wt* and *Clec2*$^{-/-}$ mice were monitored over time using flow cytometry. (C,D) To determine platelet count recovery, mice were injected with an anti-GPIbα antibody to deplete all circulating platelets. The subsequent increase in platelet count was measured by flow cytometry.

Defects in thrombopoiesis could also result in a persistent thrombocytopenia. To investigate this, platelet count recovery was monitored after antibody-induced platelet depletion. Complement-mediated immune thrombocytopenia was induced by an intravenous injection of an anti-GPIbα antibody into *Wt* and *Clec2*$^{-/-}$ mice and platelet counts were determined by

flow cytometry. Platelet counts in *Wt* as well as CLEC-2-deficient mice were close to zero after 1 h and recovered to starting values with the same kinetics (Figure 11 C). The relative values of the kinetics revealed that *Clec2*$^{-/-}$ mice recovered their platelet counts only to approx. 70% of the *Wt* animals (Figure 11 D). This result indicates that platelet production is unaltered in mice lacking CLEC-2. Further analyses are necessary to clarify whether the defects in the lymphangiogenesis and the defective lymphatic integrity are responsible for the mild thrombocytopenia observed in *Clec2*$^{-/-}$ mice.

3.1.3 CLEC-2-deficient platelets show an abolished activation response to rhodocytin

To further investigate the effect of CLEC-2 deficiency on platelets, surface receptor prevalence was determined by flow cytometry. As expected, CLEC-2 was absent on platelets of *Clec2*$^{-/-}$ mice, whereas all other tested surface receptors were expressed at normal levels (Table1).

	Wt	*Clec-2*$^{-/-}$	
CLEC-2	143 ± 11	6 ± 0	***
GPVI	49 ± 2	45 ± 7	n.s.
GPIb	390 ± 26	377 ± 13	n.s.
GPIX	439 ± 14	437± 5	n.s.
GPV	318 ± 12	324 ± 6	n.s.
CD9	1392 ± 57	1377 ± 82	n.s.
αIIbβ3	488 ± 33	478 ± 32	n.s.
α2	50 ± 2	50 ± 2	n.s.
β1	153 ± 7	149 ± 2	n.s.
platelet size	289 ± 19	305 ± 12	n.s.

Table 1. Platelet size and glycoprotein expression in *Clec2*$^{-/-}$ mice. Flow cytometric analysis of surface protein expression. Platelets were stained for 15 min at RT with the indicated fluorophore-labeled antibodies and analyzed by flow cytometry. Platelet size is given as mean FSC and was determined by FSC characteristics. Results are mean fluorescence intensities (MFI) ± SD (*n* = 4, representative of at least three independent measurements). ***, P < 0.001; n.s., not significant. (Bender *et al., Arterioscler Thromb Vasc Biol* 2013)[138]

To study the functional consequences of the CLEC-2 deficiency for platelet activation, agonist-induced activation of the major platelet integrin, αIIbβ3, and degranulation-dependent P-selectin exposure were measured by flow cytometry. The phycoerythrin (PE)-conjugated JON/A antibody specifically binds the activated form of integrin αIIbβ3.[121] Since P-selectin is stored in platelet α-granules and is not present on the platelet surface under resting conditions, detection of P-selectin on the platelet surface after agonist-induced activation served as measure for degranulation. RC-induced platelet activation was abolished in the mutant platelets, whereas responses to all other tested agonists, such as thrombin, ADP/U46619 (stable TxA_2 analogue), CRP and convulxin (CVX, a snake venom protein targeting GPVI), were unaltered (Figure 12).

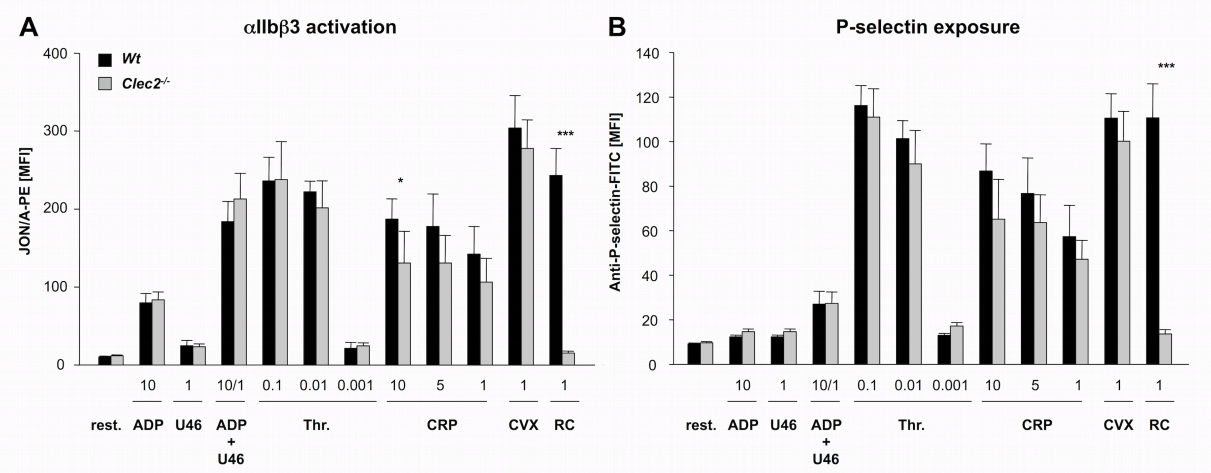

Figure 12. Integrin αIIbβ3 activation and α-granule release in *Clec2*$^{-/-}$ platelets. Flow cytometric analysis of (A) integrin αIIbβ3 activation and (B) degranulation-dependent P-selectin exposure on platelets. Washed blood was incubated with the indicated agonists for 15 min at RT and analyzed on a FACSCalibur. Results are mean ± SD (*n* = 5 mice per group, representative of three individual experiments). *, P < 0.05; ***, P < 0.001. ADP [µM]; U46619 (U46): [µM]; thrombin (Thr.): [U/ml]; collagen-related protein (CRP): [µg/ml]; convulxin (CVX): [µg/ml]; rhodocytin (RC): [µg/ml]. (Bender *et al., Arterioscler Thromb Vasc Biol* 2013)[138]

Previous studies revealed that CLEC-2 might play a role in platelet aggregate stability.[17] To test the effect of the CLEC-2 deficiency on platelet aggregate formation *in vitro*, washed platelets were stimulated with various agonists in the presence of 2 mM extracellular Ca^{2+} and light transmission traces were recorded to follow platelet aggregation. These *ex vivo* aggregation studies corroborate the results found in flow cytometry. Even at high concentrations of RC neither shape change nor aggregation could be observed for the CLEC-2-deficient platelets. However, *Clec2*$^{-/-}$ platelets aggregated normally in response to GPCR-specific agonists (ADP, U46619, thrombin) and GPVI agonists (CRP, collagen) (Figure 13). These results indicated that CLEC-2 deficiency does not affect thrombus formation or stability under conditions of standard aggregometry.

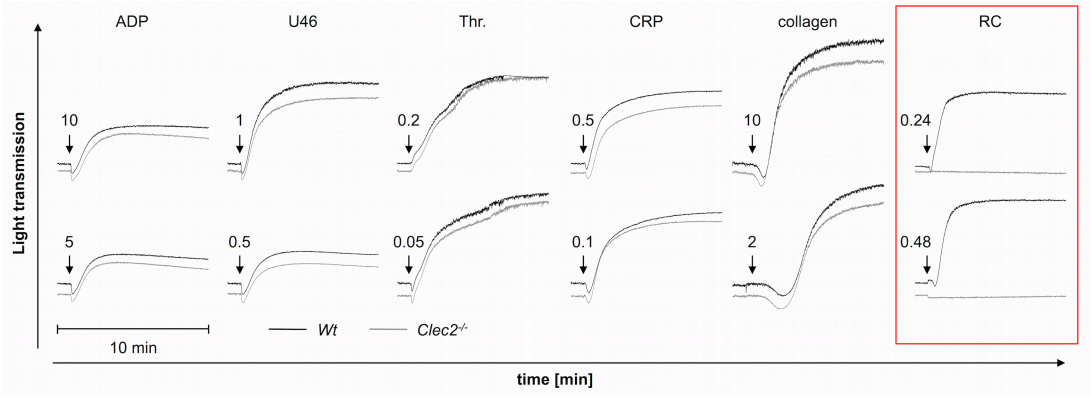

Figure 13. Abolished RC-induced aggregation in *Clec2*$^{-/-}$ platelets. Washed platelets were stimulated with the indicated agonists and light transmission was recorded in an aggregometer. Representative aggregation traces for *Wt* (black line) and *Clec2*$^{-/-}$ platelets (grey line) of at least 3 independent measurements were shown. ADP [µM]; U46619 (U46): [µM]; thrombin (thr.): [U/ml]; CRP: [µg/ml]; collagen: [µg/ml]; rhodocytin (RC): [µg/ml].

During aggregate formation, platelets require inside-out as well as outside-in activation of integrins to enable interaction with their ligands. Upon ligand binding, the αIIbβ3 integrin together with the cytoskeleton mediates clot retraction. Through the process of clot retraction platelets generate forces that contract the fibrin mesh, decrease the clot size and pull the edges of damaged tissue together to form a mechanically stable clot and to accelerate wound healing.[139] To study whether loss of CLEC-2 alters clot retraction, clot formation was induced in PRP of *Wt* and *Clec2*$^{-/-}$ mice by the addition of thrombin (5 U/ml) in the presence of 20 mM Ca^{2+} and clot retraction was monitored over time. Clot retraction started as early as 30 min after the start of the experiment and progressed to its maximum at 4 hours (Figure 14). The excess serum extruded during clot retraction was 87 ± 10.9 % for *Wt* and 92.4 ± 6.2 % for *Clec2*$^{-/-}$ of the initial PRP volume. These data show that CLEC-2 has no essential role in integrin-dependent clot retraction.

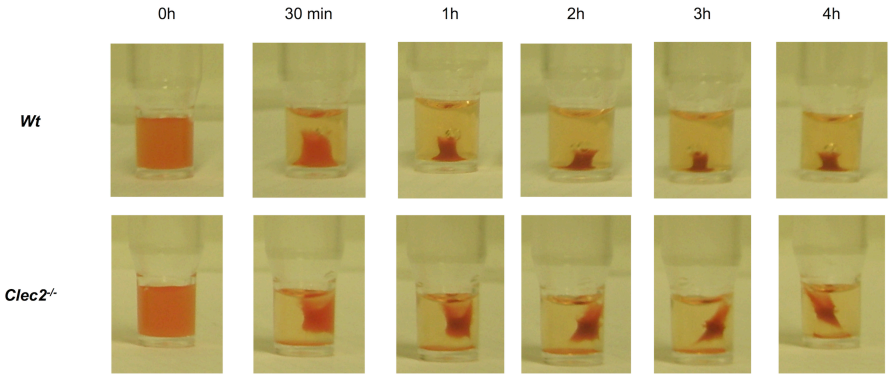

Figure 14. Unaltered integrin outside-in signaling in *Clec-2*$^{-/-}$ platelets. Clot retraction of *Wt* and CLEC-2-deficient PRP upon activation with 5 U/ml thrombin in the presence of 20 mM $CaCl_2$ was tested. Representative pictures were taken at the indicated time points.

3.1.4 CLEC-2 deficiency results in defective arterial thrombus formation and only a moderate increase in tail bleeding times

To study thrombus formation *in vivo*, mice were subjected to a model of arterial thrombosis, mesenteric arterioles were injured chemically by topical application of 20% ferric-chloride ($FeCl_3$) and subsequently thrombus formation was monitored by intravital fluorescence microscopy. The experiments were performed in collaboration with Ina Hagedorn in our laboratory. We have previously shown that injection of the anti-CLEC-2 antibody INU1 results in a depletion of CLEC-2 from circulating platelets.[17] Such CLEC-2-depleted mice display normal small aggregate formation in $FeCl_3$-injured mesenteric arterioles, but were in most cases unable to form fully occlusive thrombi.[17]

The time to beginning of thrombus formation, characterized by adhesion and accumulation of fluorescently labeled platelets, was found to be only slightly, but not significantly, delayed in

Clec2$^{-/-}$ mice compared to *Wt* animals (Figure 15 A). Full vessel occlusion was delayed or absent in most animals (Figure 15). These results indicated that immunodepletion and genetic loss of platelet CLEC-2 results in a comparable protection from occlusive thrombus formation *in vivo*.

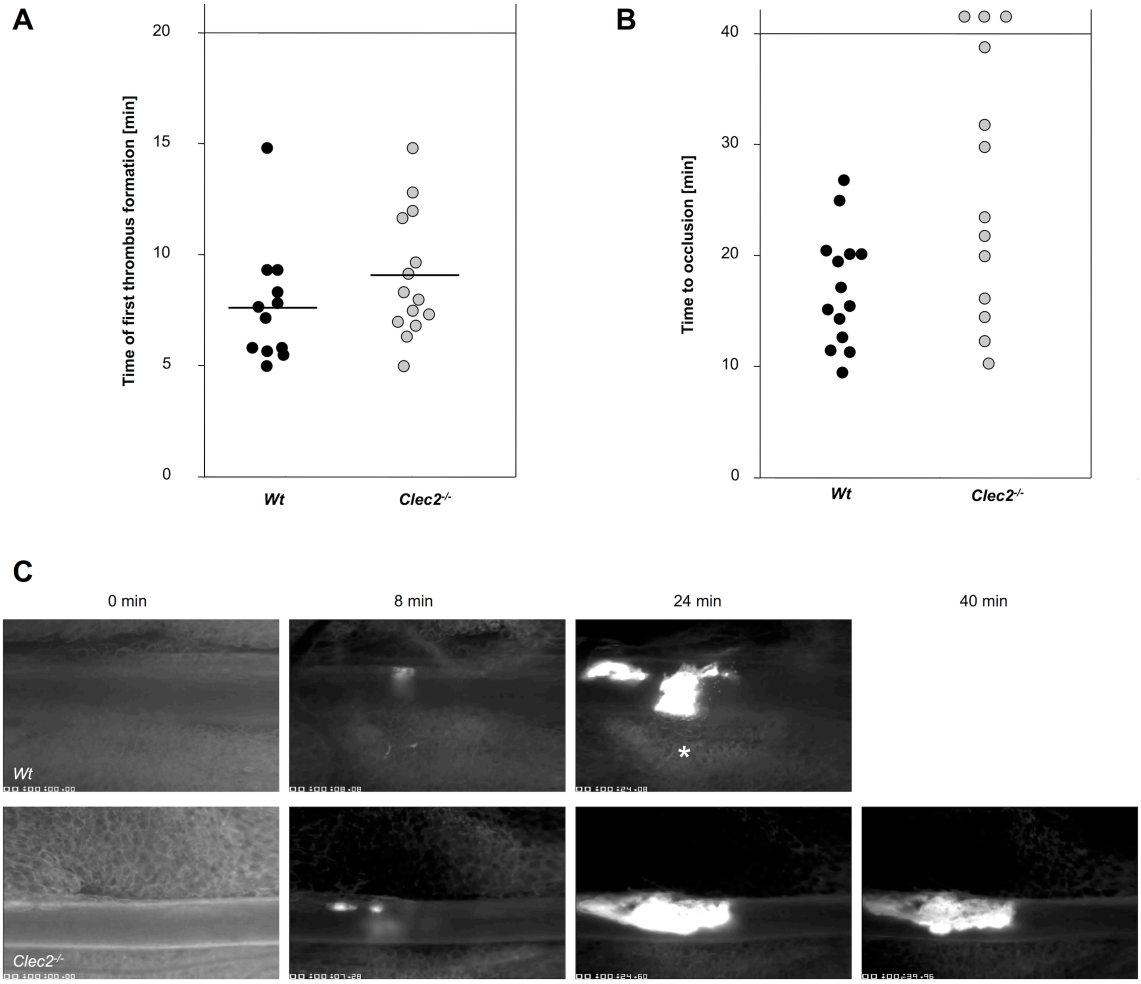

Figure 15. Defective arterial thrombus formation in *Clec2*$^{-/-}$ mice. Small mesenteric arterioles were injured using $FeCl_3$ and thrombus formation was analyzed using intravital fluorescence microscopy. (A) Time to first thrombus formation and (B) time to stable vessel occlusion are shown. Horizontal lines indicate mean values. Each symbol represents one arteriole. (C) Representative pictures are shown of the indicated time points. Asterisk indicates occlusion of the vessel. (Bender *et al., Arterioscler Thromb Vasc Biol* 2013)[138]

To investigate the consequences of CLEC-2 deficiency on hemostasis, tail-bleeding times were assessed in two different models. In the first model, a 1 mm segment from the tail tip was cut and the blood was gently absorbed with a filter paper without making contact to the wound site. We have previously shown that immunodepletion of CLEC-2 results in variable tail bleeding times.[17] The same moderately increased bleeding times could be observed in *Clec2*$^{-/-}$ mice (Figure 16 A). In addition, a second hemostatic assay was performed, which monitors the time to cessation of bleeding without using filter paper. Thereby, the cut tail tip was immersed in 37°C warm saline which allows to continuously monitoring of the blood

loss. In this model, CLEC-2-deficient mice had unaltered tail-bleeding times compared to *Wt* control (Figure 16 B). Albeit a mild prolongation of bleeding times was observed, these results show that the loss of CLEC-2 has no major impact on hemostasis.

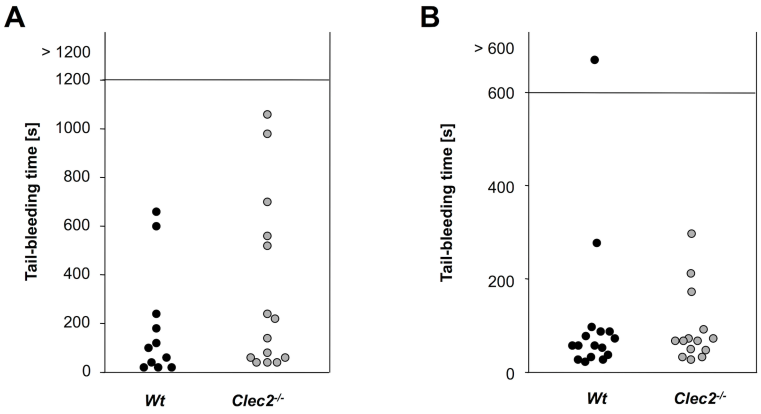

Figure 16. Mildly prolonged tail bleeding times in *Clec2*$^{-/-}$ mice. (A) A 1 mm segment from the tail tips was cut with a scalpel and (A) blood was gently absorbed with a filter paper in 20 s intervals or (B) the tail tips were immersed in 37°C warm saline. Time until bleeding has ceased is expressed as tail-bleeding time. Each symbol represents one individual. (Bender *et al., Arterioscler Thromb Vasc Biol* 2013)[138]

3.2 Characterization of CLEC-2 and GPVI double-deficient animals

3.2.1 CLEC-2/GPVI double-deficient animals display a dramatically altered lymphatic vasculature

The surface receptors CLEC-2 and GPVI are the only (hem)ITAM receptors present on murine platelets. Previously, we could show that immunodepletion of both receptors completely shut off (hem)ITAM signaling in mouse platelets without affecting signaling via GPCRs.[138] Remarkably, the simultaneous depletion of both receptors led to the complete loss of hemostatic function of platelets without causing spontaneous bleeding.[138] To test whether side effects of the antibody treatment contributed to the observed bleeding phenotype in the GPVI/CLEC-2-depleted animals, genetically double-deficient mice were generated lacking both receptors in platelets. To this end, *Gp6*$^{-/-}$ and *Clec-2*$^{fl/fl}$ mice were intercrossed obtain double-deficient animals (further referred to as *Gp6*$^{-/-}$/*Clec2*$^{-/-}$). These breedings only yielded small litters (2-6 mice) and less than 35% were *Gp6*$^{-/-}$/*Clec2*$^{-/-}$ mice, indicating increased embryonic or perinatal lethality. The surviving *Gp6*$^{-/-}$/*Clec2*$^{-/-}$ animals displayed a dramatically altered vascular structure and blood-filled lymphatic vessels in the mesentery (Figure 17 A). This phenotype was even more pronounced than that of the CLEC-2 single-deficient mice (Figure 10 A). Flow cytometric analyses confirmed the absence of both receptors in *Gp6*$^{-/-}$/*Clec2*$^{-/-}$-deficient platelets. The loss of both receptors was associated with some minor changes in the expression pattern of other surface receptors and a moderately reduced platelet count, similar to that observed in CLEC-2 single-deficient mice (Figure 17 B).

A

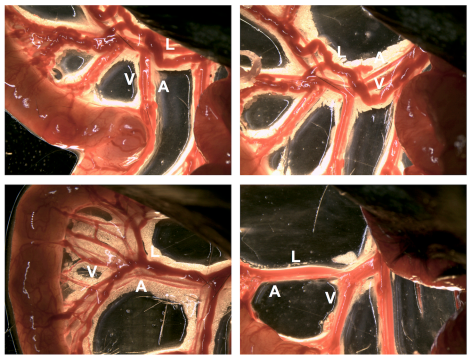

B

	Wt	*Gp6*$^{-/-}$/ *Clec-2* $^{-/-}$	
CLEC-2	123 ± 9	6 ± 1	***
GPVI	65 ± 3	5 ± 0	***
GPIb	427 ± 22	361 ± 16	**
GPIX	455 ± 12	414 ± 7	**
GPV	294 ± 22	269 ± 11	n.s.
CD9	1148 ± 63	1003 ± 71	*
αIIbβ3	438 ± 17	468 ± 29	n.s.
α2	53 ± 1	50 ± 3	n.s.
β1	127 ± 10	118 ± 3	n.s.
platelet size	352 ± 17	303 ± 9	**
platelet count	606250 ± 30000	468750 ± 55000	**

Figure 17. Analysis of *Gp6*$^{-/-}$/*Clec2*$^{-/-}$ mice. (A) Representative images of the intestine of *Gp6*$^{-/-}$/*Clec2* $^{-/-}$ mice. L= lymphatic vessel, A= arteriole, V= vein. (B) Flow cytometric analysis of surface receptor expression and platelet count. Platelets were stained for 15 min at RT with the indicated fluorophore-labeled antibodies and immediately analyzed. Platelet size is given as mean FSC and was determined by FSC characteristics. Results are mean fluorescence intensities (MFI) ± SD (*n* = 4, representative of at least three independent measurements). *, P < 0.05; **, P < 0.01; ***, P < 0.001; n.s., not significant. (Bender *et al., Arterioscler Thromb Vasc Biol* 2013)[138]

3.2.2 *Gp6*$^{-/-}$/*Clec2*$^{-/-}$-deficient platelets display a specific (hem)ITAM-specific signaling defect

To investigate the functionality of *Gp6*$^{-/-}$/*Clec2*$^{-/-}$-deficient platelets, integrin αIIbβ3 activation and α-granule release-dependent P-selectin exposure were determined upon platelet activation with different agonists using flow cytometry. As expected, these platelets showed a completely abolished responsiveness towards GPVI and CLEC-2-specific agonists indicating a complete loss of (hem)ITAM-specific signaling, while the activation response to other agonists (ADP, U46619, thrombin) remained intact (Figure 18).

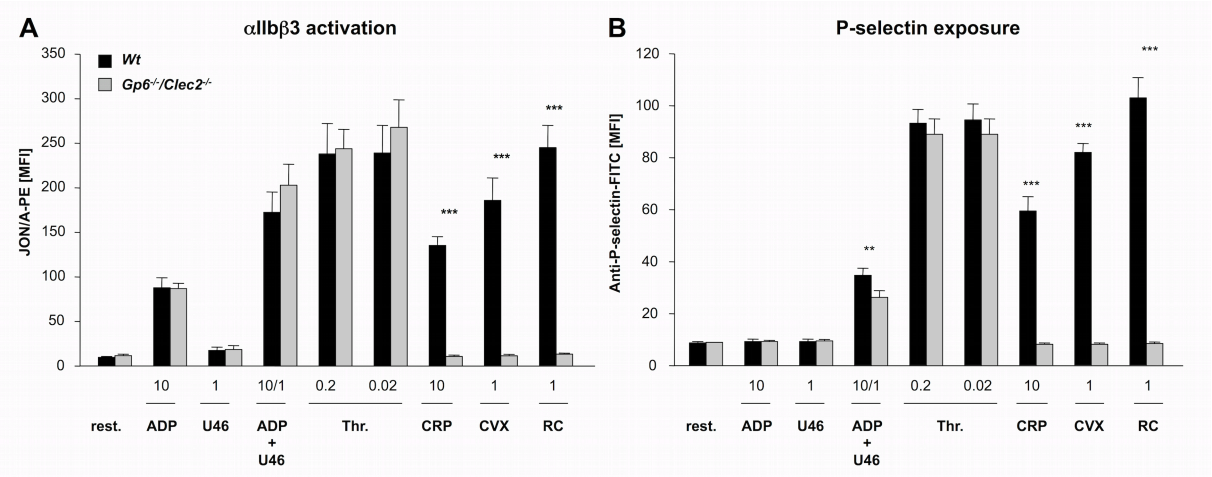

Figure 18. Integrin αIIbβ3 activation and α-granule release in *Gp6*$^{-/-}$/*Clec2*$^{-/-}$ platelets. Flow cytometric analysis of (A) integrin αIIbβ3 activation and (B) degranulation-dependent P-selectin exposure on platelets. Washed blood was incubated with the indicated agonists for 15 min at RT and analyzed on a FACSCalibur. Results are mean ± SD (*n* = 5 mice per group, representative of three individual experiments). *, P < 0.05; ***, P < 0.001. ADP [µM]; U46619 (U46): [µM]; thrombin (Thr.): [U/ml]; CRP: [µg/ml]; convulxin (CVX): [µg/ml]; rhodocytin (RC): [µg/ml]. (Bender *et al., Arterioscler Thromb Vasc Biol* 2013)[138]

Platelet tethering at the site of vascular injury represents the initial step is during the formation of a hemostatic plug under flow conditions. The key event for this first step in thrombus formation is the interaction between the platelet GPIb-V-IX receptor complex and vWF exposed on the ECM.[8] To directly investigate a possible role of GPVI and CLEC-2 in GPIb-V-IX-dependent interaction of platelets and vWF, two different assays were performed. First, adhesion of *Gp6*$^{-/-}$/*Clec2*$^{-/-}$ platelets on immobilized vWF under high shear conditions was analyzed in a flow chamber system. In this experimental setting, a shift from transient to stable platelet adhesion is dependent on αIIbβ3 integrin activation triggered by vWF-mediated stimulation of GPIb.[140] *Wt* as well as *Gp6*$^{-/-}$/*Clec2*$^{-/-}$ platelets rapidly attached to the immobilized vWF and in part firmly adhered to the surface without displaying any significant differences (Figure 19 A). Secondly, platelet spreading on a vWF-coated matrix under conditions of αIIbβ3 integrin-blockade was analyzed.[141] Under these conditions, a GPIb-specific signal is triggered and results in platelet shape change, which is limited to contraction of the cell body and filopodia formation.[142] Both, control and double-deficient

platelets efficiently extended filopodia (70% showing 3 or more filopodia, Figure 19 B). These results indicated that GPIb function was intact in GPVI/CLEC-2 double-deficient platelets.

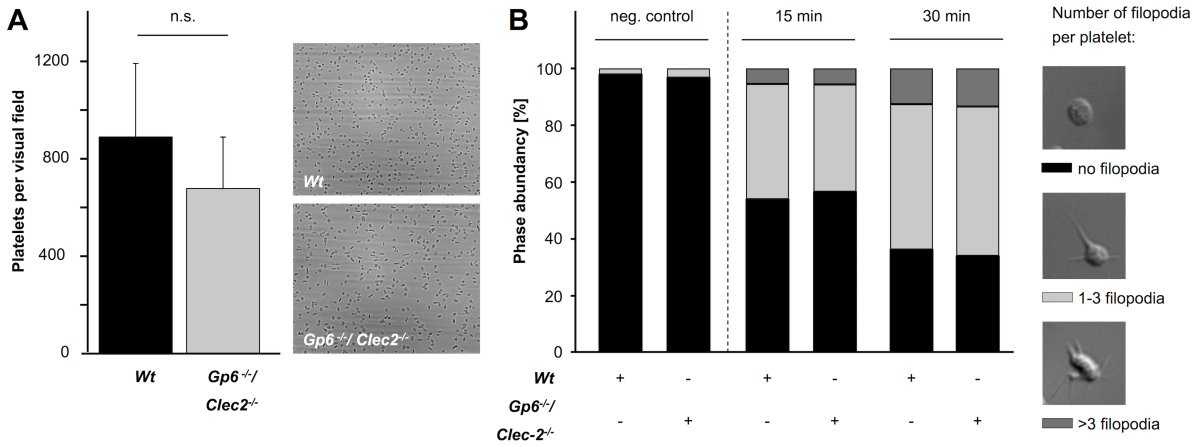

Figure 19. *Gp6*$^{-/-}$/*Clec2*$^{-/-}$ platelets have unaltered GPIb function. (A) Whole blood of *Wt* and *Gp6*$^{-/-}$/*Clec2*$^{-/-}$ mice was perfused over a vWF-coated surface at a wall shear rate of 1,700 sec^{-1} for 4 min and then washed for 4 min. Representative phase contrast images were taken at the end of the washing period. (B) Washed platelets were treated with integrilin (40 µg/ml) and botrocetin (2 µg/ml) and allowed to adhere to vWF-coated coverslips. Filopodia formation was scored according to the number of extensions per platelet at indicated the time points.

3.2.3 GPVI/CLEC-2 double-deficient animals have prolonged tail bleeding times

To test the effect of genetic GPVI/CLEC-2 double deficiency on hemostasis, tail-bleeding times were assessed using the filter paper and the saline model. *Gp6*$^{-/-}$/*Clec2*$^{-/-}$ mice showed markedly prolonged tail-bleeding times in both models compared to control or single-deficient mice (Figure 20). However, the prolongation of bleeding times was less pronounced than in double-depleted mice.[138] This may at least partially be explained by the vascular alterations and the reduced general state of health in these animals. Together, these findings demonstrate that GPVI and CLEC-2 have partially redundant functions in hemostasis.

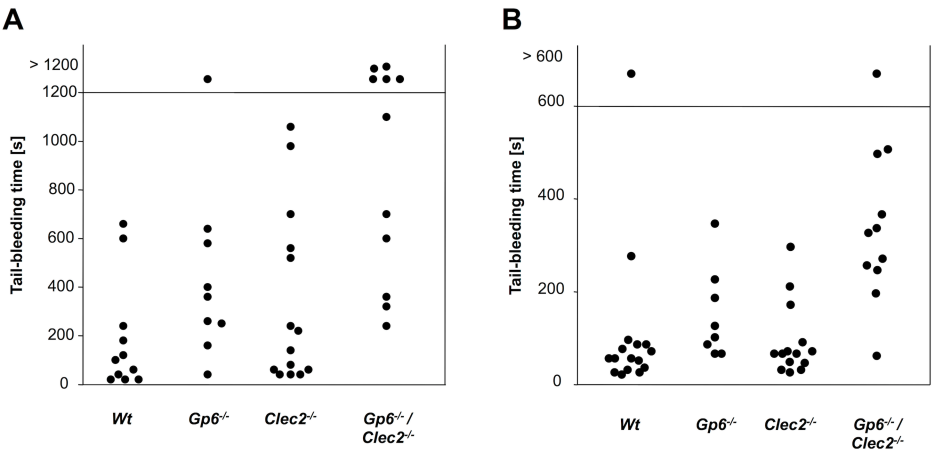

Figure 20. Defective hemostasis in mice genetically deficient for GPVI and CLEC-2. (A) A 1 mm segment from the tail tip was cut with a scalpel and (A) blood was gently absorbed with a filter paper in 20 s intervals or (B) tail tip was immersed in 37°C warm saline. Time until bleeding has ceased is expressed as bleeding time. Each symbol represents one individual. (Bender *et al., Arterioscler Thromb Vasc Biol* 2013)[138]

To further corroborate this assumption, the plasma coagulation was examined by two standard methods. (1) The prothrombin time (PT) is determined as a measure of the extrinsic coagulation pathway. Since the values for the PT, measured in seconds, highly depends on the used reagents, the percentage units (also termed pPT ratio (PTR)) were adopted for clinical use. (2) The activated partial thromboplastin time (aPTT) is measured for the intrinsic coagulation pathway. No differences were observed in PT as well as in aPTT between control and double-mutant mice (Figure 21). This excluded a major defect in the coagulation system as a possible explanation for the severely defective hemostasis in the *Gp6*$^{-/-}$/*Clec2*$^{-/-}$ mice.

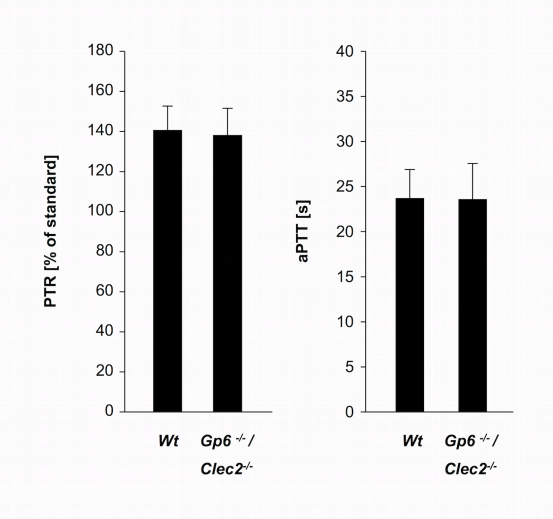

Figure 21. Intact coagulation system in GPVI/CLEC-2 double-deficient animals. Whole blood of *Wt* and *Gp6*$^{-/-}$/*Clec2*$^{-/-}$ mice was drawn in a tube containing sodium citrate and plasma was obtained by centrifugation. Plasma samples were analyzed in collaboration with the central labratory at the University hospital of Würzburg. PTR, as measured for the activation of the extrinsic pathway, was determined as [%] of standard, where the clotting time of a normal plasma standard was defined as 100%. The aPTT, as a measure for the activation of the intrinsic pathway, was determined in [s].

Notably, due to the dramatically altered vascular structure and blood-filled lymphatic vessels in the mesentery it was impossible to study thrombus formation by intravital microscopy in $FeCl_3$-injured mesenteric arterioles, as shown for the CLEC-2 single-deficient, in *Gp6*$^{-/-}$/*Clec2*$^{-/-}$ mice (Figure 17 A).

3.3 Targeted downregulation of CLEC-2 occurs through SFK-dependent internalization

CLEC-2 plays a central role in multiple physiological and pathophysiological processes, yet not much is known about the cellular regulation of CLEC-2 in murine platelets. This is of major importance for the development of pharmaceuticals that modulate CLEC-2 function under diseased conditions. We have previously demonstrated that CLEC-2 can be targeted and specifically depleted from platelets in mice by *in vivo* administration of the monoclonal antibody INU1.[17]

To study the mechanisms underlying targeted CLEC-2 downregulation *in vivo*, *Wt* mice were intravenously injected with 100 µg of the rat anti-mouse CLEC-2 antibody INU1. To determine unbound INU1 in the plasma, biotinylated INU1 was injected into *Wt* animals. Plasma of these animals was obtained at different time points and unbound antibody was measured by an enzyme-linked immunosorbent assay (ELISA). The ELISA-plate was coated with anti-rat IgG antibodies, incubated with the plasma and free INU1 was detected with horseradish peroxidase-conjugated streptavidin. As expected, the highest INU1 levels were detected directly after antibody injection and the concentration decreased over time (Figure 22). Levels were close to 0 on day 5 post injection, correlating with the appearance of the first CLEC-2- expressing platelets after this time point.

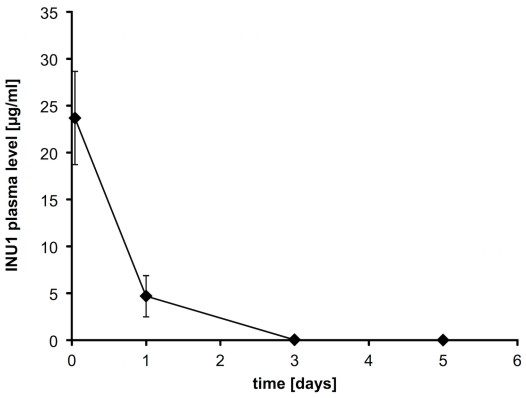

Figure 22. Plasma levels of INU1 after injection. INU1-biotin plasma levels after intravenous injection using an ELISA system. ELISA-plate was coated with anti-rat IgG antibodies, incubated with the plasma and detected with horseradish peroxidase-conjugated streptavidin.

3.3.1 INU1 binds to CLEC-2 on murine platelets and MKs *in vivo*

To use anti-CLEC-2 antibodies as potential therapeutic antibodies, it is important to obtain detailed knowledge about their biodistribution within the body. In particular it is of high interest to know whether such an antibody can bind to MKs in the bone marrow. IgG are large molecules with a molecular mass of approx. 150 kDa, yet the bone marrow has sinusoidal clefts of about 100 nm that should allow a free diffusion of large molecular weight substances, such as IgG.[143,144] To address this directly, INU1 was injected into *Wt* mice and their femora were removed at different time points post injection, fixed with 4% PFA/ 5 mM

sucrose. After fixation, the bones were transferred into 10% sucrose in PBS and dehydrated using a graded sucrose series. Subsequently, whole femora cryosections were generated and stained with anti-rat IgG-Cy3 to detect INU1. After intense washing, the sections were probed with anti-GPIb-F488 antibodies to specifically label platelets and MKs and anti-CD105-F647 antibodies to stain the endothelium. The sections revealed a robust anti-rat IgG-Cy3 signal on MKs that perfectly overlapped with the staining of anti-GPIb antibodies. Furthermore, this robust signal was observed up to five days post INU1-injection, thus showing that INU1 efficiently binds to MKs *in vivo* (Figure 23).

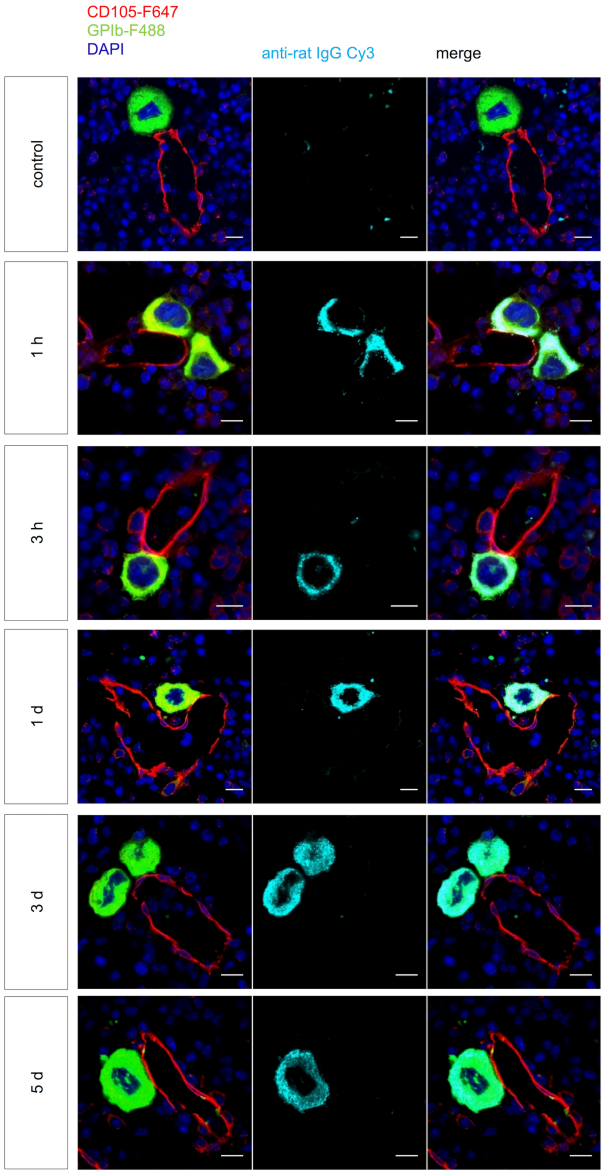

Figure 23. INU1 binds to BM MKs *in vivo*. *Wt* animals were injected with INU1 and femora were isolated at the indicated time points, fixed with 4% PFA/ 5 mM sucrose, transferred into 10% sucrose in PBS and dehydrated using a graded sucrose series. Subsequently, the samples were embedded in Cryo-Gel and frozen. 7 µm thick cryo-sections were generated using the CryoJane tape transfer system. Sections were stained with anti-rat IgG-Cy3 to detect INU1. After intense washing, the sections were probed with anti-GPIb-F488 antibodies to specifically label platelets and MKs and anti-CD105-F647 antibodies to stain the endothelium. Nuclei were stained using DAPI. Samples were visualized with a Leica TCS SP5 confocal microscope. (Scale bar 10 µm, h (hours), d (days)) (Lorenz *et al., Blood* 2015)[123]

In parallel, circulating platelets were studied *ex vivo* at different time points after INU1 injection (Figure 24). As described previously,[17] INU1 treatment caused a severe transient thrombocytopenia with platelet counts dropping below 10% of controls within the first hour and recovered back to normal levels on day three to four post injection (Figure 24 A). Newly

generated platelets lacked CLEC-2 up to day six, whereas the expression of other major glycoprotein receptors in these platelets was unaltered compared to control.[17] Western blot analyses confirmed the complete loss of platelet CLEC-2 on day 5 after INU1 injection and platelets were refractory towards the CLEC-2-specific agonist RC, whereas responses to other agonists, such as thrombin, were unaltered compared to control (Figure 24 B, C), thus confirming previous results.[17] To test whether the INU1-induced thrombocytopenia depends on platelet CLEC-2, *Clec-2*$^{-/-}$ mice were treated with 100 µg of the antibody. This treatment did not cause thrombocytopenia, thus demonstrating that the INU1-mediated effects depend on platelet CLEC-2 (Figure 24 A).

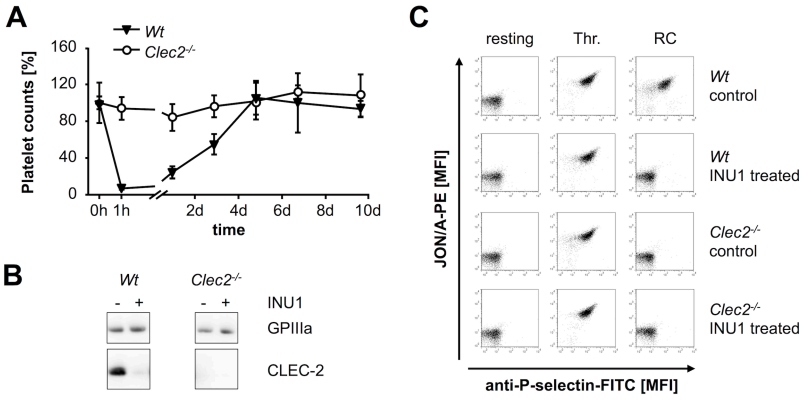

Figure 24. INU1-induced thrombocytopenia depends on platelet CLEC-2 expression. (A) *Wt* and *Clec2*$^{-/-}$ mice were intravenously injected with 100 µg INU1 and platelet counts were determined on a FACSCalibur at the indicated time points. Results are mean ± SD in % of the initial platelet counts (n=5 mice per group). (B) Western blot analysis of CLEC-2 levels, before and on day 5 post INU1 injection in platelet lysates of *Wt* and *Clec2*$^{-/-}$ mice. GPIIIa served as a loading control. (C) Flow cytometric analysis of αIIbβ3 activation (JON/A-PE) and degranulation-dependent P-selectin exposure on platelets on day 5 post INU1 injection. Washed blood was incubated with the indicated agonist for 15 min and analyzed on a FACSCalibur (rhodocytin (RC): 0.12 µg/ml, thrombin (Thr.): 0.1 U/ml). Results are representative of three individual experiments. (Lorenz *et al., Blood* 2015)[123]

3.3.2 INU1-induced thrombocytopenia occurs independently of activatory Fcγ-receptors and platelet aggregation

One possible explanation for the rapid and severe thrombocytopenia in *Wt* mice upon INU1 injection might be FcγR-dependent clearance of antibody-opsonized platelets. To address this directly, FcRγ-chain-deficient mice (*Fcer1g*$^{-/-}$,[126] further referred to as *FcRγ*$^{-/-}$) were analyzed. These animals lack the activatory Fcγ receptors (FcRγI, III and IV) and thus their macrophages are unable to phagocytose antibody-opsonized particles.[126,145] Remarkably, intravenous injection of 100 µg INU1 into *FcRγ*$^{-/-}$ mice caused a profound thrombocytopenia and a complete loss of the CLEC-2 protein in newly generated platelets comparable to *Wt* mice (Figure 25; day 5 post injection).

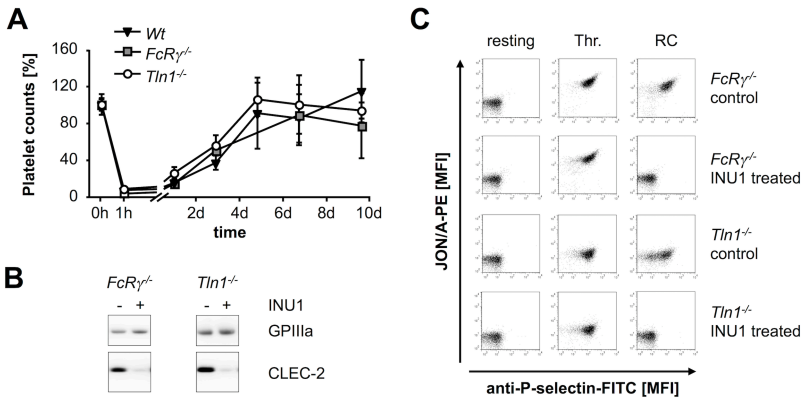

Figure 25. INU1-induced thrombocytopenia is independent of platelet integrin activation and FcγRs. (A) *Wt, FcRγ*$^{-/-}$ and *Tln1*$^{-/-}$ mice were intravenously injected with 100 µg INU1 and platelet counts were determined on a FACSCalibur at the indicated time points. Results are mean ± SD in % of the initial platelet counts (n=5 mice per group). (B) Western blot analysis of CLEC-2 levels, before and on day 5 post INU1 injection in platelet lysates of *FcRγ*$^{-/-}$ and *Tln1*$^{-/-}$ mice. GPIIIa served as a loading control. (C) Flow cytometric analysis of αIIbβ3 activation (JON/A-PE) and degranulation-dependent P-selectin exposure on platelets on day 5 post INU1 injection (rhodocytin (RC): 0.12 µg/ml, thrombin (Thr.): 0.1 U/ml). Results are representative of three individual experiments. (Lorenz *et al., Blood* 2015)[123]

We have previously shown that binding of INU1 to CLEC-2 potently induces aggregation of mouse platelets *in vitro*.[17] Therefore, we speculated that INU1 might induce the formation of platelet aggregates, which are then filtered out by the capillary bed in the lungs and/or cleared by the reticuloendothelial system, thereby causing the severe thrombocytopenia. To test this, different organs of *Wt* mice were analyzed by immunohistochemistry 1 h after the injection of 100 µg INU1 or vehicle control. Platelet aggregates were present in the microcirculation of the lungs (Figure 26 A, red: platelet-specific staining). Since integrin activation is an essential prerequisite for platelet aggregate formation, the effect of INU1 treatment in conditional talin1-deficient mice (*Tln1*$^{fl/fl\ PF4\text{-}cre}$,[124] further referred to as *Tln1*$^{-/-}$) was tested. These animals are unable to activate their platelet integrins and thus fail to form platelet aggregates. Unexpectedly, INU1-treatment of *Tln1*$^{-/-}$ mice resulted in a severe thrombocytopenia and in CLEC-2 deficiency of newly generated platelets, which was comparable to *Wt* mice (Figure 25; day 5 post injection). Of note, however, platelets of INU1-challenged *Tln1*$^{-/-}$ mice did not form aggregates and were mainly trapped in the spleen. Thereby, the normal spleen morphology consisting of red and white pulp was altered and a platelet-specific staining was visible throughout the whole organ (Figure 26 B), this suggesting a different route of platelet clearance in these animals as compared to *Wt*.

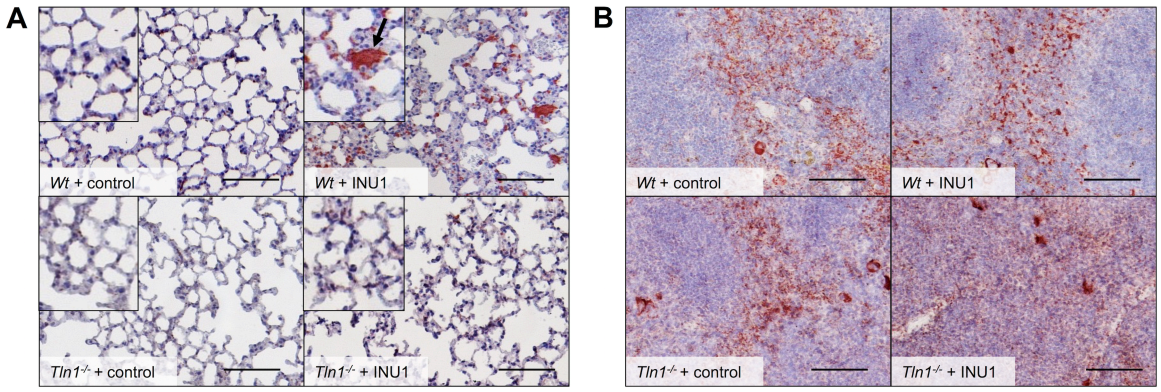

Figure 26. INU1-opsonized *Wt* platelets form microemboli, which are trapped in lung capillaries. Representative images of histological sections of *Wt* and *Tln1*$^{-/-}$ mice 1 h after treatment with 100 µg INU1 or vehicle control are displayed. (A) Lungs and (B) spleens were dissected, fixed, dehydrated and embedded in paraffin. 3 µm thick sections were stained with HRP-conjugated platelet specific anti-GPIb antibodies; detection was performed with 3-amino-9-ehylcarbazole (AEC) substrate (resulting in a red staining) and nuclei were counterstained with hematoxylin. Scale bars represent 100 µm. Arrow in A indicates a trapped aggregate in the lung of a *Wt* mouse.

Similar results were obtained when αIIbβ3 integrins were functionally blocked with F(ab)2 fragments of the anti-αIIbβ3 antibody, JON/A[121] (100 µg 1 h before the experiment; Figure 27). Together, these results indicated that the INU1-induced thrombocytopenia depends on binding of the antibody to platelet CLEC-2, but can occur independently of FcRγ-mediated phagocytosis or integrin-mediated platelet aggregation.

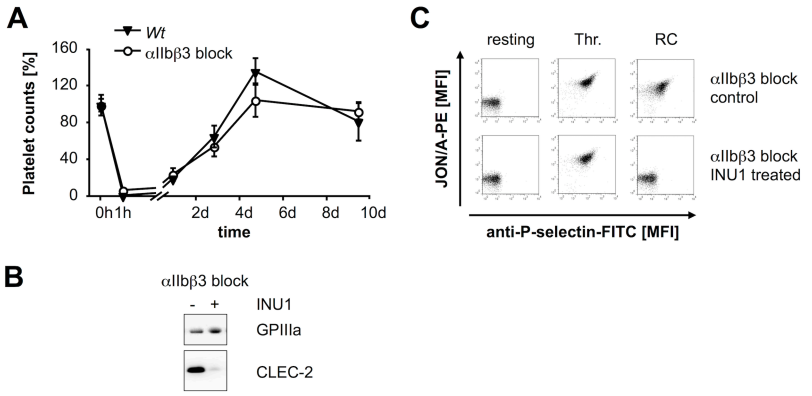

Figure 27. INU1-induced thrombocytopenia is independent of αIIbβ3 integrins. (A) *Wt* mice remained either untreated or were injected with an antibody derivative blocking αIIbβ3 (JON/A F(ab)2, 100 µg) 1 h prior to the injection with 100 µg INU1. Platelet counts were determined on a FACSCalibur at the indicated time points. Results are mean ± SD in % of the initial platelet counts (n=5 mice per group). (B) Western blot analysis of CLEC-2 levels before and on day 5 post INU1 injection in platelet lysates of mice injected with αIIbβ3 blocking F(ab)-fragment. GPIIIa served as a loading control. (C) Flow cytometric analysis of integrin αIIbβ3 activation (JON/A-PE) and degranulation-dependent P-selectin exposure on platelets on day 5 post INU1 injection (rhodocytin (RC): 0.12 µg/ml, thrombin (Thr.): 0.1 U/ml). Results are representative of three individual experiments. (Lorenz *et al., Blood* 2015)[123]

3.3.3 INU1-induced thrombocytopenia depends on CLEC-2 signaling

To test whether signaling downstream of CLEC-2 is required for INU1-induced CLEC-2 downregulation and thrombocytopenia, mice with a platelet-specific Syk-deficiency (*Syk*$^{fl/fl\ PF4\text{-}cre}$, further referred to as *Syk*$^{-/-}$) were analyzed. Platelets from these mice are refractory to ITAM-specific agonists, while activation with thrombin and other GPCR agonists was normal (Figure 28 A,[36,127]). Surprisingly, Syk-deficiency in platelets markedly attenuated INU1-triggered thrombocytopenia (1 h after injection: 56 ± 5% of control in *Syk*$^{-/-}$ mice vs. 1 ± 0% in *Wt*; Figure 28 B) and the platelets remained in a resting state as revealed by flow cytometric measurement of FSC/SSC characteristics, integrin αIIbβ3 activation and degranulation-dependent P-selectin exposure (Figure 28 C). Additionally, these platelets showed an unaltered ultrastructure in electron microscopy and a normal activation response to agonists, such as thrombin (Figure 28 C, D).

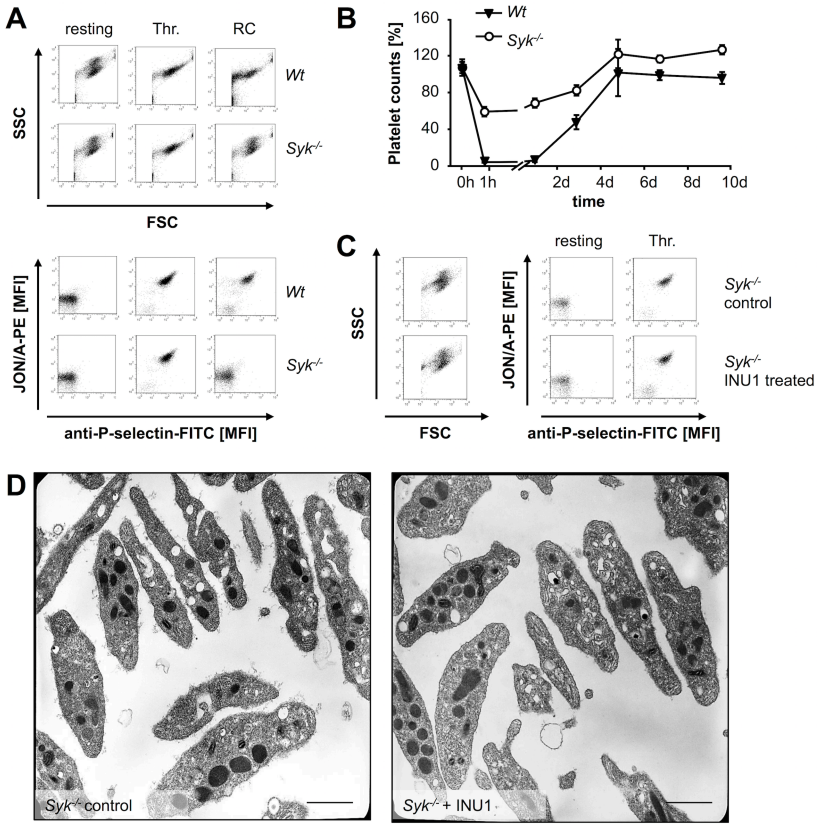

Figure 28. Attenuated INU1-induced thrombocytopenia in *Syk*$^{-/-}$ mice. (A) Flow cytometric analysis of naïve *Wt* and *Syk*$^{-/-}$ platelets incubated with various agonists. Forward scatter (FSC) and side scatter characteristics (SSC) as well as αIIbβ3 integrin activation (JON/A-PE) and degranulation-dependent P-selectin exposure are displayed (rhodocytin (RC): 0.12 µg/ml, thrombin (thr): 0.1 U/ml). (B) *Wt* and *Syk*$^{-/-}$ mice were intravenously injected with 100 µg INU1 and platelet counts were determined on a FACSCalibur at the indicated time points thereafter. Results are mean ± SD in % of the initial platelet counts (n=5 mice per group). (C) Flow cytometric analysis of control and INU1-treated *Syk*$^{-/-}$ platelets 1 h after injection. FSC and SSC as well as the αIIbβ3 integrin activation and degranulation-dependent P-selectin exposure are displayed. Results are representative of three individual experiments. (D) Transmission electron microscopy pictures of control and INU1-treated *Syk*$^{-/-}$ platelets 1 h after injection. Scale bar represents 1 µm.

Subsequently, CLEC-2 surface levels in circulating platelets were determined by flow cytometric measurements with an anti-rat Ig-FITC antibody. These levels were strongly reduced 1 h after antibody injection compared to an *in vitro* control, where platelets of untreated mice were incubated with 20 µg/ml INU1 (Figure 29 A). This result indicated that the receptor had been efficiently downregulated from the surface independently of Syk activity and cellular activation. To address this hypothesis experimentally, Western blot analysis of platelet lysates 2 h after INU1 injection were performed. CLEC-2 protein levels were reduced, but still robustly detectable in these platelets (66 ± 7% of initial protein levels), strongly suggesting that the antibody-opsonized receptor had been internalized (Figure 29 B). Similar to *Wt* mice (Figure 24 B), platelets of *Syk*$^{-/-}$ mice completely lacked CLEC-2 on day 5 after INU1 injection, indicating that the internalized receptor underwent intracellular degradation (Figure 29 B). Together, these results demonstrated for the first time that targeting of CLEC-2 by INU1 efficiently triggers downregulation of the receptor in circulating platelets. Furthermore, this process is independent of Syk and cellular activation and can be mechanistically uncoupled from the undesired antibody-induced transient thrombocytopenia.

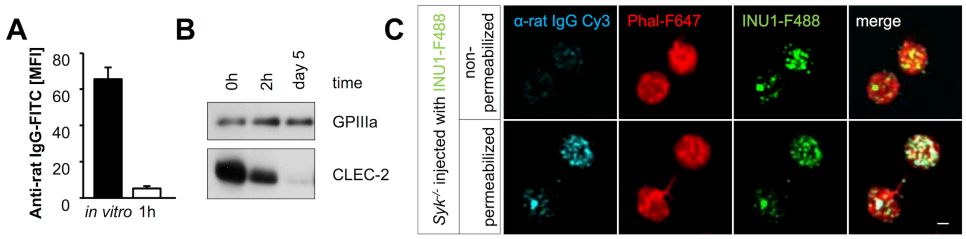

Figure 29. INU1 injection induces CLEC-2 internalization in Syk$^{-/-}$ platelets. (A) *Syk*$^{-/-}$ mice were bled 1 h after INU1 injection and washed blood was incubated with an anti-rat Ig-FITC antibody for 15 min and subsequently analyzed on a FACSCalibur. As *in vitro* control, blood from untreated mice was incubated with 20 µg/ml INU1 for 15 min, washed and incubated with an α-rat Ig-FITC antibody for 15 min. (B) Western blot analysis of CLEC-2 levels at the indicated time points post INU1-injection in platelets lysates of *Syk*$^{-/-}$ mice. GPIIIa served as a loading control. (C) *Syk*$^{-/-}$ mice were injected with 100 µg INU1-F488 antibody, 15 min after injection platelets were isolated, allowed to adhere to PLL-coated coverslips, fixed and stained with α-rat IgG-Cy3 under permeabilizing or non-permeabilizing conditions and subsequently stained with PhalF647 diluted in permeabilizing buffer. Samples were visualized using a Leica TCS SP5 confocal microscope equipped with a 100X/1.4 oil objective. Scale bar represents 1 µm. Results are representative of three individual experiments.

To address the hypothesis that INU1-induced CLEC-2 downregulation occurs through internalization in more detail, *Syk*$^{-/-}$ mice were injected with 100 µg Alexa F488-conjugated INU1 (INU1-F488) and after 15 min platelets were isolated and fixed on poly-L-lysine (PLL)-coated coverslips. To determine the localization of INU1, the cells were then stained with anti-rat IgG-Cy3 antibodies with or without membrane permeabilization. After removal of unbound antibody, all samples were counterstained with phalloidin-Atto647N (Phal-F647) under permeabilizing conditions to visualize the filamentous actin cytoskeleton. Under these

experimental conditions, a punctate distribution of INU1-F488 close to the cell membrane was found. This bound INU1-F488 antibody could, however, only be counterstained with anti-rat IgG-Cy3 antibodies under permeabilizing, but not under non-permeabilizing conditions, thus demonstrating internalization of the INU1/CLEC-2 complex (Figure 29 C).

3.3.4 INU1 induces internalization of CLEC-2 *in vitro*

These findings prompted us to test whether INU1 could also induce internalization of CLEC-2 *in vitro* and whether INU1-binding to CLEC-2 alone is sufficient to induce this process. To this end, platelets of *Wt* and *Syk*$^{-/-}$ mice were incubated with INU1-F488 for 15 min and then fixed on PLL-coated slides for 30 min followed by staining with anti-rat IgG-Cy3 antibodies with or without membrane permeabilization. Non-permeabilized *Wt* or *Syk*$^{-/-}$ platelets yielded only a very weak staining with anti-rat IgG-Cy3 antibodies, while permeabilization of the cells resulted in a strong intracellular staining with a pattern resembling and co-localizing with that of INU1-F488, confirming that the CLEC-2/INU1 complex had efficiently been internalized in both *Wt* and *Syk*$^{-/-}$ platelets (Figure 30 A).

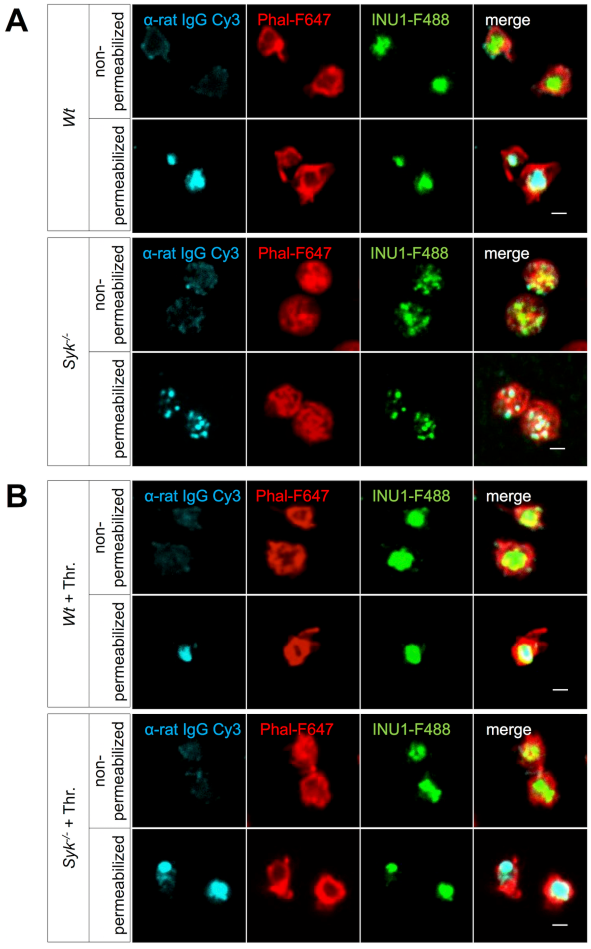

Figure 30. CLEC-2 downregulation occurs through Syk-independent internalization. (A) *Wt* and *Syk*$^{-/-}$ platelets were *in vitro* incubated with 20 µg/ml INU1-F488 for 15 min. Thereafter, platelets were stained and imaged as described in Figure 29 C. Scale bars represent 1 µm. (B) *Wt* and *Syk*$^{-/-}$ platelets were *in vitro* incubated with 20 µg/ml INU1-F488 for 15 min followed by 2 min incubation with thrombin (0.1 U/ml). Subsequently, platelets were stained and imaged as described in Figure 29 C (thrombin (Thr.)). Results are representative of three individual experiments. (Lorenz *et al., Blood* 2015)[123]

In *Wt*, but not in *Syk*$^{-/-}$ platelets, INU1 induced a pronounced shape change, reflecting cellular activation. Accordingly, the INU1-F488 signal was centralized in *Wt*, but not in *Syk*$^{-/-}$ platelets (Figure 30 A), the latter displaying a punctate staining of CLEC-2 similar to that observed in platelets from INU1-treated *Syk*$^{-/-}$ mice. To test whether the altered staining pattern for internalized CLEC-2/INU1 complexes in *Syk*$^{-/-}$ platelets was indeed due to defective CLEC-2 signaling, the experiment was repeated in the presence of thrombin, which indeed induced a strong centralization of the INU1-F488 signal in *Syk*$^{-/-}$ platelets comparable to *Wt* platelets (Figure 30 B). These results suggested that INU1-binding to platelet CLEC-2 potently induces receptor internalization under both *in vivo* and *in vitro* conditions independently of Syk and platelet activation.

3.3.5 SFK activity is essential for INU1-induced receptor internalization *in vivo*

A previous study has shown that the antibody-induced tyrosine phosphorylation of both CLEC-2 and the downstream kinase Syk is completely blocked by PP2, a potent SFK inhibitor.[36] This prompted us to test whether phosphorylation of the CLEC-2 hemITAM by SFK might be sufficient to trigger antibody-induced internalization of the receptor. To test this directly, *Wt* mice were injected with the SFK inhibitor Dasatinib (5 mg/kg) or vehicle control.[146] The injected animals were bled and PRP was obtained for aggregometry measurements. In line with previous data,[147] platelets of Dasatinib-treated mice had a (hem)ITAM-specific activation defect, whereas other signaling pathways were unaffected, thus confirming the specificity of the inhibitor (Figure 31).

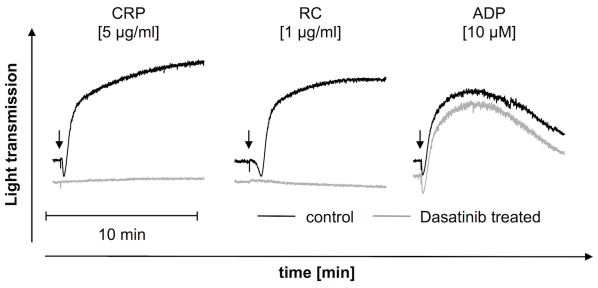

Figure 31. Platelets of Dasatinib-treated mice display a (hem)ITAM-specific activation defect. PRP of vehicle-treated (black line) and Dasatinib-treated (5 mg/kg, grey line) *Wt* mice were incubated for 5 min at 37°C and then stimulated with the indicated agonists under stirring conditions. Light transmission was recorded on an aggregometer. Results are representative of three individual experiments. (Lorenz *et al., Blood* 2015)[123]

Surprisingly, injection of 100 µg INU1 in Dasatinib-treated *Wt* mice resulted in thrombocytopenia after 2 h, albeit to a lesser extent than in vehicle-pretreated mice (Figure 32 A). The remaining platelets were in a resting state as revealed by flow cytometric measurements of FSC/SSC characteristics, integrin αIIbβ3 activation and P-selectin exposure and showed a normal activation response to agonists, such as thrombin (Figure 32 B). Importantly, INU1 was detected at maximal levels on the surface of these circulating platelets when compared to *in vitro* stained controls (Figure 32 C). This indicated

that activation of SFK upon antibody-induced CLEC-2 dimerization might be a prerequisite for the internalization of the receptor. Since under these conditions circulating platelets were opsonized with INU1, they might be cleared by Fc-dependent mechanisms. Therefore, *FcRγ*$^{-/-}$ mice were treated with Dasatinib (5 mg/kg) or vehicle 1 h before the injection of INU1. In line with our previous results (Figure 25 A), vehicle-treated *FcRγ*$^{-/-}$ mice became thrombocytopenic upon INU1-injection. In sharp contrast, platelet counts of Dasatinib-treated *FcRγ*$^{-/-}$ mice remained at 88 ± 9 % of control (Figure 32 A), indicating that the antibody-opsonized platelets were indeed cleared by FcγR-dependent mechanisms. The circulating platelets displayed robust CLEC-2 expression on their surface, which was comparable to that of *in vitro* INU1-stained control platelets (Figure 32 C). Additionally, these platelets were in a resting state and showed a normal activation response to agonists, such as thrombin (Figure 32 B). Collectively, these results provide strong *in vivo* evidence that CLEC-2 immunodepletion is an SFK-dependent internalization process.

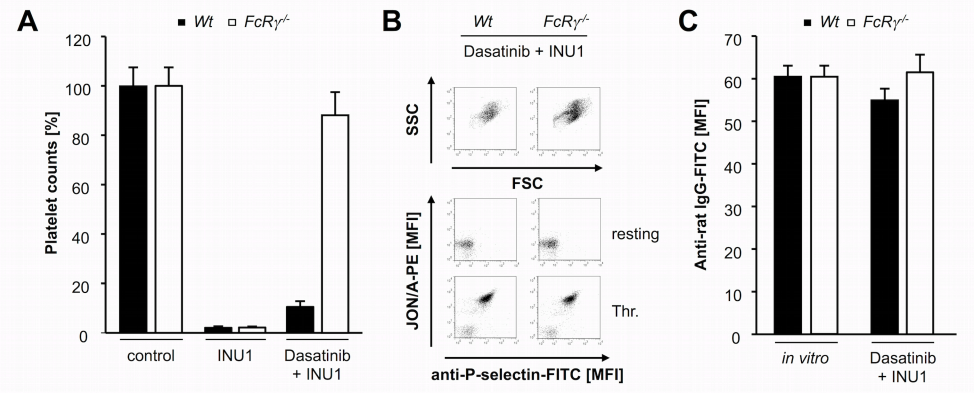

Figure 32. CLEC-2 internalization depends on SFK activity. (A) *Wt* and *FcRγ*$^{-/-}$ mice were pretreated with Dasatinib (5 mg/kg) for 1 h followed by intravenous injection of 100 µg INU1. Platelet counts were determined 2 h after injection on a FACSCalibur. Results are mean ± SD in % of starting values (n=5 mice per group). (B) Flow cytometric analysis of INU1-injected Dasatinib-treated *Wt* and *FcRγ*$^{-/-}$ platelets 2 h after injection. FSC and SSC as well as the αIIbβ3 activation and degranulation-dependent P-selectin exposure are displayed (thrombin (Thr): 0.1 U/ml). (C) 2 h after INU1 injection washed blood of Dasatinib-treated *Wt* and *FcRγ*$^{-/-}$ mice was incubated for 15 min with an anti-rat Ig-FITC antibody and subsequently analyzed on a FACSCalibur. Untreated mice were bled and used as *in vitro* control. The blood was incubated with 20 µg/ml INU1 for 15 min, washed and incubated with an anti-rat Ig-FITC antibody for 15 min. (Lorenz *et al., Blood* 2015)[123]

3.3.6 CLEC-2 internalization can be blocked *in vitro* by SFK inhibitors

To further confirm the *in vivo* findings under *in vitro* conditions, *Wt* and *Syk*$^{-/-}$ platelets were incubated with the SFK inhibitor PP2 (25 µM) or PP3 (25 µM), its inactive control. Subsequently, the platelets were by incubation with 20 µg/ml INU1-F488 for 15 min and then fixed on PLL-coated slides for 30 min followed by staining with anti-rat IgG-Cy3 antibodies with or without membrane permeabilization. PP3 did not affect INU1-induced responses of *Wt* and *Syk*$^{-/-}$ platelets, and thus resulted in CLEC-2 internalization in both genotypes and in centralization of the antibody/receptor complex in *Wt*, but not in *Syk*$^{-/-}$ platelets (Figure 33 A,

B). Antibody-induced downregulation of CLEC-2 was abolished in PP2-pretreated *Wt* and *Syk*$^{-/-}$ platelets, as revealed by the robust detection of INU1-F488 on the platelet surface using an anti-rat IgG-Cy3 antibody in the absence of permeabilization (Figure 33 A, B).

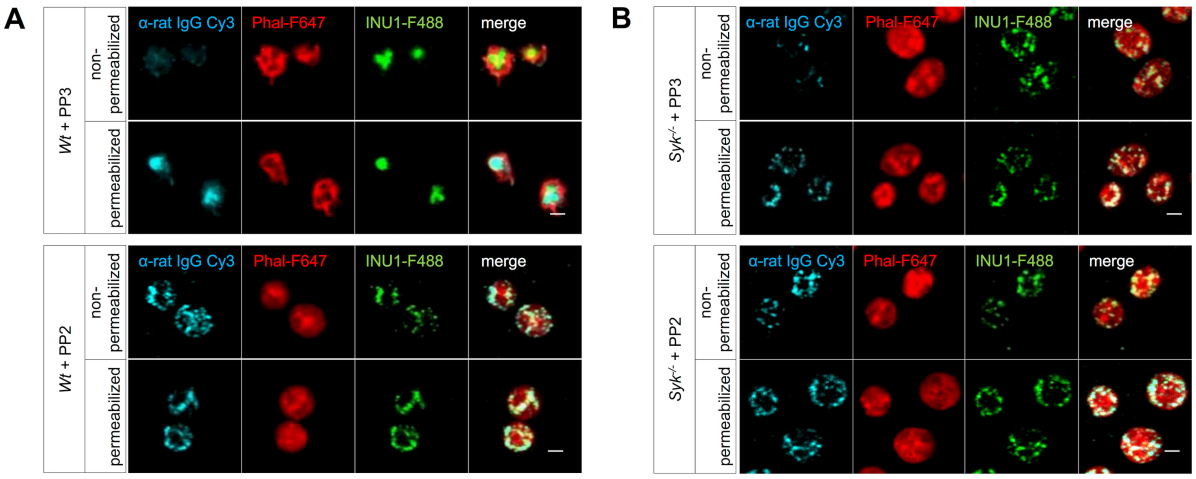

Figure 33. Inhibition of CLEC-2 internalization by the SFK inhibitor PP2. (A) *Wt* and (B) *Syk*$^{-/-}$ platelets were *in vitro* incubated for 15 min with 25 µM PP3 (negative control) or PP2 followed by an incubation with 20 µg/ml INU1-F488 for 15 min. Thereafter, platelets were processed and imaged as described in Figure 29 C.

To further corroborate these findings, flow cytometric time course experiments in *Wt* and *Syk*$^{-/-}$ platelets were performed. Platelets were preincubated with eptifibatide (40 µg/ml) – to prevent aggregate formation – and PP2 (25 µM) or PP3 followed by incubation with 20 µg/ml INU1 for up to 3 h. *Wt* platelets preincubated with PP3 had already internalized 30% of surface CLEC-2/INU1 complexes after 15 min. Only a weak signal was detectable on the surface after 60 min, demonstrating efficient internalization of INU1-opsonized CLEC-2 (Figure 34). In *Syk*$^{-/-}$ platelets, similar observations were made, albeit with a delayed time course. In sharp contrast, PP2-treated *Wt* as well as *Syk*$^{-/-}$ platelets did not show a decrease in the INU1 IgG surface signal over time (Figure 34). This clearly demonstrates that CLEC-2 internalization occurs independently of Syk, but requires SFK activity.

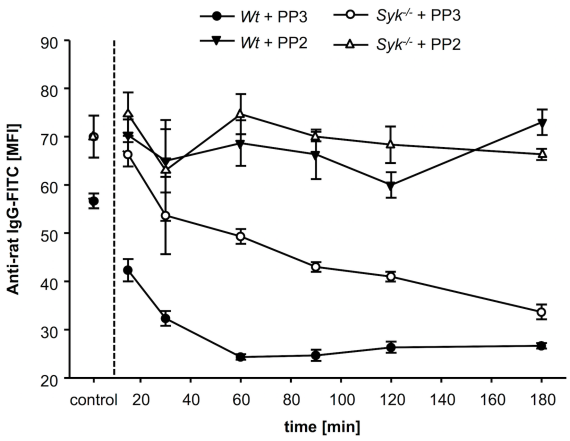

Figure 34. INU1-induced CLEC-2 internalization depends on SFK activity. *Wt* and *Syk*$^{-/-}$ platelets were *in vitro* incubated for 15 min with eptifibatide (40 µg/ml) and 25 µM PP3 or PP2 followed by 20 µg/ml INU1-F488 for the indicated times. To determine the surface prevalence of INU1, platelets were fixed with 0.5% PFA, washed and stained with anti-rat IgG FITC for 1 h. Results are mean ± SD (n=5 mice per group). For the control, *Wt* and *Syk*$^{-/-}$ platelets were incubated with 20 µg/ml INU1 for 15 min, followed by 15 min incubation with an anti-rat IgG-FITC after washing. (Lorenz *et al., Blood* 2015)[123]

To gain further insights into the INU1-mediated CLEC-2 downregulation mechanism and to confirm that SFK-dependent phosphorylation changes occur after INU1 treatment of *Wt* and *Syk*$^{-/-}$ platelets, tyrosine-phosphorylation experiments were performed (Figure 35). Isolated platelets were preincubated with eptifibatide (40 µg/ml) and PP2 (25 µM) followed by incubation with 20 µg/ml INU1. At the indicated time points, platelets were lysed and Western blot analysis was performed with the anti-phosphotyrosine antibody, 4G10, or an anti-CLEC-2 antibody. Due to the delayed internalization of CLEC-2 in the absence of Syk, prolonged incubation times after the addition of 20 µg/ml INU1 were used (Figure 34). The efficiency of the used Src kinase inhibitor PP2 already became evident under resting conditions where a decrease in the tyrosine phosphorylation pattern of different proteins could be observed (Figure 35). Moreover, INU1-induced tyrosine phosphorylation was completely abolished in PP2-treated *Wt* platelets. In contrast, Syk deficiency did not affect the tyrosine phosphorylation pattern under resting conditions. As expected, Syk phosphorylation (band migrating at approx. 65 kDa) could not be observed in *Syk*$^{-/-}$ platelets and a number of other proteins displayed a reduced intensity or delayed phosphorylation. However, several proteins were phosphorylated (at approx. 100, 80 and 20 kDa, all indicated by arrows in Figure 35), which could also be observed in *Wt* platelets upon stimulation with INU1. All of these bands were completely absent in the PP2-treated *Syk*$^{-/-}$ platelets indicating that CLEC-2 induced phosphorylation is clearly impaired in the absence of Syk, but not completely abolished – as long as SFK activity was present. Together, these results indicate that INU1-induced CLEC-2 internalization in *Syk*$^{-/-}$ platelets depends on SFK-mediated phosphorylation events. Further studies are required to reveal the identity of the phosphorylated proteins involved in this signaling cascade.

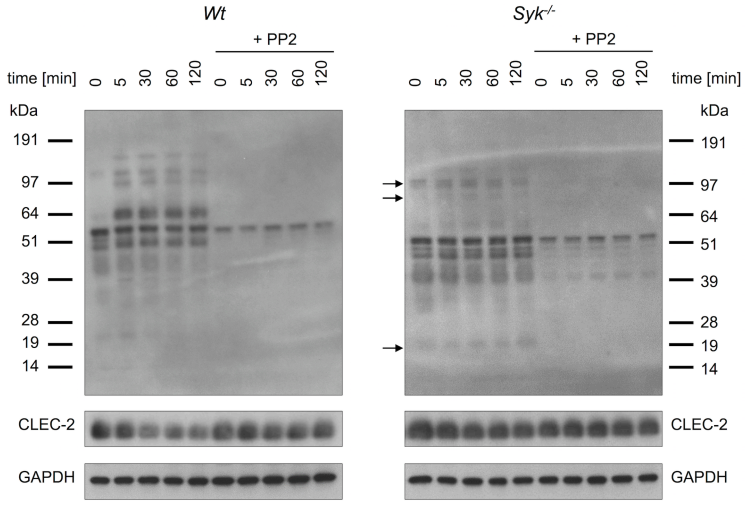

Figure 35. Abolished INU1-induced tyrosine phosphorylation in *Wt* and *Syk*$^{-/-}$ platelets after SFK inhibition. *Wt* and *Syk*$^{-/-}$ platelets were incubated with 20 µg/ml INU1 *in vitro*. Subsequently, platelets were lysed at the indicated time points. Western blot analysis was performed with the anti-phosphotyrosine antibody 4G10 or an anti-CLEC-2 antibody. GAPDH served as loading control.

3.3.7 INU1 does not induce CLEC-2 shedding *in vitro*

It is known that two major pathways exist to regulate receptor prevalence on the surface: ectodomain shedding and internalization/ intracellular clearance. To investigate whether INU1-induced ectodomain shedding of CLEC-2 contributes to the loss of the receptor from the surface, Western blot analyses of *Wt* platelets were performed. Platelets were incubated *in vitro* for different periods of time with INU1 (20 µg/ml) in the presence of eptifibatide (40 µg/ml) (Figure 36). Using an antibody recognizing the N-terminal intracellular portion of CLEC-2, no fragments or changes in the molecular weight of the CLEC-2 band were observed, but a gradual decrease of the CLEC-2 signal at later time points (>30 min). In light of the previous experiments, it appears conceivable that intracellular degradation of INU1-bound CLEC-2, but not CLEC-2 downregulation through ectodomain shedding, is responsible for the loss of the CLEC-2 signal, which is in agreement with a previous study.[148]

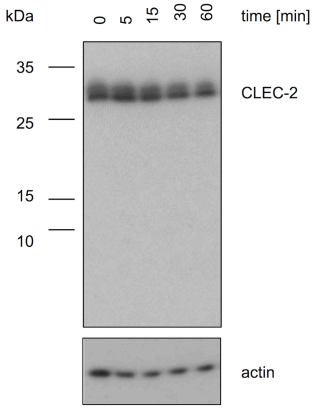

Figure 36. No evidence for INU1-induced CLEC-2 shedding in *Wt* platelets. *Wt* platelets were incubated for 5 min with eptifibatide (40 µg/ml) and 20 µg/ml INU1 *in vitro*. Subsequently, platelets were lysed at the indicated time points. Western blot analysis was performed with an antibody recognizing the intracellular N-terminal region of CLEC-2. β-actin served as a loading control. Results are representative of three individual experiments. (Lorenz *et al., Blood* 2015)[123]

3.3.8 INU1 induces CLEC-2 internalization in MKs *in vitro*

One question that still remained was how CLEC-2-deficient platelets are generated in *Wt* animals where circulating platelets undergo activation after INU1 binding. To address this *in vitro*, MK cultures were analyzed. For this mice were time-mated and the livers of 13.5 to 14.5-day-old mouse embryos were isolated and a single cell suspension was cultured for 72 h. Mature MKs were enriched on day 3 of culturing using a BSA density gradient. Thereafter, the differentiated fetal liver cell-derived MKs were incubated with INU1-F488 for different periods of time, fixed and stained with an anti-rat IgG-Cy3 antibody under membrane permeabilizing or non-permeabilizing conditions, as well as with phalloidin-F647 and DAPI diluted in permeabilizing buffer. A robust INU1-F488 signal was detectable at all time points, demonstrating the presence of the INU1/CLEC-2 complex (Figure 37). However, similar to platelets, these complexes could only be detected by the anti-rat IgG-Cy3

antibodies under permeabilizing conditions, thus arguing that the INU1/CLEC-2 complexes also become internalized in MKs (Figure 37). In contrast to platelets, however, no significant loss of total CLEC-2 was observed in MKs over time (Figure 23, 37). This might be explained by the fact that MKs – in contrast to platelets – possess a nucleus and a highly active transcriptional machinery, which may resynthesize CLEC-2 upon loss. After 24 h in culture, MKs produced protrusions, so-called proplatelets (Figure 37, 24h). Of note, both *in vitro* and *in situ* stained MKs displayed a signal for the INU1/CLEC-2 complex in proplatelet protrusions, which could only be detected by the anti-rat IgG-Cy3 antibodies under permeabilizing, but not under non-permeabilizing conditions. This indicated that degradation of the internalized CLEC-2 might occur in platelets very early in the course of their maturation within the circulation (Figure 23, 37).

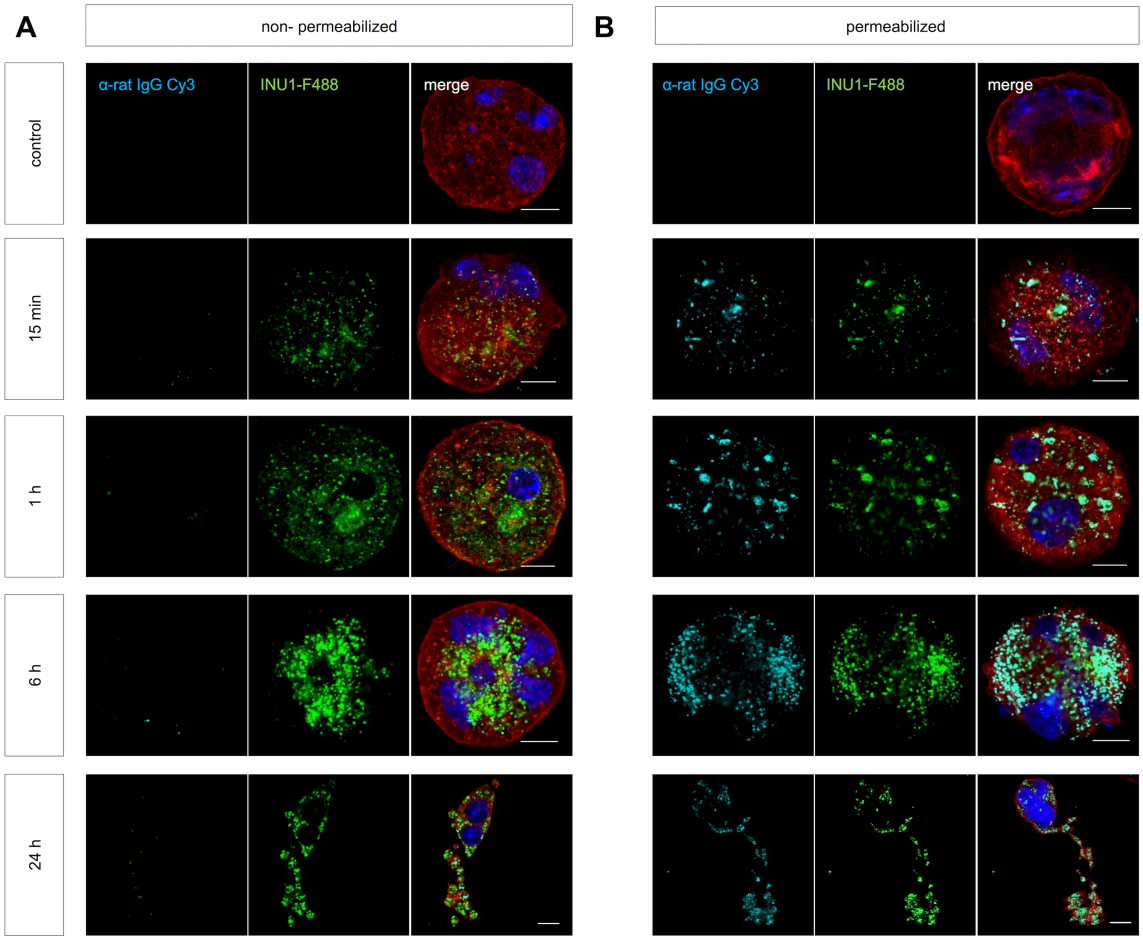

Figure 37. INU1-induced CLEC-2 internalization in fetal-liver derived MKs. The livers of 13.5 to 14.5-day-old mouse embryos were isolated from time-mated mice and single cell suspensions were cultured for 72 h and mature MKs were enriched on day 3 of culturing using a BSA density gradient. These MKs were treated with INU1-F488 for the indicated time periods. Subsequently, they were spun onto glass slides, fixed and stained with anti-rat IgG-Cy3 under (A) non-permeabilizing or (B) permeabilizing conditions, as well as with phalloidin-F647 diluted in permeabilizing buffer. Nuclei were stained using DAPI. Samples were visualized with a Leica TCS SP5 confocal microscope (Scale bar 10 µm). (Lorenz *et al., Blood* 2015)[123]

3.4 INU1 F(ab) fragments induce disseminated intravascular thrombus formation

3.4.1 INU1 F(ab) fragments induce lethality in mice

Intact antibodies of the IgG subclass are very large and can have undesired effects when used as therapeutic agents. Therefore, antibody F(ab) fragments, consisting only of the antigen-binding site, are considered to represent better pharmacological agents to block protein function. As stated above, CLEC-2 is a unique platelet receptor contributing to various physiological and pathophysiological processes, making it a potential target for their modulation. The monoclonal antibody INU1 regulates the surface prevalence of CLEC-2 by inducing its internalization. To test the utility of monovalent F(ab) fragments of INU1, the intact IgG is first digested with the nonspecific endopeptidase pepsin to yield F(ab)2 fragments and numerous small peptides of the Fc portion (Figure 38 A). The resulting F(ab)2 fragment is composed of two disulfide-connected F(ab) units and is reduced to single F(ab) fragments with DL-dithiothreitol (DTT) (Figure 38 A). The obtained antibody-fragments were purified by gel filtration via a Superdex 200 column and the purity of the preparation was controlled on a Coomassie-stained SDS gel (Figure 38 B).

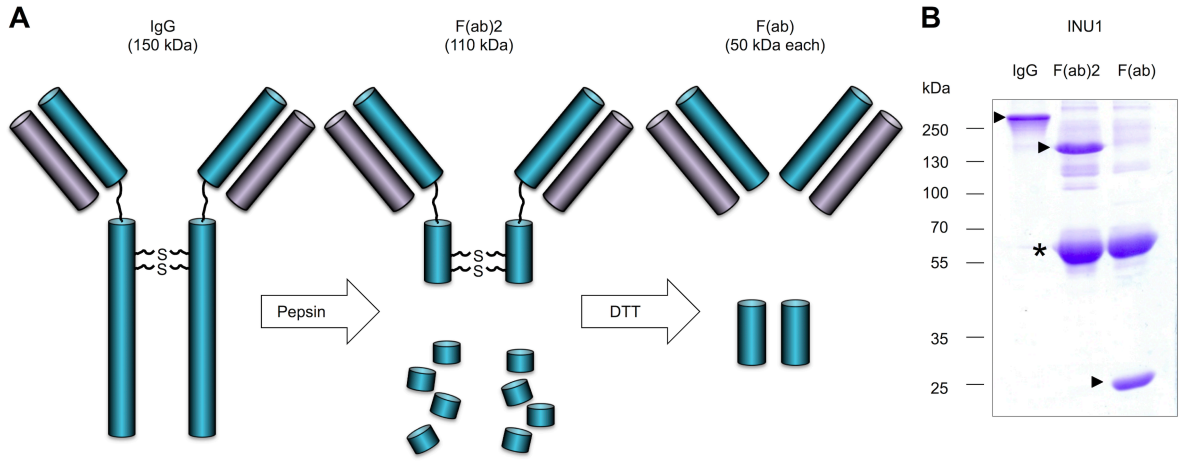

Figure 38. Preparation of monovalent F(ab) fragments. (A) The intact IgG was digested by pepsin to F(ab)2 fragments and subsequently to F(ab) fragments by DL-dithiothreitol (DTT)-meditated reduction. (B) The purity of the antibody-fragment preparation was tested on a Coomassie stained SDS gel. Of note, the F(ab) fragments should have a size of 50 kDa, as they consist of heavy and a light domain. However, under these experimental conditions a single band at 25 kDA is observed, due to a yet unknown reason. The arrowhead indicates the IgG, F(ab)2 and F(ab), respectively. The asterisk indicates residual BSA from the fragment preparation.

Monovalent INU1-F(ab) fragments are supposed to solely bind and block CLEC-2 without inducing intracellular signaling events, as they are not able to cluster the receptor. To test this directly platelet aggregation was assessed *in vitro* upon addition of INU1 IgG, F(ab)2 or

F(ab) fragments. As expected, the intact IgG as well as the F(ab)2 fragments induced aggregation in washed platelets, whereas the F(ab) fragments did not (Figure 39). Furthermore, 5 min preincubation with F(ab) could block RC-induced activation of CLEC-2 (Figure 39).

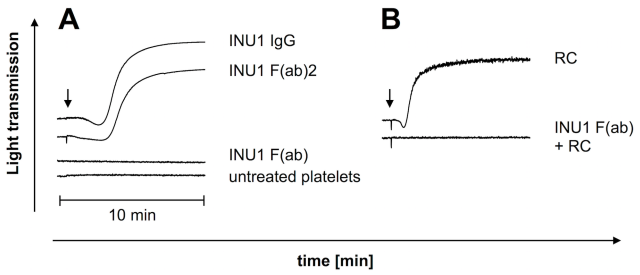

Figure 39. INU1-F(ab) fragments failed to induce platelet aggregation *in vitro*. (A) Washed platelets were stimulated with the INU1 antibody fragments as indicated under stirring conditions and light transmission was recorded on an aggregometer. (B) *Wt* platelets were preincubated with F(ab) fragments for 5 min and subsequently stimulated with rhodocytin (RC) under stirring condition and light transmission was recorded on an aggregometer. (RC: 0.24 µg/ml, antibody fragments: 20 µg/ml)

Next, the *in vivo* effects of INU1 F(ab) was tested. Unexpectedly, *in vivo* administration of 20 µg INU1-F(ab) in *Wt* animals resulted in the death of these mice within 20 to 30 min. All animals were treated with INU1 F(ab) under short-term isoflurane anesthesia. The injected animals displayed persistent generalized neurological deficits with muscle spasms, forelimb flexion, unidirectional circling and longitudinal spinning. Some animals displayed occasional episodes of paralysis. Finally, the treated animals showed symptoms of suffocation that appeared to be cause of death in most of the treated animals. Due to these deleterious results, further animal experiments were performed under deep anesthesia. These animals revealed a steady reduction in platelet counts, which over time reaching the lowest values shortly before death (Figure 40). This observation was unexpected, particularly in comparison to INU1 IgG treatment, which induced thrombocytopenia very rapidly (Figure 40).

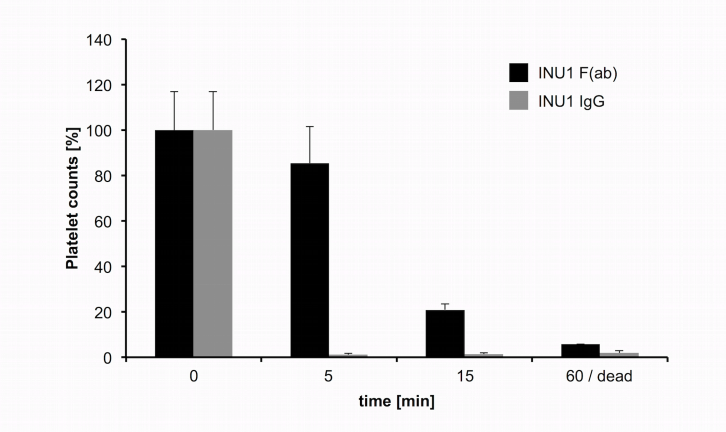

Figure 40. Delayed thrombocytopenia in INU1-F(ab) treated mice. Mice were injected with 100 µg INU1 IgG or 20 µg INU1 F(ab) and platelet counts were measured at the indicated time points by flow cytometry.

3.4.2 Accumulation of platelets in the brain after INU1 F(ab) treatment

To investigate where INU1 F(ab) opsonized platelet sequestrate, a whole body *in vivo* imaging system (IVIS) was applied. To label circulating platelets, mice were injected with 8 µg of anti-GPIX-Alexa750 antibody. After 4 h the mice were anesthetized and the abdominothoracic region was shaved. Subsequently, PBS, 20 µg INU1 F(ab) or 100 µg INU1 IgG were intravenously injected and the mice were immediately imaged for up to 1 h. Gray scale photographs showed the position of the mice and fluorescent images revealed the localization and temporal accumulation of fluorescently tagged platelets within the body (Figure 41 A). In the INU1 IgG injected animals, platelets accumulated in the spleen (Figure 41 A, white arrow). In contrast, upon INU1 F(ab) injection the labeled platelets accumulated within the lungs over time (Figure 41 A, blue arrow). After approx. 30 min, the INU1 F(ab)-injected mice were euthanized and organs of all three animals were harvested and analyzed separately in the IVIS device. After INU1 IgG and INU1 F(ab) treatment, platelet emboli were found in several organs, however, only INU1 F(ab) injection resulted in a massive accumulation of platelets within the brain (Figure 41 B). This is a very unique finding that has so far not been described for any other anti-platelet antibody derivative.

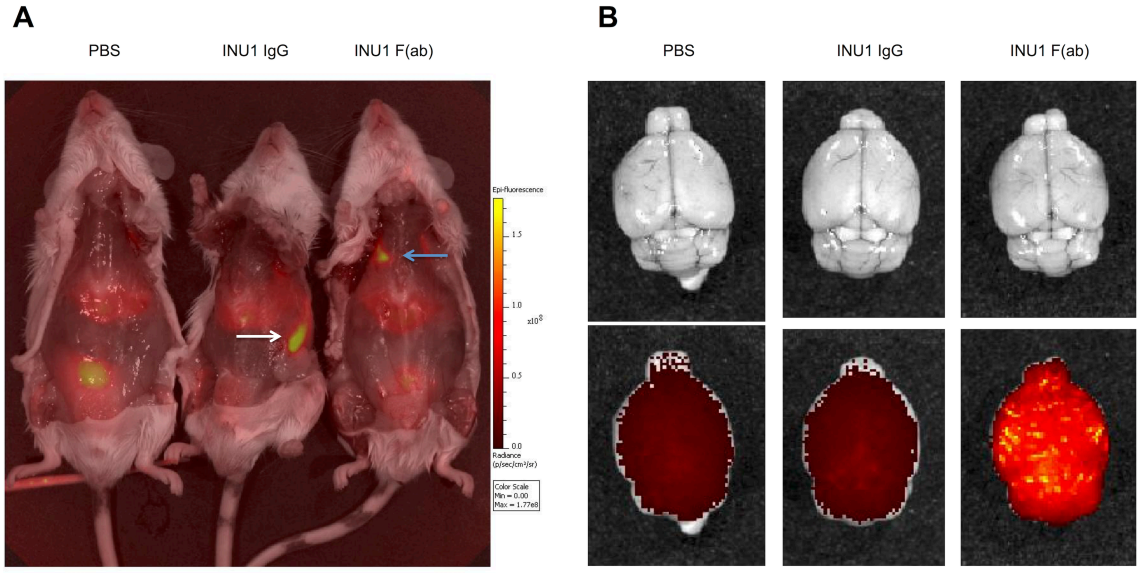

Figure 41. Whole body *in vivo* imaging after antibody treatment. (A) Mice were injected with an anti-GPIX-Alexa750 antibody 4 h prior to the experiment. Anesthetized mice were shaved, injected with PBS, 100 µg INU1 IgG or 20 µg INU1-F(ab) and images in an *in vivo* imaging system (IVIS) were acquired at a wavelength of 800 nm. After INU1 IgG treatment, platelets accumulated in the spleen (white arrow) and after INU1 F(ab) treatment in the lungs (blue arrow). (B) After sacrificing the animals, the brains were harvested and analyzed separately in the IVIS. Therein, a massive accumulation of platelets was detected after INU1 F(ab) treatment that was not present after INU1 IgG or PBS injection.

3.4.3 Platelet-rich thrombi form in the brain after INU1 F(ab) injection

To investigate the mechanism underlying the INU1 F(ab)-induced platelet accumulation within the brain, we used transcranial two photon-intravital microscopy (2P-IVM) of the brain in living mice. Therefore, mice were anesthetized and the frontopariental skull bone was thinned using a “Dremel’s” rotatory tool. After 24 h the mice were again anesthetized and placed on a customized metal stage equipped with a stereotactic holder to immobilize the head. Brain vasculature was visualized by injection of tetramethylrhodamine dextran. Platelets and MKs were labeled with an anti-GPIX-Alexa 488 antibody. Subsequently, 50 µg INU1 F(ab) were injected via a jugular vein catheter and live images were acquired with a 2P microscope equipped with a 20x water objective (Figure 42).

Approx. 15 min after INU1 F(ab) injection, the first alterations in the blood flow velocity were observed. After 20 min, bigger platelet aggregates appeared. These emboli circulated through the brain vessels and increased in size until they occluded a vessel (Figure 42). On the other hand, thrombus formation also appeared to be initiated at the vessel wall (Figure 42 B, blue arrowhead). Small platelet aggregates interacted with the vessel wall resulting in the recruitment of further platelets and in the formation of a platelet rich thrombus.

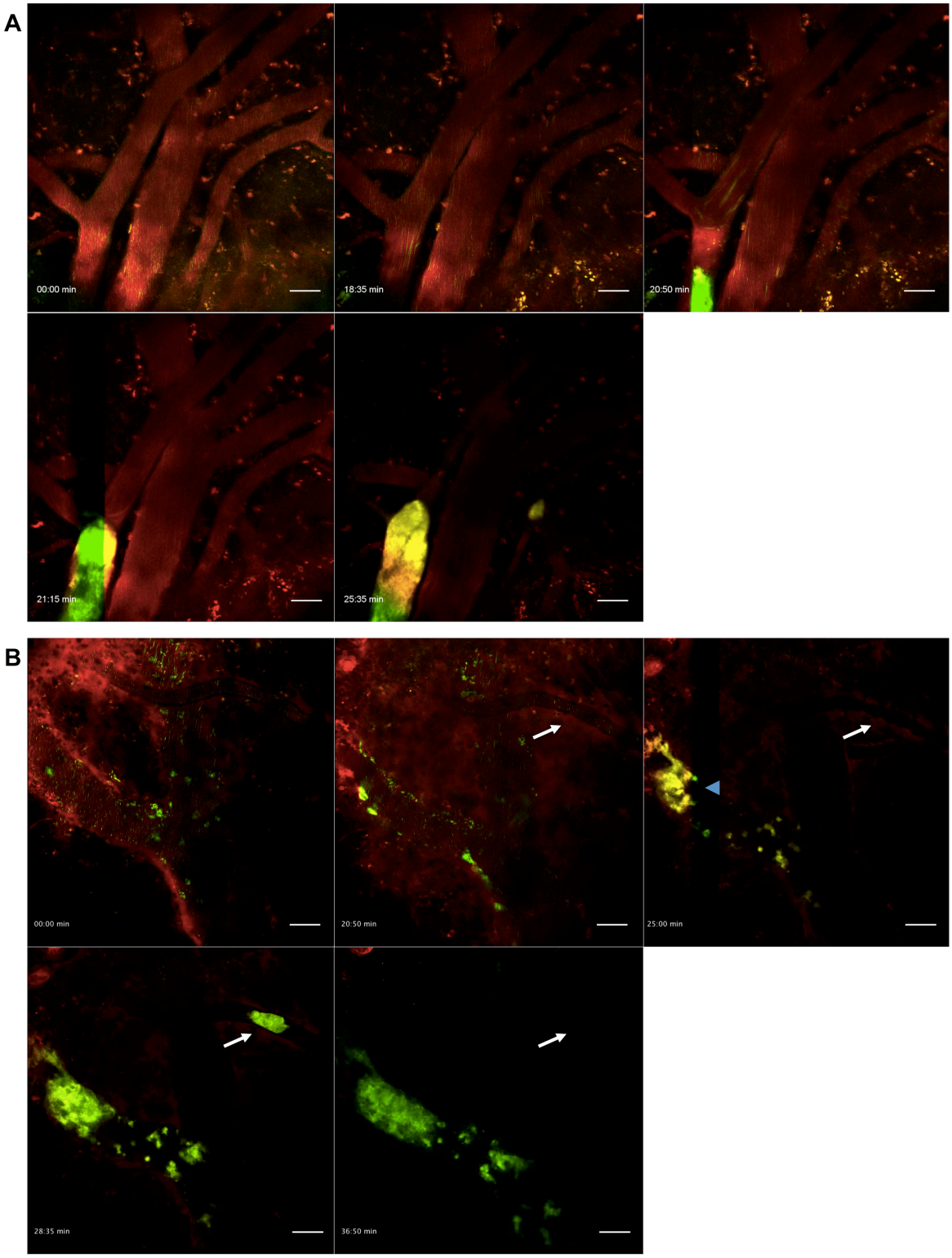

Figure 42. INU1-F(ab)-induced thrombi dissemination and formation in the brain vasculature. (A,B) Chronological images of two-photon intravital microscopy (2P-IVM) recordings of two representative mice are depicted. Mice were injected with tetramethylrhodamine dextran to label blood vessels and an anti-GPIX-Alexa488 antibody to stain MKs and platelets. 50 µg INU1 F(ab) was injected via a subclavian vein catheter and live images were acquired using a 2P microscope equipped with a 20x water objective and a TriM Scope II multiphoton system (LaVision BioTec), controlled by ImSpector Pro-V380 software (LaVision BioTec). Both, thrombus formation within the brain (blue arrowhead) as well as embolization in the brain (white arrow) could be oberserved. (Scale bar 50 µm)

3.4.4 INU1 F(ab)-induced thrombi are distributed over the entire brain

The real-time *in vivo* imaging provides very good temporal resolution of the INU1 F(ab)-induced thrombus formation, however, only a small part of the brain can be visualized. Therefore, another recently developed microscopy technique was used in collaboration with Judith van Eeuwijk. In light-sheet fluorescence microscopy (LSFM), also termed selective/ single plane illumination microscopy (SPIM), intact organs can be analyzed. A laser light sheet optically sections the tissue samples. To enable the penetration of the tissue with the laser light sheet, organs need to be transparent.

To analyze the brains with LSFM, mice were anesthetized, circulating platelets were stained with an anti-GPIX Alexa750 antibody and 50 µg INU1 F(ab) were injected. After 15 min, the mice were perfused with PBS and 4% PFA for fixation and the brains were harvested. Over the next days the brains were cleared and immersed in BABB/ clearing solution. The brains became optically transparent and could be imaged by LSFM (Figure 43). We found that platelet aggregates were distributed throughout the entire brain upon INU1 F(ab) injection. However, it is not yet clear if the thrombi were formed within the arterial or venous system of the brain, as this distinction is so far not possible with LSFM.

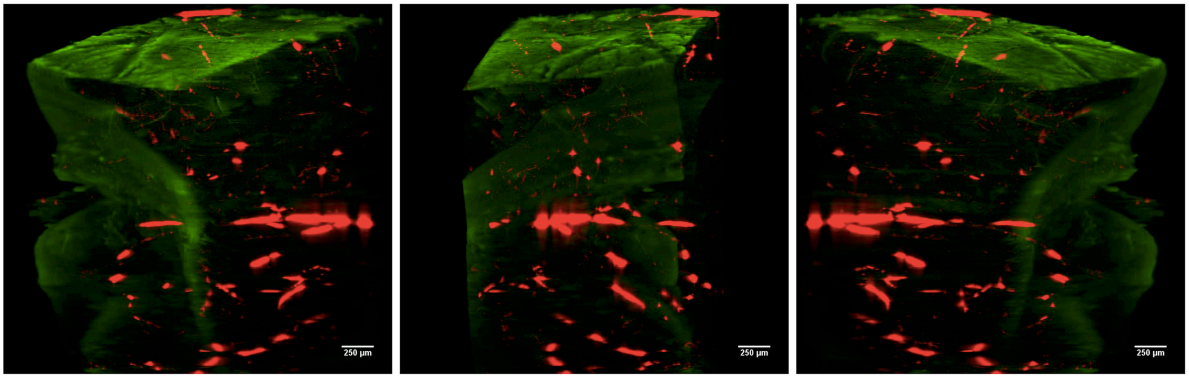

Figure 43. INU1 F(ab)-induced thrombi were distributed through out the entire brain. Mice were injected with 20 µg INU1 F(ab) and after 15 min perfused with PBS and 4% PFA. Subsequently, the brains were dissected, cleared and visualized using LSFM. Circulating platelets were labeled with an anti-GPIX Alexa750 antibody and visualized platelet aggregate formation. The brain tissue is depicted in green (second harmonic). (Scale bar 250 µm)

To address this question directly, transmission electron microscopy (TEM) of brain sections was performed in collaboration with Prof. Süleyman Ergün from the Institute of Anatomy and Cell Biology. Mice were anesthetized, injected with PBS or 20 µg INU1 F(ab) and 15 min later perfused with PBS and 2% glutaraldehyde/ 1% PFA for fixation. Skulls containing the brains were dissected and after decalcification brains were processed for TEM as described in the methods section. In control brains, arteries and veins were visible and distinguishable by their morphology (Figure 44 A). After INU1 F(ab) treatment no thrombi were observed

within the veins, however, the arteries were occupied with platelet-rich thrombi containing fibrin fibers and soluble fibrin (Figure 44 B).

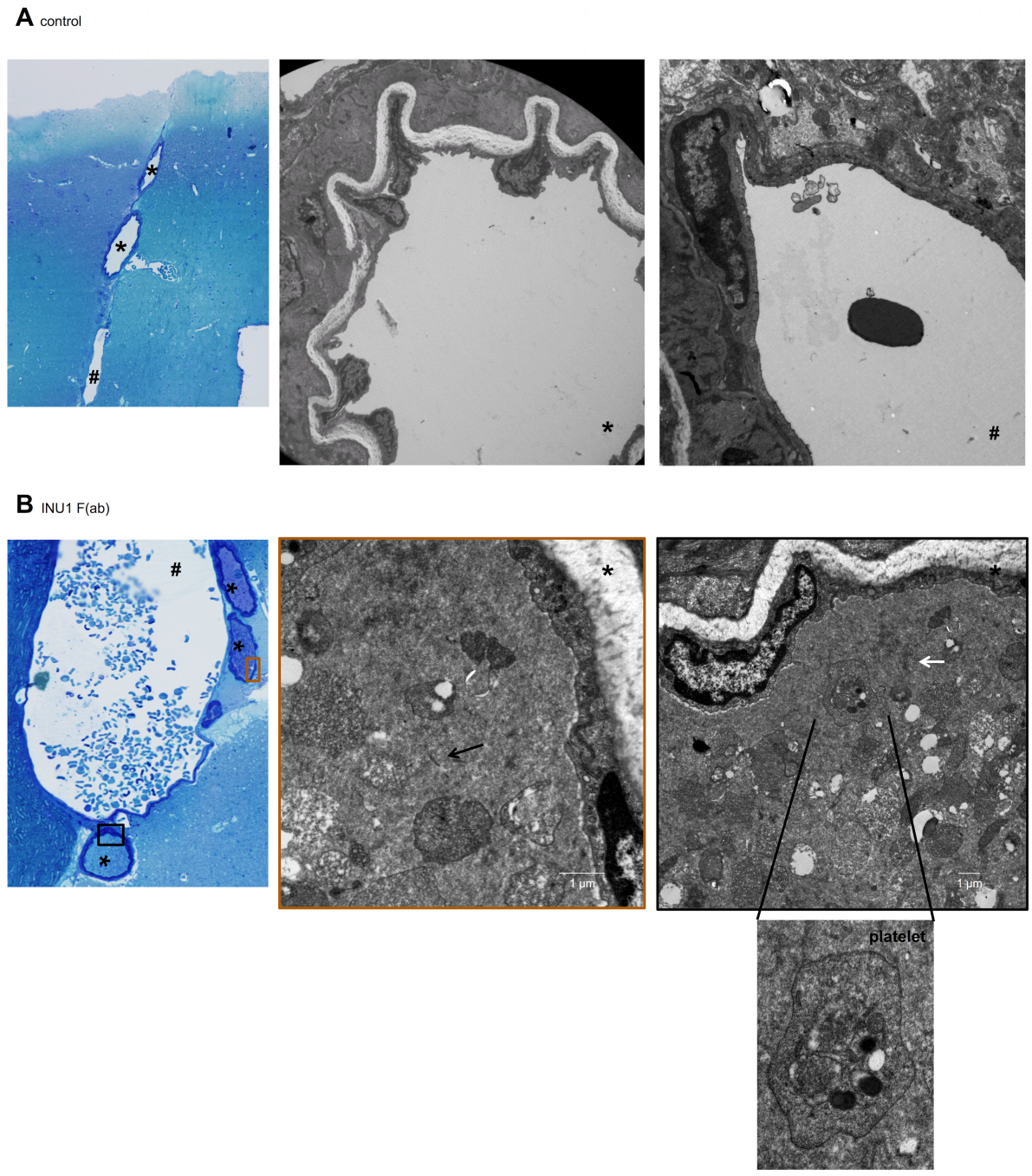

Figure 44. INU1 F(ab)-induced platelet-rich thrombi are trapped in arteries. Mice were injected with PBS as control or INU1 F(ab) and perfused with PBS and 2% glutaraldehyde/ 1% PFA for fixation. Skulls containing the brains were dissected and after decalcification the brains were processed for TEM. Semi-thin sections were stained with methylene blue to locate positions for TEM samples. These sections were inspected with an LEO912AB electron microscope (LEO, Oberkochen, Germany). The asterisk indicates arteries, the hashtag indicates veins. Soluble fibrin is indicated by the white arrow and fibrin fibers are indicated by the black arrow.

3.4.5 INU1 F(ab)-induced platelet aggregation is not restricted to the brain

As mentioned above, whole body imaging showed that fluorescently labeled platelets accumulated not solely in the brain but emboli rather were found in various organs. To investigate the morphology and dissemination of these emboli in more detail, paraffin sections of brain, liver, kidney, lung, heart and spleen of PBS and INU1 F(ab)-treated mice were analyzed. Emboli-occluded blood vessels were observed in the sections of different organs (Figure 45, black arrow). This indicated that the INU1 F(ab)-induced platelet aggregation is not limited to the brain but is rather a general process that occurs within the blood stream.

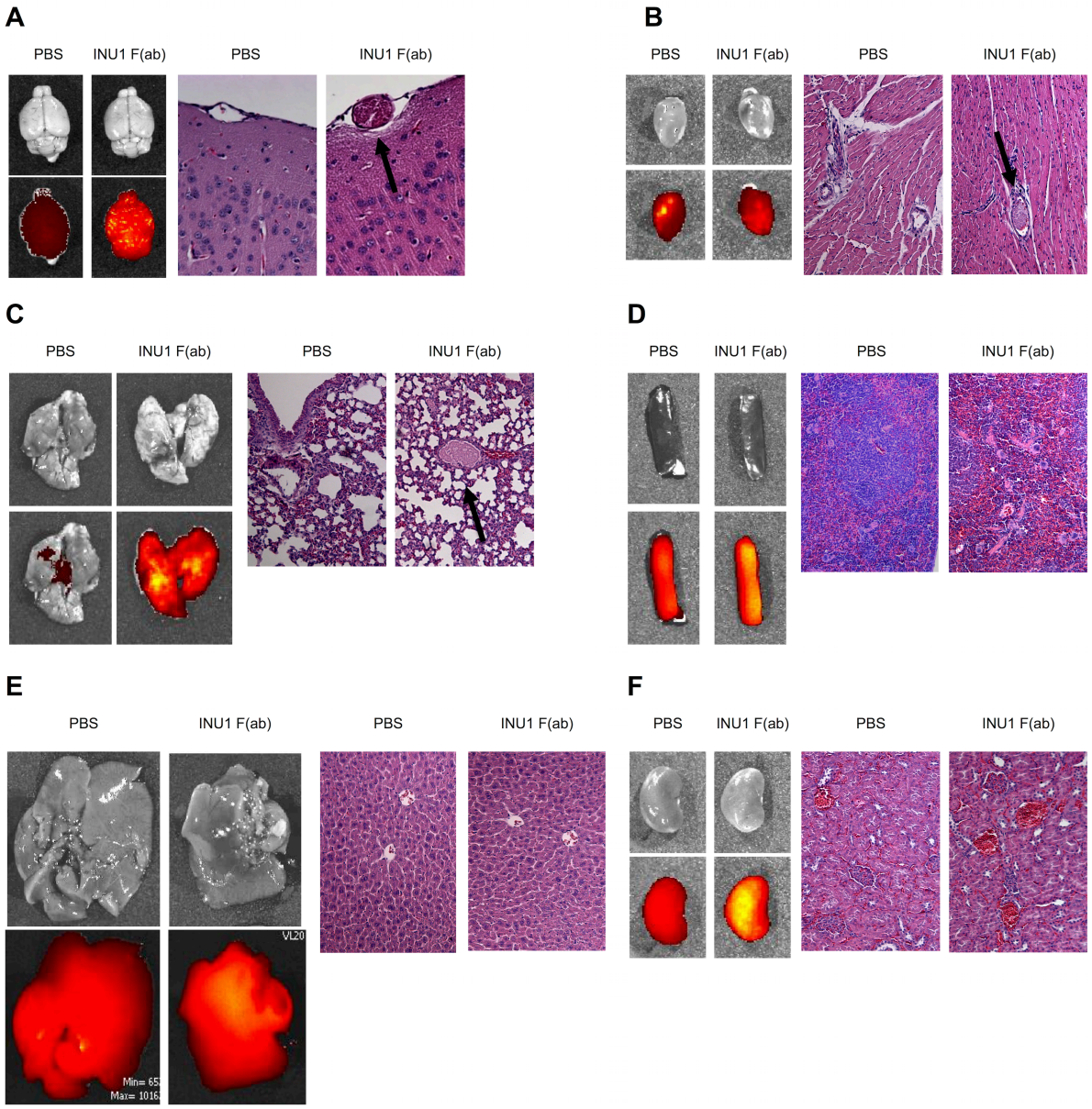

Figure 45. Platelet aggregates were found in different organs after INU1 F(ab) injection. Mice were injected with an anti-GPIX-Alexa750 antibody 4 h prior to the experiment. Anesthetized mice were injected with PBS or 20 µg INU1-F(ab), organs were harvested and imaged using an IVIS. Thereafter, organs were fixed and paraffin-sections were stained with eosin and hematoxylin. Representative sections for (A) brain, (B) heart, (C) lung, (D) spleen, (E) liver and (F) kidney are shown. Arrows indicate occluded vessels.

3.4.6 INU1 F(ab)-induced thrombus formation depends on platelet CLEC-2 and platelet aggregation

Based on the finding of ubiquitous embolization, the mechanisms underlying the INU1 F(ab)-induced thrombus formation were analyzed in more detail. To elucidate the involvement of CLEC-2 signaling, granule release, platelet aggregation and the role of other blood cells, different genetically modified mouse strains and interventions were used (Table 2).

Table 2: Overview of different mouse strains injected with INU1 F(ab). Mouse strains that did not shown neurological reactions upon INU1 F(ab) injection are highlighted in red. (depl.: depleted, mut.: mutated, bl.: blocked, n. d.: not determined)

	Animals with neurological symptoms (death)	total no. animals	no. experiments	comments/ observations
Wt	103 (81)	103	n > 30	thrombocytopenia
platelet depl.	0 (0)	9	n = 3	-
CLEC-2 depl.	0 (0)	9	n = 3	no thrombocytopenia
Clec1b$^{fl/fl\ PF4cre}$	0 (0)	7	n = 2	no thrombocytopenia
hemITAM mut. (Y7A) (fetal liver chimeras)	0 (0)	8	n = 1	no thrombocytopenia
Dasatinib-treated	0 (0)	3	n = 1	n. d.
Syk$^{ZAP\ KIN}$ [127]	0 (0)	4	n = 1	n. d.
Lat$^{-/-}$	5 (3)	12	n = 4	thrombocytopenia
Grb-2$^{fl/fl\ PF4cre}$ [128]	4 (4)	4	n = 1	n. d.
SLAP$^{-/-}$*/SLAP2*$^{-/-}$ [129]	9 (0)	*9*	*n = 2*	thrombocytopenia
GPIIbIIa bl. (JON/A F(ab))	0 (0)	15	n = 4	no thrombocytopenia
Tln1$^{fl/fl\ PF4cre}$	0 (1)	11	n = 3	no thrombocytopenia
CD41-YFP ^{KIN} (GPIIb)	0 (0)	5	n = 1	no thrombocytopenia
Gp5$^{-/-}$	4 (4)	4	n = 1	n. d.
GPIb bl. (p0p/B)	6 (6)	9	n = 3	thrombocytopenia
vWF$^{-/-}$	5 (0)	5	n =1	thrombocytopenia
Clopidogrel-treated	8 (3)	8	n = 3	n. d.
Hirudin-treated	7 (7)	7	n = 2	n. d.
F12$^{-/-}$ [133]	6 (5)	6	n =2	thrombocytopenia
Neutrophils depl.	3 (3)	3	n = 1	n. d.
Nbeal2$^{-/-}$ [134]	0 (0)	21	n = 4	delayed/ reduced thrombocytopenia
Munc13-4 KO (*Unc13d*$^{-/-}$) [135]	0 (0)	14	n = 4	temporary neurological deficits; thrombocytopenia

Neurological symptoms induced by INU1 F(ab) depended on the presence of platelets and the presence of CLEC-2 on the platelet surface. Furthermore, receptor-mediated signal transduction was required, as the inhibition of SFK by Dasatinib, the deficiency of Syk or mutation of the hemITAM tyrosine (Y7A) prevented neurological deficits and eventual mortality. However, the lack of certain adaptor proteins, such as Lat, the Src-like adaptor protein (SLAP)/ SLAP2 and the growth factor receptor-bound protein-2 (Grb-2) could not prevent the appearance of neurological reactions. This indicates that INU1 F(ab) induces classical CLEC-2 signaling that leads to platelet activation *in vivo*.

In line with this hypothesis, platelet aggregation was observed within the brain in 2P-IVM. Accordingly, interference with integrin function by genetic approaches or antibody-treatment prevented platelet aggregate formation and thus INU1 F(ab)-induced thrombocytopenia and lethality (Figure 46 A). Of note, the INU1 F(ab)-opsonized platelets circulated in a resting state in *Tln1*$^{fl/fl\ PF4cre}$ mice, thus indicating that the activation of integrins plays a crucial role in INU1 F(ab)-induced platelet activation (Figure 46 B, C). TEM analysis revealed that the INU1 F(ab)-induced thrombi are formed in arteries, where higher shear rates prevail as found compared to veins. It is known that under high shear conditions the interaction between the GPIb-V-IX complex and vWF is mandatory to allow platelet adhesion. However, neither the deficiency of GPV or vWF or the inhibition of GPIb had an effect on the INU1 F(ab)-associated neurological symptoms. This suggests that the INU1 F(ab)-induced thrombus formation is triggered by a yet unknown mechanism potentially mediated by an unknown ligand which binds to INU1 F(ab)-opsonized CLEC-2.

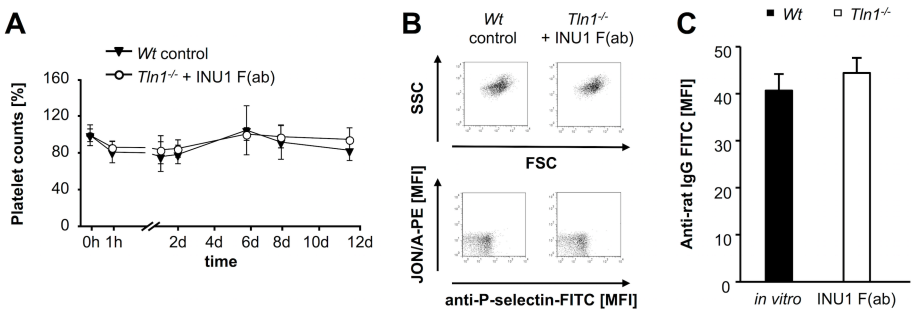

Figure 46. *Tln1*$^{-/-}$ mice are protected from INU1 F(ab) induced lethality. (A) *Tln1*$^{-/-}$ mice were injected with 20 µg INU1 F(ab) and platelet counts were determined on a FACSCalibur at the indicated time points. (B) Flow cytometric analysis of *Wt* control and INU1 F(ab)-injected *Tln1*$^{-/-}$ platelets 24 h after injection. FSC and SSC as well as the αIIbβ3 activation and degranulation-dependent P-selectin exposure are displayed. (C) 24h after INU1 F(ab) injection washed blood of *Tln1*$^{-/-}$ mice was incubated for 15 min with an anti-rat Ig-FITC antibody and subsequently analyzed on a FACSCalibur. As *in vitro* control, blood from untreated mice was incubated with 20 µg/ml INU1 F(ab) for 15 min, washed and incubated with an anti-rat Ig-FITC antibody for 15 min.

Interestingly, treatment of mice with the widely used anti-platelet drug clopidogrel, which irreversibly inhibits the ADP receptor $P2Y_{12}$, could not inhibit the INU1 F(ab)-induced effects. Similar results were obtained upon pretreatment of mice with hirudin, a potent direct thrombin

inhibitor. Furthermore, to investigate whether the intrinsic coagulation cascade is involved in the INU1 F(ab)-induced thrombus formation, coagulation factor XII (FXII)-deficient animals were tested. These animals are protected from pathological thrombus formation due to reduced fibrin formation.[133] However upon injection of INU1 F(ab), these animals developed severe neurological deficits and died shortly thereafter. This indicates that INU1 F(ab)-induced thrombosis occurs independently of the intrinsic coagulation cascade.

Activated platelets are able to bind to adherent neutrophils, which result in robust neutrophil activation and the formation of neutrophil extracellular traps (NETs).[149] This extracellular DNA could provide a scaffold for thrombus formation.[150] To analyze whether NET formation contributes to INU1 F(ab)-induced thrombus formation, neutrophils were depleted by intravenously injection of an anti-Ly6G antibody (5 mg/kg body weight) 24 h prior to the experiments.[151] The depletion of neutrophils was confirmed by flow cytometry directly before the experiment. Subsequently, the mice were injected with INU1 F(ab). All injected animals still displayed robust intravascular thrombus formation and died. This suggests that INU1 F(ab)-triggered thrombus formation did not depend on the interaction of platelets with leucocytes but rather on a component that gets released by platelets.

Therefore, different genetically modified mouse strains were applied to the INU1 F(ab) treatment that either displayed an abolished platelet dense granule secretion and a reduced α-granule release (Munc13-4 knock out (*Unc13d*$^{-/-}$))[135] or completely lack α-granules (*Nbeal2*$^{-/-}$).[134] Mice of both strains were protected from INU1 F(ab)-induced mortality. However, Munc13-4-deficient animals temporarily showed some neurological symptoms including muscle spasms and longitudinal spinning for approx. 1 h after INU1 F(ab) injection. However, approx. 30 min later these symptoms ceased and the behavior of the injected animals was indistinguishable from control animals. Of note, the platelet counts of these animals decreased during this period of time. In contrast, non of the INU F(ab)-injected *Nbeal2*$^{-/-}$ mice showed any neurological symptoms. *Nbeal2*$^{-/-}$ mice have a moderate thrombocytopenia with approx. 60% platelet count as compared to *Wt* animals.[134] Upon injection of INU1 F(ab) platelet counts in these mice decreased to approx. 40% of the starting values and circulating platelets were opsonized with the F(ab) fragments (Figure 47). This striking result suggests that a component within the platelet α-granules may play a critical role in INU1 F(ab)-induced thrombus formation responsible for in the neurological deficits and death of the animals.

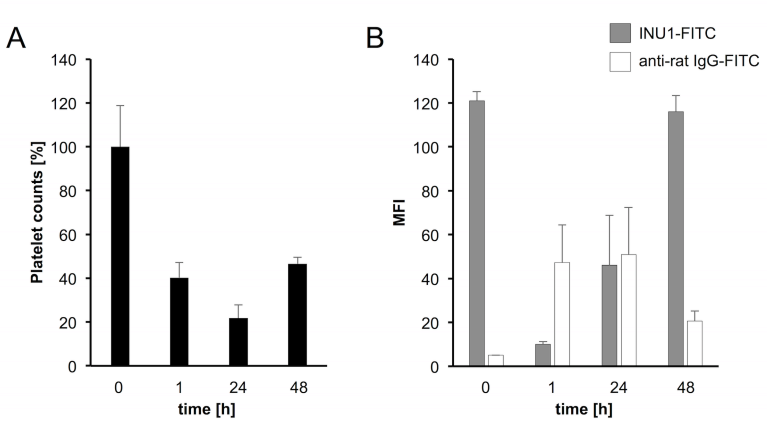

Figure 47. Nbeal2 deficiency protects from INU1 F(ab)-induced mortality. *Nbeal2*$^{-/-}$ mice were injected with 20 µg INU1 F(ab) and were bled at the indicated time points. (A) Platelet counts, (B) INU1 FITC and anti-rat IgG-FITC signals were measured by flow cytometry.

3.4.7 INU1 F(ab) induces platelet aggregation under flow conditions *in vitro*

The previous results from the 2P-IVM indicated that INU1 F(ab)-opsonized platelets have the capacity to interact with the vessel wall and to induce a yet not fully understood mechanism of thrombus formation. To gain more insight into this new mechanism, platelet spreading on different matrices was analyzed in the presence or absence of INU1 F(ab) (Figure 48).

Washed platelets were allowed to spread on a fibrinogen-coated surface after stimulation with 0.01 U/ml thrombin. Interestingly, INU1 F(ab)-treated platelets formed filopodia and lamellipodia to the same extent and with the same kinetics as control platelets (Figure 48 A). In a next step, spreading on a vWF-coated surface was analyzed and found to be slightly inhibited upon preincubation of platelets with INU F(ab) (Figure 48 B). Moreover, incubation of platelets under static conditions on a INU1 F(ab)-coated surface did not induce any platelet activation or spreading (Figure 48 C). Together, these results demonstrate that the *in vivo* observed INU1 F(ab)-induced platelet activation and aggregate formation could not be reproduced *in vitro* under stirring (Figure 39) or static conditions (Figure 48).

A flow based *in vitro* assay was performed, to adjust the *in vitro* conditions to those occurring *in vivo*. Washed platelets, platelet-rich plasma or whole blood was perfused over a BSA-blocked coverslips with at a shear rate of 1700 s^{-1}, which represents the prevailing shear in arterioles (Figure 49 A-C).

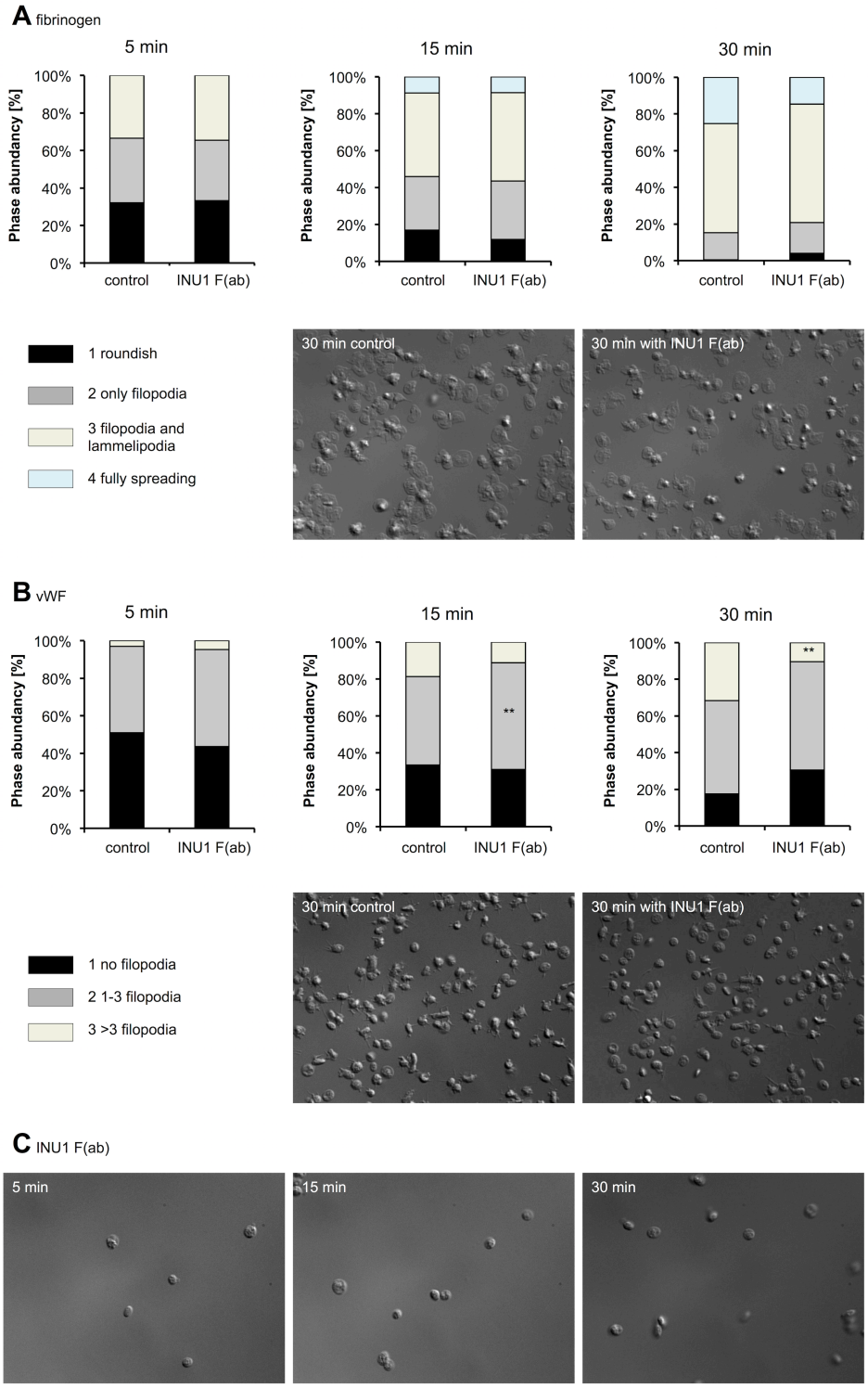

Figure 48. INU F(ab) does not induce platelet spreading. Washed *Wt* platelets were allow to spread on different matrices in the presence of Ca^{2+}. Representative DIC images were taken at the indicated time points and statistical analysis spread platelet at the different spreading stages is shown. (A) Spreading was performed on fibrinogen-coated coverslips and platelets were stimulated with 0.01 U/ml thrombin. (B) Spreading was performed on vWF-coated coverslips in the presence of integrilin (40 µg/ml) and botrocetin (2 µg/ml). (C) Spreading was performed on a INU1 F(ab)-coated coverslip without additional stimulation.

The flow through from the flow chamber was collected, fixed in 4% PFA and stained with anti-GPIX-Alexa647 antibodies for 15 min. Thereafter, representative images were captured. Under all conditions, untreated *Wt* platelets were still present as single platelets after passing the flow chamber (Figure 49 A-C). Treatment of washed platelets or PRP with 20 µg/ml INU1 F(ab) yielded the same results observed for the untreated platelets (Figure 49 A, B). In contrast, after perfusion of INU1 F(ab)-treated whole blood, large platelet aggregates were observed in the flow through (Figure 49 C). As a control experiment, this was repeated with INU1 F(ab)-treated whole blood from *Nbeal2*$^{-/-}$ mice. Here, the flow did not induce thrombus formation and again single platelets were visible (Figure 49 D). This approach allowed the reproduction of the INU1 F(ab)-induced platelet activation and aggregate formation under *in vitro* conditions. It corroborates the assumption that a potential component in platelet α-granules contributes to the INU1 F(ab) induced phenotype. Furthermore, this could provide the basis for further experiments striving to identify a possible, yet still unknown ligand playing a crucial role in INU1-induced thrombus formation and CLEC-2-dependent thrombus stabilization.

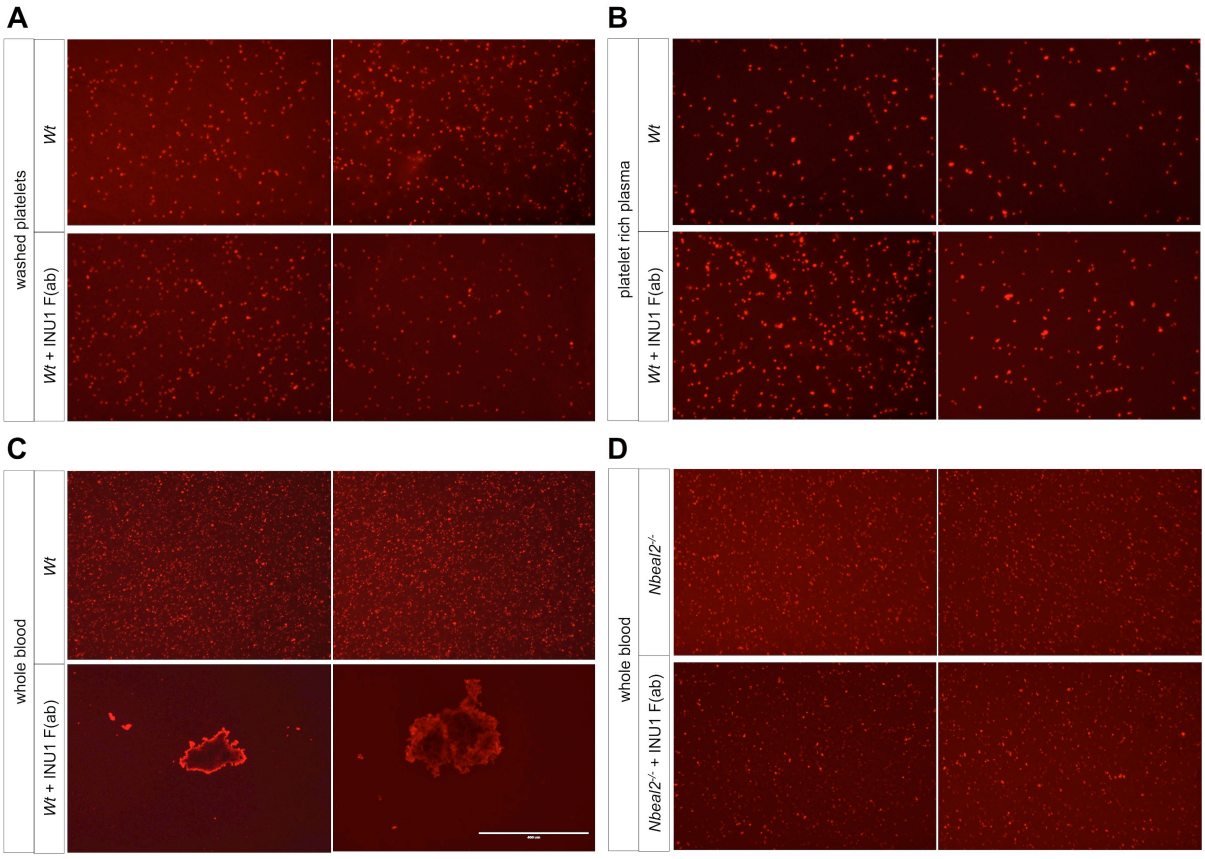

Figure 49. INU1 F(ab)-induces platelet aggregation in whole blood under flow conditions *in vitro*. (A) Washed platelets, (B) platelet-rich plasma or whole blood from (C) *Wt* or (D) *Nbeal2*$^{-/-}$ mice was either untreated or incubated with 20 µg/ml INU1 F(ab) for 15 min followed by perfusion over a BSA-blocked coverslip at a shear rate of 1700s^{-1}. The flow through was collected in 4% PFA and platelets were stained with an anti-GPIX-Alexa647 antibody for 15 min. Representative pictures were taken. (Scale bar 400 µm) (n = 4, representative of at least three independent experiments)

4 DISCUSSION

Platelet activation and aggregation at sites of vascular injury is essential to limit blood loss, but under pathological conditions it may lead to complete vessel occlusion and, due to the occurrence of emboli, to stroke. Therefore, platelet signaling has become an important field of biomedical research over the last decades yielding many widely used drugs for the treatment and prevention of cerebro- and cardiovascular diseases. Aspirin and clopidogrel are perhaps the most common ones, acting by inhibition of platelet function. However, application of any currently available antithrombotic agents is often associated with an increased bleeding risk, which may outweigh it therapeutic effect or even possibly lead to life-threatening complications. Hence, the detailed analysis of platelet activation, the regulation of surface receptors and the respective signaling pathways has become a rapidly developing field of research during the last decades with the aim identified new therapeutic options.

The mouse has become an indispensible model system for thrombosis research, as they have striking similarities to humans in anatomy, physiology and genetics. 99% of mouse genes have direct counterparts in humans.[152] Mice are a cost-effective and efficient tool, as they are small, highly fertile and have a short generation time. In platelet research there are some concerns about the transferability of results from mice to humans due to differences in the expression of some platelet surface receptors. However, mouse models are established that mimic human platelet disorders such as the gray platelet syndrome (GPS),[153,154] Glanzmann's thrombasthenia[155] or Bernard-Soulier syndrome.[156] The possibility to directly manipulate the mouse genome provides a powerful tool to modify platelet surface receptors. This enables the identification of potential targets for anti-thrombotic therapy, as multiple *in vivo* models are established to study e.g. thrombosis, ischemic stroke or myocardial infarction in mice.

The recently identified C-type lectin-like receptor 2 (CLEC-2) and the major collagen receptor GPVI have been proposed as promising new anti-thrombotic targets based on the results of several murine studies.[25,35,75] Both receptors can be depleted from the surface of circulating platelets by antibodies.[17,74] Previously it has been shown that GPVI downregulation occurs through two distinct pathways, namely ectodomain shedding or internalization/ intracellular clearance.[92] The results presented in this thesis demonstrate for the first time that CLEC-2 is downregulated from the platelet surface by internalization *in vitro* and *in vivo*. Single deficiency of either GPVI or CLEC-2 results in protection from occlusive arterial thrombus formation without compromising hemostasis in mice. However, double-deficient animals show a dramatic hemostatic defect revealing partially redundant functions of these receptors.

Furthermore, we generated F(ab) fragments of the CLEC-2-binding antibody INU1, which could block CLEC-2-dependent signaling *in vitro*. Unexpectedly, treatment of mice with INU1 F(ab) resulted in widespread intravascular thrombus formation in different organs, including the brain. This is a very unique finding that has been so far not described for any other anti-platelet antibody derivative. The mechanism underling this pathogenic effect has not been clarified yet, but it potentially depends on binding of a still unknown ligand to the antibody-fragment opsonized CLEC-2.

Together, these data provide new insights into the regulation and function of CLEC-2 and GPVI and may be important for the development of potential future therapeutics.

4.1 GPVI and CLEC-2 have partially redundant function in hemostasis

4.1.1 CLEC-2 plays a central role in lymphatic vessel development and pathological thrombus formation

In the present study, a conditional knock out approach using the PF4-Cre/loxP system was used to investigate the effect of CLEC-2 deficiency on embryonic development and platelet function *in vitro* and *in vivo*. It was found that MK/ platelet-specific deletion of CLEC-2 resulted in a defective lymphatic vessel development, a mild thrombocytopenia, reduced thrombus stability with consecutive embolization as previously published.[45,46] Hemostasis, however, was largely normal in these animals. These results confirm our previous findings obtained from antibody-induced depletion of CLEC-2.[17]

This study shows that MK/ platelet-specific CLEC-2-deficient animals exhibit impaired lymphatic vessel development resulting in the appearance of blood-filled lymphatic vessels in the mesenteries (Figure 10 A). This result corresponds to previous studies describing “non-separating” phenotypes in mice deficient for proteins involved in CLEC-2 signaling pathway, namely Syk,[46] SLP-76,[50-52] and PLCγ2.[53] In mice, lymphatic endothelial cells (LEC) first differentiate in the anterior cardinal vein around embryonic day 9.5 (E9.5) when a subset of venous endothelia cells expresses the transcription factor Prox1 and the lymphatic vessel hyaluronan receptor-1 (LYVE-1).[157,158] Lymphatic vascular development requires separation of blood and lymphatic vasculature, sprouting of lymphatic vessels and subsequent vascular maturation.[158] Platelets are important for keeping both vascular systems apart through the interaction of podoplanin expressed on the lymphatic endothelium and CLEC-2 on platelets.[43,49] MK/ platelet-specific CLEC-2 knock out animals develop a peripheral lymphatic system exhibiting a defective separation from the blood vasculature and an impaired lymphatic vascular organization (Figure 10 A). These results are in line with previous findings described in podoplanin knock out mice were similar defects have been described.[157] One

possible explanation for the phenotype seen in MK/ platelet-specific CLEC-2 knock out animals might be that, during primitive hematopoiesis in the yolk sac, the rapid formation of platelets enables residual levels of CLEC-2 protein. The expression pattern of the PF4-cre transgene during early embryogenesis is not clear and a recent publication described that recombination was observed in liver MKs as soon as E11.5 and persisted at E16.5.[159] Primitive hematopoiesis from MK/ erythroid progenitors starts at E7.5 and first yolk sac-derived platelets appear at E9.5.[160-162] About the same time the lymphatic development starts and residual levels of CLEC-2 might be present in platelets so that the lymphatic development might be initiated. However, for sealing blood-lymphatic connections and maintaining of the lymphatic integrity throughout life, the persistent interaction of platelet CLEC-2 and podoplanin seems to be necessary. This assumption is supported by studies in irradiated mice transplanted with fetal liver cells from CLEC-2-deficient embryos.[46] These animals develop the same clinical phenotype with blood-filled lymphatic vessels as observed in MK/ platelet-specific CLEC-2 knock out animals. The exact contribution of platelet CLEC-2 to lymphatic vessel development and integrity is an important area for further investigations.

Over the last years several groups have intensively studied the role of CLEC-2 in platelet function. Here, we showed that platelet CLEC-2 deficiency results in severely impaired thrombus formation under flow conditions *in vivo*, as revealed by intravital microscopy using the ferric chloride injury model (Figure 15). This finding is corroborated by the observation that antibody-induced depletion of CLEC-2 results in a similar thrombus formation defect.[17] The initial adhesion of CLEC-2-deficient platelets on the injured vessel was unaltered, as was indicated by the regular formation of small aggregates at the site of injury (Figure 15). This finding is further supported by a previous *in vitro* study demonstrating that antibody-induced CLEC-2-depleted platelets normally adhere on a collagen-coated surface, however further platelets failed to firmly interact with the adherent platelets and were permanently released.[17] This is not surprising as this first tethering/ adhesion process is mediated by the actions of GPIb, GPVI, $\alpha 2\beta 1$ and $\alpha IIb\beta 3$ integrins.[15,163] CLEC-2-dependent signaling appears to be rather important for the stabilization of direct platelet-platelet contacts in the growing thrombus, as single platelets were constantly released and also small aggregate fragments frequently detached from the surface of the thrombus (Figure 15). Consequently, these animals were significantly protected from arterial vessel occlusion. The importance of CLEC-2 for thrombus stabilization *in vitro* and *in vivo* was subsequently supported by Suzuki-Inoue *et al.*, who used another genetic knock out approach.[25] The group generated CLEC-2-deficient chimeric mice by transplanting fetal liver cells from constitutive CLEC-2 knock out embryos into irradiated *Wt* mice.[25] The authors reported normal adhesion but a significantly reduced thrombus propagation of CLEC-2-deficient platelet on a collagen surface under flow *in vitro*.[25] Furthermore, in line with data of the here presented study, these CLEC-2-deficient

mice displayed virtually abolished aggregate and thrombus formation in a model of laser-induced injury of mesenteric arterioles.[25] This defect was apparent by the frequent release of only loosely attached platelets from the vessel wall or from platelet aggregates finally preventing vessel occlusion.

The mechanism underlying CLEC-2 activation and function in thrombus formation remains elusive as the only known physiological ligand of the receptor, podoplanin, is widely expressed outside the blood vasculature.[35,47] According to the data presented here, one may speculate that the potential ligand of CLEC-2 may circulate in the plasma or may be expressed/immobilized on the surface of activated platelets supporting thrombus stabilization. In agreement with this assumption, Suzuki-Inoue *et al.*, recently proposed an interesting mechanism for thrombus stabilization involving CLEC-2 itself as a ligand candidate.[45] They demonstrated in different *in vitro* analyses that CLEC-2 molecules are able to undergo direct homophilic associations.[45] This means that CLEC-2 on one platelet might be able to bind a CLEC-2 molecule on another platelet.[45] However, the importance of this interaction for thrombus formation and the mechanism that regulates a possible switch between different homophilic binding affinities of CLEC-2 on resting and activated platelets remains to be determined.

On the contrary to the aforementioned findings, CLEC-2 on platelets seems to have only minor influence on hemostasis as CLEC-2-deficient mice have only mildly prolonged or no altered tail-bleeding time at all (Figure 16). We have previously shown that antibody-induced CLEC-2-depleted mice display variable bleeding times when assessed in a filter paper model.[17] The extent of the bleeding was, however, rather mild compared to the hemostatic defect caused by integrin αIIbβ3 blockade.[114] In a later study, Hughes *et al.* reported that radiation chimeric mice, lacking CLEC-2 in the hematopoietic system, have unaltered tail-bleeding times compared to *Wt* controls using a tail-bleeding model without filter paper.[44] Furthermore, we designed and performed a third version of the assay, namely monitoring of bleeding into saline, where we found no prolongation of the tail-bleeding times in the MK/platelet-specific CLEC-2-deficient animals compared to *Wt* controls (Figure 16 B). In line with these findings, CLEC-2-depleted mice did not show a significant hemostatic defect when bleeding times were determined in saline.[138] These results suggest that the mechanism contributing to hemostasis may be partially different in the various bleeding time models and that the antibody-induced CLEC-2 depletion mirrors genetic loss of CLEC-2 in platelets. Although bleeding times are no valid parameter that allows reliable predictions of a potential bleeding risk,[164] it is tempting to speculate that an anti-CLEC-2 therapy might be associated with a relatively small risk of hemorrhagic complications.

4.1.2 GPVI and CLEC-2 double deficiency severely compromises hemostasis

This study shows that the combined loss of the two major platelet (hem)ITAM receptors, GPVI and CLEC-2, results in a severe hemostatic defect and virtually abolished thrombus formation in mice. These findings reveal for the first time that GPVI and CLEC-2 have partially redundant functions in normal hemostasis and pathological thrombus formation. Their simultaneous targeting may be an effective, but not necessarily safe antithrombotic approach.

CLEC-2 and GPVI are the only (hem)ITAM receptors present on murine plateletsand the immunodepletion of both receptors completely shuts off (hem)ITAM signaling in mouse platelets, without affecting GPCR-mediated signaling.[138] We generated genetically double-deficient mice lacking both receptors on their platelets. These double-deficient animals displayed a dramatically altered vascular structure and blood-filled lymphatic vessels in the mesenteries (Figure 17 A). This phenotype was clearly more pronounced than in CLEC-2 single-deficient animals (Figure 10 A) and not observed in GPVI single-deficient animals at all. This is the first description that GPVI might be involved in the lymphatic development and that CLEC-2 and GPVI might have partially redundant functions in this process. During lymphatic vascular development, LECs transdifferentiate in the anterior cardinal vein from preexisting venous endothelial cells. Thereafter, lymphatic structures develop through budding and sprouting of LECs. One hypothesis is that podoplanin on LECs is crosslinked by direct contact with CLEC-2 on platelets resulting in altered constitutive signaling, which leads to inhibition of LEC migration.[46] A recent study of Osada *et al.* proposed a modified model where the contents released from the granules of activated platelets, but not platelet aggregates themselves, are important for the development and integrity of the vascular systems.[54] They hypothesized that podoplanin activates platelets through CLEC-2 whereby the transforming growth factor family protein, bone morphogenetic protein-9 (BMP-9), is released, inhibiting the proliferation, migration and tube formation of LECs until blood and lymphatic vessels are separated.[54] However, the authors did not show any firm *in vivo* evidence for their hypothesis. They only demonstrated that released granule contents from platelets, activated with a GPVI-specific agonist, inhibited LEC migration, proliferation and tube formation *in vitro*.[54] In contrast, a later study from Finney *et al.* could not confirm this result using granule releases after platelet stimulation with a CLEC-2-specific agonist.[46] Based on these observations, we hypothesized that in CLEC-2 single-deficient animals, during lymphatic development, platelets might become activated through GPVI and release their granule contents, thereby promoting lymphatic development. Of note, this GPVI-dependent degranulation might only be important in CLEC-2-deficient animals as GPVI-deficient or degranulation incompetent mice have normal lymphatic vessels. However, in the

double-deficient animals CLEC-2- and GPVI-depended pathways are impaired resulting in a more pronounced phenotype with poorly differentiated lymphatic vessels.

The only well established ligands for GPVI are collagen, a component of the ECM, and fibrin.[11,165] Furthermore, Ozaki *et al.* published that GPVI is able to bind to laminins, another major ECM component.[166] They reported that platelets adhere to laminin through integrin $\alpha6\beta1$ and become activated through GPVI.[166] These laminins are normally not present on endothelial cells, but Saito *et al.* showed that LECs contain and are able to secret laminin heterotrimers composed of $\alpha4$, $\beta2$ and $\gamma1$ chains (laminin-421).[167] This led to the hypothesis that platelets might be activated by secreted laminis through GPVI and thereby facilitating the lymphatic vessel development in CLEC-2 single-deficient animals. However, further investigations are required to clarify the contribution of GPVI for the vascular development in CLEC-2 single-deficient animals.

Both activatory receptors have been proposed as possible pharmacological targets for antithrombotic therapy as they can easily be immunodepleted from circulating platelets *in vivo*, resulting in a knock out-like phenotype for the respective receptor over a prolonged period of time.[17,74] Such a targeted downregulation of GPVI or CLEC-2 provides profound antithrombotic protection in different models of thrombosis while having only moderate effects on normal hemostasis.[17,44,45,74,122] The GPVI immunodepletion is specific as GPVI-depleted and *Gp6*$^{-/-}$ mice display virtually identical defects in different thrombosis models and a comparable minor prolongation of tail bleeding times.[122] As mentioned above, the same is true when comparing antibody-induced downregulation of CLEC-2 with MK/ platelet-specific knock out in mice.[17,138]

Furthermore, GPVI and CLEC-2 can be simultaneously depleted from circulating platelets by injection of both antibodies.[138] The combined loss of GPVI and CLEC-2 resulted in markedly impaired hemostasis and a severe thrombus formation defect that exceeded the effect seen in GPVI- or CLEC-2 single-depleted animals by far.[138] To exclude that off-target effects of the antibody treatment account for the pronounced defect, *Gp6*$^{-/-}$/*Clec2*$^{-/-}$ mice were analyzed. These animals fully reproduced the thrombotic defects, although to a somewhat lesser extent in terms of the hemostatic defect, which might at least partially be explained by the mixture of their blood and lymphatic vessel with a consecutively reduced blood pressure (Figure 20). Furthermore, the coagulation system in these double-knock out animals was not impaired as the aPTT and PT were unaltered compared to *Wt* animals (Figure 21). These findings indicate that the simultaneous inhibition of these two receptors impairs the hemostatic function of platelets through mechanisms that remain to be determined.

For normal hemostasis, however, classic (hem)ITAM signaling downstream of the two receptors appears not to be essential as mice lacking Syk, a crucial proximal molecule within

this signaling pathway, did not show such pronounced bleeding defects.[168] Similarly, it has been reported that the Syk inhibitor, PRT060318, did not affect hemostasis in mice.[169] Together, these findings point to functions of GPVI, CLEC-2 or both receptors in hemostasis and possibly also thrombosis independent of their classical signal transduction pathways. Based on this assumption, one may speculate that adhesive functions of these receptors and/or their ability to bind and activate putative counter receptors in platelets might account for this unexpected activity. However, currently no intravascular ligands for CLEC-2 are known but based on our findings we speculate that they might exist.

Taken together, this data demonstrates that simultaneous downregulation of the platelet activating proteins, GPVI and CLEC-2, is possible and revealed unexpected redundant functions of these two receptors in arterial thrombus formation and more important in normal hemostasis in mice. Although data obtained in mice cannot be directly extrapolated to the human system (which is further complicated by the possible role of a third ITAM receptor, FcγRIIa, which is absent in mouse platelets), these results indicate that anti-GPVI or anti-CLEC-2 treatment might bear the risk of uncontrolled bleeding in patients exhibiting defects in the respective other (hem)ITAM signaling pathway. Although there are no known CLEC-2-deficient patients, most probably because CLEC-2 is critically involved in lymphatic vascular development in embryogenesis,[25,43] it might be possible that patients with an acquired loss of CLEC-2, e.g. caused by autoimmune disease, exist. However, as GPVI-deficient patients have already been described, the scenario of massive bleeding complications upon an anti-CLEC-2 therapy in these individuals appears to be the more relevant problem. This assumption is supported by a murine model, where *Gp6*$^{-/-}$ mice were injected with the CLEC-2-depleting antibody INU1. Pathological thrombus formation after $FeCl_3$-induced injury, as well as normal hemostasis, was severely affected in these mice similar to the observed defects in the double-depleted animals.[138]

In summary, this part of the study demonstrated that the simultaneous depletion of the (hem)ITAM-bearing receptors GPVI and CLEC-2 results in a virtually abolished thrombus formation *in vivo*, severely compromising hemostasis in these animals. These results may have important implications for the development and application of anti-GPVI and/or anti-CLEC-2 based therapeutics.

4.2 Targeted downregulation of CLEC-2 occurs through Syk-independent internalization in murine platelets

In the second part of the thesis, mechanisms underlying the antibody-induced regulation of CLEC-2 were studied. It is demonstrated that the targeted downregulation of CLEC-2 occurs through SFK-dependent, but Syk-independent internalization in circulating platelets. In contrast, anti-CLEC-2 antibody-induced thrombocytopenia depends on SFK- and Syk-mediated platelet activation, thereby allowing the mechanistic uncoupling of these two processes.

CLEC-2 has increasingly been recognized as a central activatory platelet receptor in thrombus formation and stabilization as well as tumor metastasis and maintenance of vascular integrity during inflammation. The presented data provide the first evidence that anti-CLEC-2 antibody treatment results in CLEC-2 immunodepletion via internalization, presumably followed by intracellular degradation (Figure 29 C, 30 A). To our knowledge, CLEC-2 is so far the second receptor to be downregulated from the surface of circulating platelets through antibody targeting, with this process previously described for GPVI in mouse and human platelets.[116,170] However, in the case of GPVI, the major pathway of immunodepletion is ectodomain shedding, while internalization becomes the prevailing mechanism only under conditions of impaired GPVI signaling.[92] The presented results show for the first time that the major route of CLEC-2 downregulation in platelets and MKs is internalization while there is no evidence for ectodomain shedding of CLEC-2 under any of the tested experimental conditions *in vitro* and *in vivo* (Figure 36). This finding is in line with a previous *in vitro* study, which also found no evidence for ectodomain shedding of CLEC-2 following auto-activation or in response to activation of ITAM receptors in human platelets.[148] Interestingly, however, in that study Western blot and flow cytometric analyses indicated that CLEC-2 surface expression was not regulated at all.[148] Different experimental conditions and reagents may explain why CLEC-2 internalization was not detected in this previous study. For example, in our *in vitro* studies, the αIIbβ3 blocker eptifibatide was used to inhibit platelet aggregate formation and enabled the analysis of activated single platelets (Figure 34). Under these conditions, INU1 binding very efficiently induces virtually complete internalization of CLEC-2 in platelets *in vitro*. In agreement with previous findings, no downregulation of surface CLEC-2 was observed after stimulation with other agonists such as thrombin (data not shown).[148] Furthermore, in the previous study a different anti-CLEC-2 antibody (AYP1) was used, which detects CLEC-2 on human platelets. It is likely that AYP1 binds a different epitope in the extracellular domain of CLEC-2 than INU1. Thus, epitope-specific differences could be one reason for the discrepancies between the two studies. This would, however, stand in stark contrast to the targeted downregulation of GPVI, which occurs epitope independently.[91] The contradictory findings may as well be explained by species-specific

differences, however, this is considered very unlikely. Unfortunately, INU1 antibody does not cross-react with human CLEC-2 thus excluding studies on human platelets. In conclusion, further studies and the development of new anti-CLEC-2 antibodies will be required to assess if CLEC-2 is similarly downregulated in human platelets.

The results obtained in the course of this thesis demonstrate that INU1-induced CLEC-2 internalization is strictly dependent on SFK activity *in vitro* and *in vivo*, strongly suggesting that phosphorylation of the CLEC-2 hemITAM is a critical step required for this process to occur (Figure 32). Indeed, Dasatinib, a widely used anti-cancer drug for patients with e.g. Imatinib-resistant chronic myelogenous leukemia or prostate cancer[171-174] that efficiently inhibits SFK activity prevented INU1-induced CLEC-2 downregulation *in vivo* (Figure 32). It was previously shown that upon stimulation of CLEC-2 by multimeric ligands such as RC and presumably podoplanin, hemITAM phosphorylation by Syk is sufficient to trigger downstream signaling and platelet activation. In contrast, for dimeric activation with ligands such as antibodies, SFK are essential,[36] indicating that signal strength might affect CLEC-2 phosphorylation and thereby CLEC-2 regulation. Although it is currently unclear under which conditions CLEC-2 internalization occurs in normal physiology, it is likely that this mechanism may regulate platelet reactivity. Given the multimeric nature of podoplanin it appears unlikely that CLEC-2 is internalized upon binding to this ligand. Podoplanin is, however, not present in the blood stream and the relevance of CLEC-2 for thrombus formation and stabilization[17] argues for the presence of different, hitherto unidentified, CLEC-2 ligand, which could trigger internalization of the receptor. Further studies are required to identify novel CLEC-2 ligands and assess their effect on CLEC-2 surface expression. Of note, a decrease in CLEC-2 surface expression upon stimulation with RC was reported recently, which was, however, ascribed to steric hindrance between RC and the anti-CLEC-2 antibody.[148] In the context of thrombus formation, CLEC-2 downregulation might also represent a negative feedback-regulation of platelet reactivity. This could be of particular relevance, since it was recently shown that CLEC-2-mediated platelet activation is insensitive towards 'classical' inhibitors such as nitric oxide or prostacyclin (PGI_2).[175] Further studies are required to understand whether this might play a role in limiting stability of a growing thrombus – or during lymph-vessel development – thereby preventing overshooting aggregation responses.

The data clearly shows that whereas INU1-induced CLEC-2 downregulation is strictly dependent on hemITAM signaling through the receptor, it still efficiently occurs in the absence of Syk *in vitro* and *in vivo* (Figure 29 C, 30 A). This result was unexpected as it was shown, in line with previous reports,[25,36,127] that *Syk*$^{-/-}$ platelets are entirely refractory to stimulation with CLEC-2 agonists, including RC and INU1 (Figure 28 A). This proposes that a hemITAM-triggered signaling pathway downstream of CLEC-2 exists in platelets that trigger internalization of the receptor independently of classic cellular activation. This is of particular

relevance, as the severe transient thrombocytopenia seen in INU1-treated *Wt* mice was not observed in *Syk*$^{-/-}$ mice (Figure 28 B) and hence seems to depend on the classical activation pathway. Together, our data demonstrate for the first time that the targeted downregulation of CLEC-2 occurs in circulating platelets *in vivo* and can be mechanistically uncoupled from the undesired associated thrombocytopenia.

Interestingly, a similar downregulation mechanism has been described for the T-cell receptor that is as well dependent on SFK, in this case Lck, but independent of Syk.[176] Phosphorylation of the T-cell receptor by Lck results in recruitment of adaptor proteins and ubiquitin ligases leading to internalization and degradation.[176] It was recently shown that the anti-CLEC-2-antibody-induced phosphorylation of the CLEC-2 hemITAM depends on the SFK Lyn[36] and our results support the concept of SFK being upstream of Syk in hemITAM signaling.

This thesis also demonstrated that INU1 could induce thrombocytopenia in two different ways – one that is platelet activation-dependent and FcγR-independent and a second one that depends on FcγRs. The first mechanism applies to the situation in *Wt* mice, where platelets are directly activated and internalize the CLEC2/INU1 complexes. These activated platelets are then rapidly cleared from the circulation independently of FcγRs (Figure 24, 25). FcγR-dependent platelet clearance, however, becomes relevant in Dasatinib-treated mice, where INU1 does not cause platelet activation and remains on the surface of the cells (due to blocked internalization, Figure 32). In *Syk*$^{-/-}$ mice, however, INU1 does not cause platelet activation and is rapidly internalized and thus inaccessible to FcγRs. As a result, INU1-induced thrombocytopenia is largely prevented in these animals (Figure 28). The partial drop in platelet counts in Syk-deficient mice most likely represents a short time frame of FcγR-dependent platelet clearance until full internalization of the CLEC-2 has occurred. In line with this, blockade of FcγRs further reduced INU1-induced thrombocytopenia in Syk-deficient mice (Figure 50).

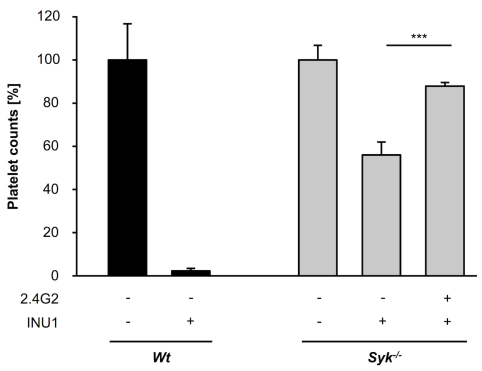

Figure 50. Blockade of Fcγ receptors using the monoclonal antibody 2.4G2 ameliorates INU1-induced thrombocytopenia in Syk-deficient mice. *Wt* and *Syk*$^{-/-}$ mice were pretreated with 2.4G2 (24 h and 1 h before INU1 injection; 100 µg intraperitoneally) followed by intravenously injected with 100 µg INU1. After 1 h platelet counts were determined on a FACSCalibur. Results are mean ± SD in % of the initial platelet counts (n=5 mice per group). (Lorenz *et al., Blood* 2015)[123]

Taken together, the results presented in this thesis provide the first evidence of an active mechanism that regulates CLEC-2 surface abundance in mouse platelets that strongly depends on phosphorylation events mediated via SFK (Figure 51). Moreover, Syk appears to be the central molecular checkpoint that is dispensable for CLEC-2 immunodepletion but required for INU1 induced thrombocytopenia (Figure 51). This offers the possibility to mechanistically uncouple targeted CLEC-2 downregulation from the undesired anti-CLEC-2 induced platelet activation and consumption. Furthermore, the data shows that MKs also can downregulate CLEC-2 from their surface through internalization, which may explain the appearance of CLEC-2-deficient platelets in the circulation of *Wt* mice 2-3 days after anti-CLEC-2 antibody treatment. These results may have implications for the development of therapeutic agents to interfere with CLEC-2 activity in thrombotic, inflammatory or malignant diseases.

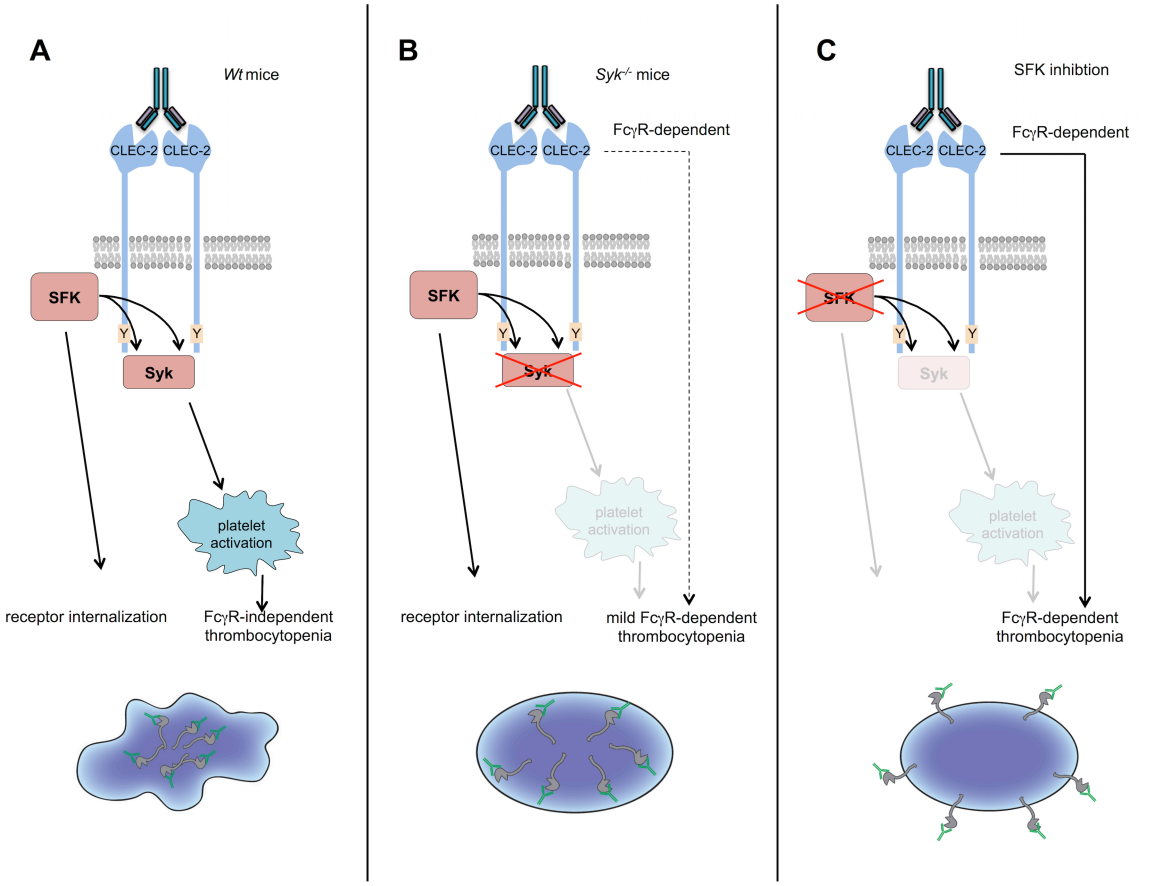

Figure 51. Schematic representation of INU1-induced thrombocytopenia and CLEC-2 regulation. (A) In *Wt* mice, where platelets are rapidly activated and internalize the CLEC-2/ INU1 complexes. The activated platelets were cleared from the circulation independently of FcγRs. (B) In *Syk*$^{-/-}$ mice INU1-induced platelet activation is impaired and the CLEC-2/ INU1 complex is rapidly internalized. Therefore, INU1-induced thrombocytopenia is largely prevented in these animals. However, a partial drop in platelet counts in Syk-deficient mice most likely represents a short time frame of FcγR-dependent platelet clearance until full internalization of the CLEC-2 has occurred. (C) After SFK inhibition in *Wt* mice platelets were rapidly FcγR-dependent cleared, as INU1 does not cause platelet activation and remains on the surface of the cells (due to blocked internalization).

Finally, we started to investigate the regulation of CLEC-2 in MKs to address the question how CLEC-2-deficient platelets were generated in *Wt* animals upon INU1 injection. Intravenously injected INU1 binds robustly to MKs in the bone marrow (Figure 23). Furthermore, *in vitro* studies demonstrated that fetal-liver derived MKs internalize the INU1/CLEC-2 complex (Figure 37). MKs are platelet progenitor cells, whose principal role is to maintain the normal blood platelet counts. As platelet have little or no capacity to *de novo* synthesize proteins, MKs must express most, if not all, platelet proteins. Hence, many receptors may exist in MKs solely for later use in hemostasis, but they could also play a role in MK development. Senis *et al.* analyzed the transcriptome of mature murine MKs and identified that 17 of the 25 most MK-specific expressed genes encoded transmembrane proteins, including the GPIb-V-IX complex, integrin αIIb and CLEC-2.[177] Their studies suggest that these proteins are expressed on the MK surface.[177] The assumption that CLEC-2 is expressed on the MK surface, is corroborated by our findings demonstrating the internalization of the CLEC-2/INU1 complex. As these MKs give rise to normal platelets, we hypothesized that CLEC-2 expression on the MK surface might be dispensable for platelet production. Furthermore, both *in vitro* and *in situ* stained MKs displayed an intracellular signal for the INU1/CLEC-2 complex in proplatelet protrusions, which indicates that degradation of the internalized CLEC-2 might occur in platelets very early in the course of their maturation within the circulation (Figure 23, 37). However, further studies are needed to elucidate the function and downregulation of CLEC-2 in MKs.

4.3 INU1 F(ab) fragments induce disseminated intravascular thrombosis

Monoclonal antibodies (mAbs) are widely used in the treatment of various diseases.[103] Intact antibodies (IgG) may, however, have unwanted effects; therefore antibody fragments (F(ab)) consisting of only of the antigen-binding domain are considered better pharmacological agents for inhibition. We generated F(ab) fragments of the CLEC-2-binding antibody INU1 and tested their function *in vivo*. Unexpectedly, injection of INU1 F(ab) resulted in a widespread intravascular thrombus formation leading to neurological deficits and consecutive death of the animals. This intravascular thrombus formation is the result of CLEC-2-dependent platelet activation aggregation.

Bergmeier *et al.* published that monoclonal antibodies directed against GPIbα on platelets induced rapid and persisting thrombocytopenia *in vivo*.[178] It is speculated that these effects are induced because of the divalent antibody structure as the same results were obtained when incubating platelet with the divalent F(ab)2 fragments.[178] However, incubation with or injection of the monovalent F(ab) fragment functionally blocks the interaction of GPIb with its

ligand vWF without inducing platelet activation or thrombocytopenia *in vitro* and *in vivo*.[178-180] We yielded similar results with INU1 IgG. Occupancy of CLEC-2 with INU1 IgG resulted in platelet aggregate formation *in vitro* (Figure 39) and rapid thrombocytopenia with trapped micro-emboli in the pulmonary capillaries *in vivo* (Figure 26). Furthermore, *in vitro* incubation of platelets with INU1 F(ab) fragments led solely to the blockade of CLEC-2-dependent signal transduction without inducing any activation elucidated by aggregation measurements (Figure 39). In sharp contrast, injection of INU1 F(ab) resulted in a delayed activation and aggregate formation in mice and platelet-rich aggregates where observed in different organs including the brain (Figure 42, 45). These aggregates lead to persistent neurological deficits in the injected animals, followed by symptoms of suffocation and death in most of the treated animals. To our knowledge, such a dramatic reaction after antibody-injection, whether IgG or F(ab) fragments, has never been observed before. However, Cueni *et al.* published a similar finding after expression of podoplanin-Fc in the skin of animals.[181] They described that 15% of the transgenic animals died suddenly between 3 to 6 weeks of age. The death appeared to be provoked by intense activity or exposure to stress.[181] The authors showed that although podoplanin-Fc was expressed via a promoter, which is exclusively active in the skin, free podoplanin-Fc was detected in the plasma and as well as in and around blood vessels of tissues other than the skin.[181] Furthermore, podoplanin-positive thrombi were found in the lamina propria, the heart, lung, liver, kidney and even the brain.[181] Podoplanin as well as INU1 F(ab) bind specifically to CLEC-2 on platelets and induce disseminated intravascular thrombosis. This closely resembles the conditions found in septic humans with disseminated intravascular coagulation (DIC), which is characterized by the deposition of fibrin leading to microvascular thrombi occurrence in various organs. This leads to multiple organ failures thereby increasing the overall mortality of patients with DIC.[182] DIC exists in both acute and chronic forms and is potentially life threatening. Therefore INU1 F(ab) might be a new model to investigate the underlying mechanism in more detail and may allow to determined new therapeutic approaches.

In histological sections platelet-rich thrombi were found in arteries after INU1 F(ab) injection (Figure 44, 45). It is well established that platelets can form thrombi under different shear conditions. Under pathological conditions, arterial thrombi are typically formed under high blood flow conditions. Siedlecki *et al.* reported that under high shear conditions the large multimeric plasma glycoprotein vWF undergoes a shear stress-induced conformational transition from a globular state to an extended chain conformation.[183] Thereby, intra-molecular globular domains are exposed, which can be bound by GPIb, facilitating platelet adhesion.[183] Integrins are also known to change their extracellular confirmations upon platelet activation to enable ligand binding.[184] This process is termed “inside-out” signaling, as early stages of platelet activation trigger intracellular pathways.[184] Based on these

findings, we hypothesized that binding of INU1 F(ab) might either induce a shear dependent conformational change or an intracellular signal, resulting in the change of the extracellular domain. Subsequently the binding of a yet unknown ligand might be facilitated, resulting in platelet aggregation.

We based this hypothesis on our findings that the INU1 F(ab) induced platelet aggregation is not limited to the brain but is rather a general mechanism occurring in the blood stream meaning that there must be a more ubiquitous mechanism involved rather than a tissues specific ligand (Figure 45). Furthermore, our findings indicate that the thrombus formation depends on the expression of CLEC-2 on platelets, CLEC-2-induced intracellular signaling, presence of α-granules and finally platelet aggregation (Table 2). A prerequisite for platelet aggregation is the activation of integrins, which is impaired in talin1-deficient animals.[124] These mice were therefore protected from INU1 F(ab)-induced intravascular thrombus formation. Moreover, we observed that the INU1 F(ab)-opsonized platelets circulated in a resting state in these animals. Previous studies showed that a “crosstalk” between integrins and ITAM-coupled receptors exists. As mentioned above, integrins require “inside-out” signaling to induce their active confirmation to bind their ligands.[185] Further studies showed that cell surface clustering of integrin receptors resulted in phosphorylation and activation of the intracellular tyrosine kinase Syk, potentially through engagement of ITAM-containing receptors.[186] That observation suggests a mechanism of integrin “outside-in” signaling that makes use of the classical ITAM signaling pathway components.[186] This interaction might play a central role for INU1 F(ab)-induced platelet activation, however the exact mechanism is currently still unclear and needs further investigation.

INU1 F(ab) did not induce platelet activation *in vitro* under stirring conditions (Figure 39). Further studies in a modified *in vitro* flow chamber model revealed that F(ab)-opsonized *Wt* platelets were able to form aggregates without further stimulation (Figure 49). This indicates that INU1 F(ab) triggered thrombus formation depends on a component that is released from platelets. Nbeal2-deficient animals have an impaired α-granules biogenesis resulting in a lack of these granules in mature platelets (Figure 52).[134,153] These Nbeal2-deficient animals are protected in models of arterial thrombosis due to the formation of unstable platelet aggregates and continuous detachment of small thrombi.[134] Furthermore, the mutant animals had a strong hemostatic defect and were protected in a model of stroke indicating that α-granule secretion is critical for platelet plug formation and stability.[134] Additionally, we found that Nbeal2-deficient animals were protected from the INU1 F(ab) induced thrombus formation, as these animals did not show neurological deficits and exhibit only a mild thrombocytopenia. Based on these observations one may speculate that α-granules might contain a potential ligand for CLEC-2 facilitating CLEC-2-dependent thrombus formation and stabilization. Platelet α-granules store more than 300 different proteins that upon release

support various physiological and pathophysiological purposes including platelet adhesiveness (e.g. vWF, fibrinogen), inflammation (e.g. P-selectin, interleukin-1β (IL-1β), IL-8, platelet factor 4 (PF4, CXCL4), angiogenesis (e.g. platelet-derived growth factor), wound healing (e.g. transforming growth factor beta), antimicrobial host defense and malignancy.[187] Several proteins secreted from platelet α-granules, including vWF and coagulation factor V, are known to be important for platelet function in hemostasis at sites of blood vessel injury.[188,189] Absence of α-granules is thought to contribute to a mild to moderate bleeding phenotype in gray platelet syndrome (GPS). This is a rare bleeding disorder characterized by macrothrombocytopenia, with platelet lacking α-granules due to a mutation in *NBEAL2*.[154,190,191] The content of α-granules includes both membrane bound proteins that are upon granule release expressed on the platelet surface and soluble proteins that are released into the extracellular space.[192] Further studies are needed to identify a possible ligand facilitating the INU1 F(ab)-induced intravascular thrombus formation.

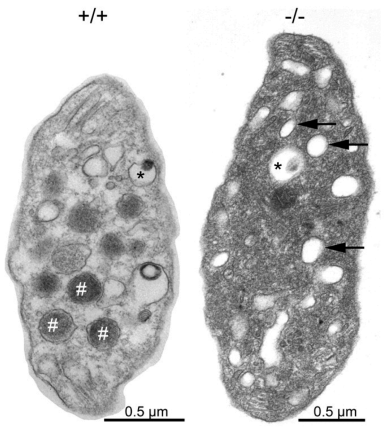

Figure 52. Ultrastructure of *Nbeal2*$^{-/-}$ platelets. Representative TEM images of resting *Wt* (+/+) and *Nbeal2*$^{-/-}$ (−/−) platelets. Nbeal2-deficient platelets both show lack of α-granules (#) and an increased number of vacuoles (arrows) while platelet size was increased and dense granule (*) content was unaltered. (Taken from Deppermann *et al.*, *Rare Dis* 2013)[153]

These very unexpected results demonstrate that binding of CLEC-2 might induce changes in the extracellular domain resulting in disseminated intravascular thrombus formation and should be considered, when thinking of CLEC-2 as a potential therapeutic target. However, identification of an intravascular CLEC-2 ligand is of high interest as the receptor is involved in various physiological and pathophysiological processes thus making it an interesting target to modulate these processes.

4.4 CLEC-2 as a potential anti-thrombotic target

CLEC-2 has been intensively discussed as a potential novel anti-thrombotic target.[17,25,35] In medicine an ideal anti-thrombotic treatment would protect from thrombotic events while leaving the hemostasis unaffected. CLEC-2-deficient animals display largely normal hemostasis in different bleeding time models, but a significant protection from occlusive

thrombus formation in a murine thrombosis model.[17,45,138] Furthermore, we demonstrated that CLEC-2 can be specifically targeted and functionally inactivated *in vivo* by antibodies resulting in the comparable protection from pathological thrombus formation.[17,123] However, antithrombotic agents are typically administered over a long period of time, especially when used to prevent ischemic events. Studies in irradiated mice showed that reconstitution with CLEC-2-deficient hematopoietic cells resulted in appearance of blood-filled lymphatic vessels in the mesenteric within some weeks.[46] This might indicate that long term targeting of CLEC-2 might have unwanted effects, due to its function in maintaining lymphatic vascular integrity.

Furthermore, this study provided evidence that deficiency in CLEC-2 combined with a deficiency of GPVI resulted in a dramatic hemostatic defect.[138] So far, CLEC-2-deficient patients have not been described, whereas patients with an acquired GPVI deficiency due to production of autoantibodies are well described in the litarature.[116,117] Therefore, a scenario of massive bleeding complications upon an anti-CLEC-2 therapy in these individuals might be a clinically relevant problem. Besides this, anti-CLEC-2 antibody injection resulted in a transient thrombocytopenia in mice. Although this effect was attenuated in signaling incompetent Syk-deficient mice[123] and it has been experimentally proven that a dramatic drop of platelet count does not *per se* cause spontaneous bleeding,[63] it may limit the therapeutic use of anti-CLEC-2 antibodies. Additionally, the presented data indicated that binding of CLEC-2 by a monovalent antibody F(ab) fragment induced thrombus formation. This is highly relevant, as the F(ab) fragments should only block the receptor and inhibit further signaling, as shown for the anti-platelet agents such as abciximab (“ReoPro”).

In summary, these findings question the suitability of CLEC-2 as an adequate antithrombotic target for prophylactic use. However, CLEC-2 might be a suitable target for treatment of an acute embolization via an *in loco* administration. Furthermore, several publications showed that CLEC-2 on platelets plays a significant role in tumor metastasis as podoplanin is expressed on several tumor cells including squamous cell carcinoma, mesothelioma, testicular seminoma and brain tumors.[47,65,67] Hence, CLEC-2 might be an interesting target to inhibit tumor cell spreading in cancer patients.

Therefore, more studies are needed to understand the function of CLEC-2 and identify potential ligands to develop blocking compounds or inhibitors that do not induce intracellular signaling, but rather manipulate the receptor in the desired way.

4.5 Closing remarks and further prospects

The work presented here showed for the first time that CLEC-2 can be targeted and downregulated from the platelet surface by internalization without inducing thrombocytopenia. Further studies demonstrated that binding of CLEC-2 with an antibody F(ab) resulted in disseminated intravascular thrombus formation, but the underlying mechanism remained unknown. In addition, mice with a double deficiency in both (hem)ITAM receptors, GPVI and CLEC-2, were analyzed. These animals had a dramatic bleeding phenotype that demonstrated a redundant function of these two receptors in hemostasis.

Further studies are planned in our laboratory to investigate the regulation and function of CLEC-2 on MKs and platelets in more detail. Therefore, further CLEC-2 specific antibodies should be generated. During the last four years, three more rats were repeatedly immunized with native CLEC-2 protein immunoprecipitated from platelet lysate using INU1, their spleens were isolated, hybridoma cells were generated and tested. However, these attempts failed to produce another CLEC-2 antibody. A reason why the antibody generation turned out to be this difficult could be that the protein structure of mouse and rat CLEC-2 share a high homology of 90.0%, especially in the extracellular domain of the protein. Hence, further attempts are necessary potentially using other immunization strategies.

Initial studies demonstrated that the CLEC-2-specific antibody INU1 binds to MKs *in vivo* and induces CLEC-2 internalization on fetal-liver derived MKs *in vitro*. Further studies are required to elucidate the underlying mechanisms. Furthermore, little is known about the regulation of GPVI on MKs. Injection of the GPVI-specific antibody JAQ1 resulted in a long-term GPVI deficiency in circulating platelets. In platelet the major pathway for GPVI regulation is ectodomain shedding. Further studies are planned to identify the pathways underlying the long-term GPVI-downregulation in MKs.

Injection of INU1 F(ab) in Nbeal2-deficient animals revealed that a potential CLEC-2 ligand might be stored in platelet α-granules. Further experiments are planed to identify this ligand. One approach is a modified flow chamber model, where INU1 F(ab)-opsonized *Wt* but not Nbeal2-deficient platelet form stable thrombi.

Moreover, a new mouse line was generated with a point mutation in the hemITAM tyrosine (Y7A), which abolishes CLEC-2 signaling transduction. These mice should be analyzed with regard to their embryonic development to get a more detailed understanding of CLEC-2 and its signaling during lymphatic development and blood-lymphatic vessel separation. Initial results indicate that these animals resemble the CLEC-2 knock out phenotype, however further analyses are needed to asses this in detail.

5 REFERENCES

1. Italiano JE, Jr., Patel-Hett S, Hartwig JH. Mechanics of proplatelet elaboration. *J Thromb Haemost*. 2007;5 Suppl 1:18-23.

2. Junt T, Schulze H, Chen Z, et al. Dynamic visualization of thrombopoiesis within bone marrow. *Science*. 2007;317(5845):1767-1770.

3. Ruggeri ZM. Platelets in atherothrombosis. *Nature medicine*. 2002;8(11):1227-1234.

4. Stegner D, Dutting S, Nieswandt B. Mechanistic explanation for platelet contribution to cancer metastasis. *Thromb Res*. 2014;133 Suppl 2:S149-157.

5. Nurden AT, Nurden P, Sanchez M, Andia I, Anitua E. Platelets and wound healing. *Front Biosci*. 2008;13:3532-3548.

6. Jenne CN, Kubes P. Platelets in inflammation and infection. *Platelets*. 2015;26(4):286-292.

7. Nieswandt B, Pleines I, Bender M. Platelet adhesion and activation mechanisms in arterial thrombosis and ischaemic stroke. *J Thromb Haemost*. 2011;9 Suppl 1:92-104.

8. Savage B, Almus-Jacobs F, Ruggeri ZM. Specific synergy of multiple substrate-receptor interactions in platelet thrombus formation under flow. *Cell*. 1998;94(5):657-666.

9. Nieswandt B, Brakebusch C, Bergmeier W, et al. Glycoprotein VI but not alpha2beta1 integrin is essential for platelet interaction with collagen. *EMBO J*. 2001;20(9):2120-2130.

10. Furie BC, Furie B. Tissue factor pathway vs. collagen pathway for in vivo platelet activation. *Blood cells, molecules & diseases*. 2006;36(2):135-138.

11. Nieswandt B, Watson SP. Platelet-collagen interaction: is GPVI the central receptor? *Blood*. 2003;102(2):449-461.

12. Offermanns S. Activation of platelet function through G protein-coupled receptors. *Circulation research*. 2006;99(12):1293-1304.

13. Clemetson KJ. Platelet activation: signal transduction via membrane receptors. *Thrombosis and haemostasis*. 1995;74(1):111-116.

14. Jung SM, Moroi M. Platelets interact with soluble and insoluble collagens through characteristically different reactions. *The Journal of biological chemistry*. 1998;273(24):14827-14837.

15. Varga-Szabo D, Pleines I, Nieswandt B. Cell adhesion mechanisms in platelets. *Arteriosclerosis, thrombosis, and vascular biology*. 2008;28(3):403-412.

16. Brass LF, Zhu L, Stalker TJ. Minding the gaps to promote thrombus growth and stability. *The Journal of clinical investigation*. 2005;115(12):3385-3392.

17. May F, Hagedorn I, Pleines I, et al. CLEC-2 is an essential platelet-activating receptor in hemostasis and thrombosis. *Blood*. 2009;114(16):3464-3472.

18. Stegner D, Nieswandt B. Platelet receptor signaling in thrombus formation. *J Mol Med (Berl)*. 2011;89(2):109-121.

19. Braun A, Vogtle T, Varga-Szabo D, Nieswandt B. STIM and Orai in hemostasis and thrombosis. *Front Biosci (Landmark Ed)*. 2011;16:2144-2160.

20. Colonna M, Samaridis J, Angman L. Molecular characterization of two novel C-type lectin-like receptors, one of which is selectively expressed in human dendritic cells. *European journal of immunology*. 2000;30(2):697-704.

21. Yokoyama WM, Plougastel BF. Immune functions encoded by the natural killer gene complex. *Nature reviews Immunology*. 2003;3(4):304-316.

22. Sobanov Y, Bernreiter A, Derdak S, et al. A novel cluster of lectin-like receptor genes expressed in monocytic, dendritic and endothelial cells maps close to the NK receptor genes in the human NK gene complex. *European journal of immunology*. 2001;31(12):3493-3503.

23. Chaipan C, Soilleux EJ, Simpson P, et al. DC-SIGN and CLEC-2 mediate human immunodeficiency virus type 1 capture by platelets. *J Virol*. 2006;80(18):8951-8960.

24. Tang T, Li L, Tang J, et al. A mouse knockout library for secreted and transmembrane proteins. *Nature biotechnology*. 2010;28(7):749-755.

25. Suzuki-Inoue K, Fuller GL, Garcia A, et al. A novel Syk-dependent mechanism of platelet activation by the C-type lectin receptor CLEC-2. *Blood*. 2006;107(2):542-549.

26. Wang L, Ren S, Zhu H, et al. Structural and functional conservation of CLEC-2 with the species-specific regulation of transcript expression in evolution. *Glycoconj J*. 2012;29(5-6):335-345.

27. Zelensky AN, Gready JE. The C-type lectin-like domain superfamily. *FEBS J*. 2005;272(24):6179-6217.

28. Osorio F, Reis e Sousa C. Myeloid C-type lectin receptors in pathogen recognition and host defense. *Immunity*. 2011;34(5):651-664.

29. Drickamer K. C-type lectin-like domains. *Current opinion in structural biology*. 1999;9(5):585-590.

30. Drickamer K, Fadden AJ. Genomic analysis of C-type lectins. *Biochem Soc Symp*. 2002(69):59-72.

31. Pyz E, Marshall AS, Gordon S, Brown GD. C-type lectin-like receptors on myeloid cells. *Annals of medicine*. 2006;38(4):242-251.

32. Weis WI, Taylor ME, Drickamer K. The C-type lectin superfamily in the immune system. *Immunological reviews*. 1998;163:19-34.

33. Weis WI, Drickamer K. Structural basis of lectin-carbohydrate recognition. *Annu Rev Biochem*. 1996;65:441-473.

34. Watson AA, Brown J, Harlos K, Eble JA, Walter TS, O'Callaghan CA. The crystal structure and mutational binding analysis of the extracellular domain of the platelet-activating receptor CLEC-2. *J Biol Chem*. 2007;282(5):3165-3172.

35. O'Callaghan CA. Thrombomodulation via CLEC-2 targeting. *Curr Opin Pharmacol*. 2009;9(2):90-95.

36. Severin S, Pollitt AY, Navarro-Nunez L, et al. Syk-dependent phosphorylation of CLEC-2: a novel mechanism of hem-immunoreceptor tyrosine-based activation motif signaling. *J Biol Chem*. 2011;286(6):4107-4116.

37. Watson AA, Christou CM, James JR, et al. The platelet receptor CLEC-2 is active as a dimer. *Biochemistry*. 2009;48(46):10988-10996.

38. Fuller GL, Williams JA, Tomlinson MG, et al. The C-type lectin receptors CLEC-2 and Dectin-1, but not DC-SIGN, signal via a novel YXXL-dependent signaling cascade. *J Biol Chem*. 2007;282(17):12397-12409.

39. Pollitt AY, Grygielska B, Leblond B, Desire L, Eble JA, Watson SP. Phosphorylation of CLEC-2 is dependent on lipid rafts, actin polymerization, secondary mediators, and Rac. *Blood*. 2010;115(14):2938-2946.

40. Dhanjal TS, Ross EA, Auger JM, et al. Minimal regulation of platelet activity by PECAM-1. *Platelets*. 2007;18(1):56-67.

41. Mori J, Pearce AC, Spalton JC, et al. G6b-B inhibits constitutive and agonist-induced signaling by glycoprotein VI and CLEC-2. *J Biol Chem*. 2008;283(51):35419-35427.

42. Watson SP, Herbert JM, Pollitt AY. GPVI and CLEC-2 in hemostasis and vascular integrity. *J Thromb Haemost*. 2010;8(7):1456-1467.

43. Bertozzi CC, Schmaier AA, Mericko P, et al. Platelets regulate lymphatic vascular development through CLEC-2-SLP-76 signaling. *Blood*. 2010;116(4):661-670.

44. Hughes CE, Navarro-Nunez L, Finney BA, Mourao-Sa D, Pollitt AY, Watson SP. CLEC-2 is not required for platelet aggregation at arteriolar shear. *J Thromb Haemost*. 2010;8(10):2328-2332.

45. Suzuki-Inoue K, Inoue O, Ding G, et al. Essential in vivo roles of the C-type lectin receptor CLEC-2: embryonic/neonatal lethality of CLEC-2-deficient mice by blood/lymphatic misconnections and impaired thrombus formation of CLEC-2-deficient platelets. *J Biol Chem*. 2010;285(32):24494-24507.

46. Finney B, Schweighoffer E, Navarro-Núñez L, et al. CLEC-2 and Syk in the megakaryocytic/platelet lineage are essential for development. *Blood*. 2012;119(7):1747-1756.

47. Suzuki-Inoue K, Kato Y, Inoue O, et al. Involvement of the snake toxin receptor CLEC-2, in podoplanin-mediated platelet activation, by cancer cells. *J Biol Chem*. 2007;282(36):25993-26001.

48. Wicki A, Christofori G. The potential role of podoplanin in tumour invasion. *British journal of cancer*. 2007;96(1):1-5.

49. Uhrin P, Zaujec J, Breuss JM, et al. Novel function for blood platelets and podoplanin in developmental separation of blood and lymphatic circulation. *Blood*. 2010;115(19):3997-4005.

50. Abtahian F, Guerriero A, Sebzda E, et al. Regulation of blood and lymphatic vascular separation by signaling proteins SLP-76 and Syk. *Science*. 2003;299(5604):247-251.

51. Clements JL, Lee JR, Gross B, et al. Fetal hemorrhage and platelet dysfunction in SLP-76-deficient mice. *The Journal of clinical investigation*. 1999;103(1):19-25.

52. Sebzda E, Hibbard C, Sweeney S, et al. Syk and Slp-76 mutant mice reveal a cell-autonomous hematopoietic cell contribution to vascular development. *Developmental cell*. 2006;11(3):349-361.

53. Wang D, Feng J, Wen R, et al. Phospholipase Cgamma2 is essential in the functions of B cell and several Fc receptors. *Immunity*. 2000;13(1):25-35.

54. Osada M, Inoue O, Ding G, et al. Platelet activation receptor CLEC-2 regulates blood/lymphatic vessel separation by inhibiting proliferation, migration, and tube formation of lymphatic endothelial cells. *J Biol Chem*. 2012;287(26):22241-22252.

55. Tammela T, Alitalo K. Lymphangiogenesis: Molecular mechanisms and future promise. *Cell*. 2010;140(4):460-476.

56. Hess PR, Rawnsley DR, Jakus Z, et al. Platelets mediate lymphovenous hemostasis to maintain blood-lymphatic separation throughout life. *J Clin Invest*. 2014;124(1):273-284.

57. Herzog BH, Fu J, Wilson SJ, et al. Podoplanin maintains high endothelial venule integrity by interacting with platelet CLEC-2. *Nature*. 2013;502(7469):105-109.

58. von Andrian UH, Mempel TR. Homing and cellular traffic in lymph nodes. *Nat Rev Immunol*. 2003;3(11):867-878.

59. Butcher EC, Picker LJ. Lymphocyte homing and homeostasis. *Science*. 1996;272(5258):60-66.

60. Drayton DL, Liao S, Mounzer RH, Ruddle NH. Lymphoid organ development: from ontogeny to neogenesis. *Nat Immunol*. 2006;7(4):344-353.

61. Rosen SD. Ligands for L-selectin: homing, inflammation, and beyond. *Annu Rev Immunol*. 2004;22:129-156.

62. Girard JP, Moussion C, Forster R. HEVs, lymphatics and homeostatic immune cell trafficking in lymph nodes. *Nat Rev Immunol*. 2012;12(11):762-773.

63. Goerge T, Ho-Tin-Noe B, Carbo C, et al. Inflammation induces hemorrhage in thrombocytopenia. *Blood*. 2008;111(10):4958-4964.

64. Boulaftali Y, Hess PR, Getz TM, et al. Platelet ITAM signaling is critical for vascular integrity in inflammation. *J Clin Invest*. 2013;123(2):908-916.

65. Chaipan C, Steffen I, Tsegaye TS, et al. Incorporation of podoplanin into HIV released from HEK-293T cells, but not PBMC, is required for efficient binding to the attachment factor CLEC-2. *Retrovirology*. 2010;7:47.

66. Christou CM, Pearce AC, Watson AA, et al. Renal cells activate the platelet receptor CLEC-2 through podoplanin. *Biochem J*. 2008;411(1):133-140.

67. Kato Y, Kaneko MK, Kunita A, et al. Molecular analysis of the pathophysiological binding of the platelet aggregation-inducing factor podoplanin to the C-type lectin-like receptor CLEC-2. *Cancer Sci*. 2008;99(1):54-61.

68. Bambace NM, Holmes CE. The platelet contribution to cancer progression. *J Thromb Haemost*. 2011;9(2):237-249.

69. Gay LJ, Felding-Habermann B. Contribution of platelets to tumour metastasis. *Nat Rev Cancer*. 2011;11(2):123-134.

70. Jurasz P, Alonso-Escolano D, Radomski MW. Platelet--cancer interactions: mechanisms and pharmacology of tumour cell-induced platelet aggregation. *Br J Pharmacol*. 2004;143(7):819-826.

71. Nieswandt B, Hafner M, Echtenacher B, Mannel DN. Lysis of tumor cells by natural killer cells in mice is impeded by platelets. *Cancer Res*. 1999;59(6):1295-1300.

72. Clemetson JM, Polgar J, Magnenat E, Wells TN, Clemetson KJ. The platelet collagen receptor glycoprotein VI is a member of the immunoglobulin superfamily closely related to FcalphaR and the natural killer receptors. *The Journal of biological chemistry*. 1999;274(41):29019-29024.

73. Jandrot-Perrus M, Busfield S, Lagrue AH, et al. Cloning, characterization, and functional studies of human and mouse glycoprotein VI: a platelet-specific collagen receptor from the immunoglobulin superfamily. *Blood*. 2000;96(5):1798-1807.

74. Nieswandt B, Schulte V, Bergmeier W, et al. Long-term antithrombotic protection by in vivo depletion of platelet glycoprotein VI in mice. *The Journal of experimental medicine*. 2001;193(4):459-469.

75. Dutting S, Bender M, Nieswandt B. Platelet GPVI: a target for antithrombotic therapy?! *Trends Pharmacol Sci*. 2012;33(11):583-590.

76. Andrews RK, Suzuki-Inoue K, Shen Y, Tulasne D, Watson SP, Berndt MC. Interaction of calmodulin with the cytoplasmic domain of platelet glycoprotein VI. *Blood*. 2002;99(11):4219-4221.

77. Suzuki-Inoue K, Tulasne D, Shen Y, et al. Association of Fyn and Lyn with the proline-rich domain of glycoprotein VI regulates intracellular signaling. *The Journal of biological chemistry*. 2002;277(24):21561-21566.

78. Gibbins J, Asselin J, Farndale R, Barnes M, Law CL, Watson SP. Tyrosine phosphorylation of the Fc receptor gamma-chain in collagen-stimulated platelets. *The Journal of biological chemistry*. 1996;271(30):18095-18099.

79. Berlanga O, Tulasne D, Bori T, et al. The Fc receptor gamma-chain is necessary and sufficient to initiate signalling through glycoprotein VI in transfected cells by the snake C-type lectin, convulxin. *European journal of biochemistry / FEBS*. 2002;269(12):2951-2960.

80. Gibbins JM, Okuma M, Farndale R, Barnes M, Watson SP. Glycoprotein VI is the collagen receptor in platelets which underlies tyrosine phosphorylation of the Fc receptor gamma-chain. *FEBS letters*. 1997;413(2):255-259.

81. Clemetson KJ, Clemetson JM. Platelet collagen receptors. *Thromb Haemost*. 2001;86(1):189-197.

82. Asazuma N, Wilde JI, Berlanga O, et al. Interaction of linker for activation of T cells with multiple adapter proteins in platelets activated by the glycoprotein VI-selective ligand, convulxin. *The Journal of biological chemistry*. 2000;275(43):33427-33434.

83. Batuwangala T, Leduc M, Gibbins JM, Bon C, Jones EY. Structure of the snake-venom toxin convulxin. *Acta Crystallogr D Biol Crystallogr*. 2004;60(Pt 1):46-53.

84. Gibbins JM. Platelet adhesion signalling and the regulation of thrombus formation. *Journal of cell science*. 2004;117(Pt 16):3415-3425.

85. Fujii C, Yanagi S, Sada K, Nagai K, Taniguchi T, Yamamura H. Involvement of protein-tyrosine kinase p72syk in collagen-induced signal transduction in platelets. *European journal of biochemistry / FEBS*. 1994;226(1):243-248.

86. Yanaga F, Poole A, Asselin J, et al. Syk interacts with tyrosine-phosphorylated proteins in human platelets activated by collagen and cross-linking of the Fc gamma-IIA receptor. *The Biochemical journal*. 1995;311 (Pt 2):471-478.

87. Zhang W, Trible RP, Samelson LE. LAT palmitoylation: its essential role in membrane microdomain targeting and tyrosine phosphorylation during T cell activation. *Immunity*. 1998;9(2):239-246.

88. Gross BS, Melford SK, Watson SP. Evidence that phospholipase C-gamma2 interacts with SLP-76, Syk, Lyn, LAT and the Fc receptor gamma-chain after stimulation of the collagen receptor glycoprotein VI in human platelets. *European journal of biochemistry / FEBS*. 1999;263(3):612-623.

89. Watson SP, Auger JM, McCarty OJ, Pearce AC. GPVI and integrin alphaIIb beta3 signaling in platelets. *Journal of thrombosis and haemostasis : JTH*. 2005;3(8):1752-1762.

90. Gardiner EE, Karunakaran D, Shen Y, Arthur JF, Andrews RK, Berndt MC. Controlled shedding of platelet glycoprotein (GP)VI and GPIb-IX-V by ADAM family metalloproteinases. *Journal of thrombosis and haemostasis : JTH*. 2007;5(7):1530-1537.

91. Schulte V, Rabie T, Prostredna M, Aktas B, Gruner S, Nieswandt B. Targeting of the collagen-binding site on glycoprotein VI is not essential for in vivo depletion of the receptor. *Blood*. 2003;101(10):3948-3952.

92. Rabie T, Varga-Szabo D, Bender M, et al. Diverging signaling events control the pathway of GPVI down-regulation in vivo. *Blood*. 2007;110(2):529-535.

93. Bergmeier W, Piffath CL, Cheng G, et al. Tumor necrosis factor-alpha-converting enzyme (ADAM17) mediates GPIbalpha shedding from platelets in vitro and in vivo. *Circ Res*. 2004;95(7):677-683.

94. Bender M, Hofmann S, Stegner D, et al. Differentially regulated GPVI ectodomain shedding by multiple platelet-expressed proteinases. *Blood*. 2010;116(17):3347-3355.

95. Stegner D, Haining EJ, Nieswandt B. Targeting glycoprotein VI and the immunoreceptor tyrosine-based activation motif signaling pathway. *Arterioscler Thromb Vasc Biol*. 2014;34(8):1615-1620.

96. Nieswandt B, Bergmeier W, Schulte V, Rackebrandt K, Gessner JE, Zirngibl H. Expression and function of the mouse collagen receptor glycoprotein VI is strictly

dependent on its association with the FcRgamma chain. *J Biol Chem*. 2000;275(31):23998-24002.

97. Gardiner EE, Arthur JF, Kahn ML, Berndt MC, Andrews RK. Regulation of platelet membrane levels of glycoprotein VI by a platelet-derived metalloproteinase. *Blood*. 2004;104(12):3611-3617.

98. Bergmeier W, Rabie T, Strehl A, et al. GPVI down-regulation in murine platelets through metalloproteinase-dependent shedding. *Thromb Haemost*. 2004;91(5):951-958.

99. Hughes CE, Pollitt AY, Mori J, et al. CLEC-2 activates Syk through dimerization. *Blood*. 2010;115(14):2947-2955.

100. Hughes CE, Auger JM, McGlade J, Eble JA, Pearce AC, Watson SP. Differential roles for the adapters Gads and LAT in platelet activation by GPVI and CLEC-2. *J Thromb Haemost*. 2008;6(12):2152-2159.

101. Manne BK, Badolia R, Dangelmaier C, et al. Distinct pathways regulate Syk activation downstream of ITAM and hemITAM receptors in platelets. *J Biol Chem*. 2015.

102. Spalton JC, Mori J, Pollitt AY, Hughes CE, Eble JA, Watson SP. The novel Syk inhibitor R406 reveals mechanistic differences in the initiation of GPVI and CLEC-2 signaling in platelets. *J Thromb Haemost*. 2009;7(7):1192-1199.

103. Elbakri A, Nelson PN, Abu Odeh RO. The state of antibody therapy. *Human immunology*. 2010;71(12):1243-1250.

104. Khazaeli MB, Conry RM, LoBuglio AF. Human immune response to monoclonal antibodies. *J Immunother Emphasis Tumor Immunol*. 1994;15(1):42-52.

105. ter Meulen J. Monoclonal antibodies for prophylaxis and therapy of infectious diseases. *Expert Opin Emerg Drugs*. 2007;12(4):525-540.

106. Zhu L, van de Lavoir MC, Albanese J, et al. Production of human monoclonal antibody in eggs of chimeric chickens. *Nat Biotechnol*. 2005;23(9):1159-1169.

107. Ma JK, Chikwamba R, Sparrow P, Fischer R, Mahoney R, Twyman RM. Plant-derived pharmaceuticals--the road forward. *Trends Plant Sci*. 2005;10(12):580-585.

108. Ma JK, Drake PM, Christou P. The production of recombinant pharmaceutical proteins in plants. *Nat Rev Genet*. 2003;4(10):794-805.

109. Albrecht H, Radosevich JA, Babich M. Fundamentals of antibody-related therapy and diagnostics. *Drugs Today (Barc)*. 2009;45(3):199-211.

110. Meadows TA, Bhatt DL. Clinical aspects of platelet inhibitors and thrombus formation. *Circulation research*. 2007;100(9):1261-1275.

111. Holmes DR, Jr., Kereiakes DJ, Kleiman NS, Moliterno DJ, Patti G, Grines CL. Combining antiplatelet and anticoagulant therapies. *Journal of the American College of Cardiology*. 2009;54(2):95-109.

112. Use of a monoclonal antibody directed against the platelet glycoprotein IIb/IIIa receptor in high-risk coronary angioplasty. The EPIC Investigation. *The New England journal of medicine*. 1994;330(14):956-961.

113. Gruner S, Prostredna M, Koch M, et al. Relative antithrombotic effect of soluble GPVI dimer compared with anti-GPVI antibodies in mice. *Blood*. 2005;105(4):1492-1499.

114. Kleinschnitz C, Pozgajova M, Pham M, Bendszus M, Nieswandt B, Stoll G. Targeting platelets in acute experimental stroke: impact of glycoprotein Ib, VI, and IIb/IIIa blockade on infarct size, functional outcome, and intracranial bleeding. *Circulation*. 2007;115(17):2323-2330.

115. Massberg S, Gawaz M, Gruner S, et al. A crucial role of glycoprotein VI for platelet recruitment to the injured arterial wall in vivo. *J Exp Med*. 2003;197(1):41-49.

116. Boylan B, Chen H, Rathore V, et al. Anti-GPVI-associated ITP: an acquired platelet disorder caused by autoantibody-mediated clearance of the GPVI/FcRgamma-chain complex from the human platelet surface. *Blood*. 2004;104(5):1350-1355.

117. Moroi M, Jung SM, Okuma M, Shinmyozu K. A patient with platelets deficient in glycoprotein VI that lack both collagen-induced aggregation and adhesion. *The Journal of clinical investigation*. 1989;84(5):1440-1445.

118. Boylan B, Berndt MC, Kahn ML, Newman PJ. Activation-independent, antibody-mediated removal of GPVI from circulating human platelets: development of a novel NOD/SCID mouse model to evaluate the in vivo effectiveness of anti-human platelet agents. *Blood*. 2006;108(3):908-914.

119. Gruner S, Prostredna M, Aktas B, et al. Anti-glycoprotein VI treatment severely compromises hemostasis in mice with reduced alpha2beta1 levels or concomitant aspirin therapy. *Circulation*. 2004;110(18):2946-2951.

120. Nieswandt B, Bergmeier W, Rackebrandt K, Gessner JE, Zirngibl H. Identification of critical antigen-specific mechanisms in the development of immune thrombocytopenic purpura in mice. *Blood*. 2000;96(7):2520-2527.

121. Bergmeier W, Schulte V, Brockhoff G, Bier U, Zirngibl H, Nieswandt B. Flow cytometric detection of activated mouse integrin alphaIIbbeta3 with a novel monoclonal antibody. *Cytometry*. 2002;48(2):80-86.

122. Bender M, Hagedorn I, Nieswandt B. Genetic and antibody-induced glycoprotein VI deficiency equally protects mice from mechanically and FeCl(3) -induced thrombosis. *J Thromb Haemost*. 2011;9(7):1423-1426.

123. Lorenz V, Stegner D, Stritt S, et al. Targeted downregulation of platelet CLEC-2 occurs through Syk-independent internalization. *Blood*. 2015.

124. Nieswandt B, Moser M, Pleines I, et al. Loss of talin1 in platelets abrogates integrin activation, platelet aggregation, and thrombus formation in vitro and in vivo. *The Journal of experimental medicine*. 2007;204(13):3113-3118.

125. Tiedt R, Schomber T, Hao-Shen H, Skoda RC. Pf4-Cre transgenic mice allow the generation of lineage-restricted gene knockouts for studying megakaryocyte and platelet function in vivo. *Blood*. 2007;109(4):1503-1506.

126. Takai T, Li M, Sylvestre D, Clynes R, Ravetch JV. FcR gamma chain deletion results in pleiotrophic effector cell defects. *Cell*. 1994;76(3):519-529.

127. Konigsberger S, Prodohl J, Stegner D, et al. Altered BCR signalling quality predisposes to autoimmune disease and a pre-diabetic state. *EMBO J*. 2012;31(15):3363-3374.

128. Dutting S, Vogtle T, Morowski M, et al. Growth factor receptor-bound protein 2 contributes to (hem)immunoreceptor tyrosine-based activation motif-mediated signaling in platelets. *Circ Res*. 2014;114(3):444-453.

129. Cherpokova D, Bender M, Morowski M, et al. SLAP/SLAP2 prevent excessive platelet (hem)ITAM-signaling in thrombosis and ischemic stroke in mice. *Blood*. 2014.

130. Zhang J, Varas F, Stadtfeld M, Heck S, Faust N, Graf T. CD41-YFP mice allow in vivo labeling of megakaryocytic cells and reveal a subset of platelets hyperreactive to thrombin stimulation. *Exp Hematol*. 2007;35(3):490-499.

131. Kahn ML, Diacovo TG, Bainton DF, Lanza F, Trejo J, Coughlin SR. Glycoprotein V-deficient platelets have undiminished thrombin responsiveness and Do not exhibit a Bernard-Soulier phenotype. *Blood*. 1999;94(12):4112-4121.

132. Ni H, Denis CV, Subbarao S, et al. Persistence of platelet thrombus formation in arterioles of mice lacking both von Willebrand factor and fibrinogen. *J Clin Invest*. 2000;106(3):385-392.

133. Renne T, Pozgajova M, Gruner S, et al. Defective thrombus formation in mice lacking coagulation factor XII. *J Exp Med*. 2005;202(2):271-281.

134. Deppermann C, Cherpokova D, Nurden P, et al. Gray platelet syndrome and defective thrombo-inflammation in Nbeal2-deficient mice. *J Clin Invest*. 2013.

135. Stegner D, Deppermann C, Kraft P, et al. Munc13-4-mediated secretion is essential for infarct progression but not intracranial hemostasis in acute stroke. *J Thromb Haemost*. 2013;11(7):1430-1433.

136. Ono A, Westein E, Hsiao S, et al. Identification of a fibrin-independent platelet contractile mechanism regulating primary hemostasis and thrombus growth. *Blood*. 2008;112(1):90-99.

137. Stolla M, Stefanini L, Andre P, et al. CalDAG-GEFI deficiency protects mice in a novel model of Fcgamma RIIA-mediated thrombosis and thrombocytopenia. *Blood*. 2011;118(4):1113-1120.

138. Bender M, May F, Lorenz V, et al. Combined in vivo depletion of glycoprotein VI and C-type lectin-like receptor 2 severely compromises hemostasis and abrogates arterial thrombosis in mice. *Arterioscler Thromb Vasc Biol*. 2013;33(5):926-934.

139. Tucker KL, Sage T, Gibbins JM. Clot retraction. *Methods Mol Biol*. 2012;788:101-107.

140. Elvers M, Stegner D, Hagedorn I, et al. Impaired alpha(IIb)beta(3) integrin activation and shear-dependent thrombus formation in mice lacking phospholipase D1. *Sci Signal*. 2010;3(103):ra1.

141. David T, Ohlmann P, Eckly A, et al. Inhibition of adhesive and signaling functions of the platelet GPIb-V-IX complex by a cell penetrating GPIbalpha peptide. *J Thromb Haemost*. 2006;4(12):2645-2655.

142. Yuan Y, Kulkarni S, Ulsemer P, et al. The von Willebrand factor-glycoprotein Ib/V/IX interaction induces actin polymerization and cytoskeletal reorganization in rolling platelets and glycoprotein Ib/V/IX-transfected cells. *J Biol Chem*. 1999;274(51):36241-36251.

143. Clauss MA, Jain RK. Interstitial transport of rabbit and sheep antibodies in normal and neoplastic tissues. *Cancer Res*. 1990;50(12):3487-3492.

144. Jain RK. Physiological barriers to delivery of monoclonal antibodies and other macromolecules in tumors. *Cancer Res*. 1990;50(3 Suppl):814s-819s.

145. Nimmerjahn F, Ravetch JV. Fcgamma receptors: old friends and new family members. *Immunity*. 2006;24(1):19-28.

146. Luo FR, Yang Z, Camuso A, et al. Dasatinib (BMS-354825) pharmacokinetics and pharmacodynamic biomarkers in animal models predict optimal clinical exposure. *Clin Cancer Res*. 2006;12(23):7180-7186.

147. Gratacap MP, Martin V, Valera MC, et al. The new tyrosine-kinase inhibitor and anticancer drug dasatinib reversibly affects platelet activation in vitro and in vivo. *Blood*. 2009;114(9):1884-1892.

148. Gitz E, Pollitt AY, Gitz-Francois JJ, et al. CLEC-2 expression is maintained on activated platelets and on platelet microparticles. *Blood*. 2014;124(14):2262-2270.

149. Clark SR, Ma AC, Tavener SA, et al. Platelet TLR4 activates neutrophil extracellular traps to ensnare bacteria in septic blood. *Nat Med*. 2007;13(4):463-469.

150. Fuchs TA, Brill A, Duerschmied D, et al. Extracellular DNA traps promote thrombosis. *Proc Natl Acad Sci U S A*. 2010;107(36):15880-15885.

151. Daley JM, Thomay AA, Connolly MD, Reichner JS, Albina JE. Use of Ly6G-specific monoclonal antibody to deplete neutrophils in mice. *J Leukoc Biol*. 2008;83(1):64-70.

152. Mouse Genome Sequencing C, Waterston RH, Lindblad-Toh K, et al. Initial sequencing and comparative analysis of the mouse genome. *Nature*. 2002;420(6915):520-562.

153. Deppermann C, Nurden P, Nurden AT, Nieswandt B, Stegner D. The Nbeal2(-/-) mouse as a model for the gray platelet syndrome. *Rare Dis*. 2013;1:e26561.

154. Kahr WH, Hinckley J, Li L, et al. Mutations in NBEAL2, encoding a BEACH protein, cause gray platelet syndrome. *Nat Genet*. 2011;43(8):738-740.

155. Hodivala-Dilke KM, McHugh KP, Tsakiris DA, et al. Beta3-integrin-deficient mice are a model for Glanzmann thrombasthenia showing placental defects and reduced survival. *J Clin Invest*. 1999;103(2):229-238.

156. Ware J, Russell S, Ruggeri ZM. Generation and rescue of a murine model of platelet dysfunction: the Bernard-Soulier syndrome. *Proc Natl Acad Sci U S A*. 2000;97(6):2803-2808.

157. Schacht V, Ramirez MI, Hong YK, et al. T1alpha/podoplanin deficiency disrupts normal lymphatic vasculature formation and causes lymphedema. *EMBO J*. 2003;22(14):3546-3556.

158. Schulte-Merker S, Sabine A, Petrova TV. Lymphatic vascular morphogenesis in development, physiology, and disease. *J Cell Biol*. 2011;193(4):607-618.

159. Gauvrit S, Philippe J, Lesage M, Tjwa M, Godin I, Germain S. The role of RNA interference in the developmental separation of blood and lymphatic vasculature. *Vasc Cell*. 2014;6(1):9.

160. Xu MJ, Matsuoka S, Yang FC, et al. Evidence for the presence of murine primitive megakaryocytopoiesis in the early yolk sac. *Blood*. 2001;97(7):2016-2022.

161. Xie X, Chan RJ, Johnson SA, et al. Thrombopoietin promotes mixed lineage and megakaryocytic colony-forming cell growth but inhibits primitive and definitive erythropoiesis in cells isolated from early murine yolk sacs. *Blood*. 2003;101(4):1329-1335.

162. Tober J, Koniski A, McGrath KE, et al. The megakaryocyte lineage originates from hemangioblast precursors and is an integral component both of primitive and of definitive hematopoiesis. *Blood*. 2007;109(4):1433-1441.

163. Ruggeri ZM, Mendolicchio GL. Adhesion mechanisms in platelet function. *Circulation research*. 2007;100(12):1673-1685.

164. Rodgers RP, Levin J. A critical reappraisal of the bleeding time. *Seminars in thrombosis and hemostasis*. 1990;16(1):1-20.

165. Mammadova-Bach E, Ollivier V, Loyau S, et al. Platelet glycoprotein VI binds to polymerized fibrin and promotes thrombin generation. *Blood*. 2015.

166. Ozaki Y, Suzuki-Inoue K, Inoue O. Novel interactions in platelet biology: CLEC-2/podoplanin and laminin/GPVI. *J Thromb Haemost*. 2009;7 Suppl 1:191-194.

167. Saito N, Hamada J, Furukawa H, et al. Laminin-421 produced by lymphatic endothelial cells induces chemotaxis for human melanoma cells. *Pigment Cell Melanoma Res*. 2009;22(5):601-610.

168. Law DA, Nannizzi-Alaimo L, Ministri K, et al. Genetic and pharmacological analyses of Syk function in alphaIIbbeta3 signaling in platelets. *Blood*. 1999;93(8):2645-2652.

169. Andre P, Morooka T, Sim D, et al. Critical role for Syk in responses to vascular injury. *Blood*. 2011;118(18):5000-5010.

170. Nieswandt B, Schulte V, Bergmeier W. Flow-cytometric analysis of mouse platelet function. *Methods Mol Biol*. 2004;272:255-268.

171. Talpaz M, Shah NP, Kantarjian H, et al. Dasatinib in imatinib-resistant Philadelphia chromosome-positive leukemias. *N Engl J Med*. 2006;354(24):2531-2541.

172. Shah NP, Tran C, Lee FY, Chen P, Norris D, Sawyers CL. Overriding imatinib resistance with a novel ABL kinase inhibitor. *Science*. 2004;305(5682):399-401.

173. Tokarski JS, Newitt JA, Chang CY, et al. The structure of Dasatinib (BMS-354825) bound to activated ABL kinase domain elucidates its inhibitory activity against imatinib-resistant ABL mutants. *Cancer Res*. 2006;66(11):5790-5797.

174. Agarwal N, Di Lorenzo G, Sonpavde G, Bellmunt J. New agents for prostate cancer. *Ann Oncol*. 2014;25(9):1700-1709.

175. Borgognone A, Navarro-Nunez L, Correia JN, et al. CLEC-2-dependent activation of mouse platelets is weakly inhibited by cAMP but not by cGMP. *J Thromb Haemost*. 2014;12(4):550-559.

176. Myers MD, Sosinowski T, Dragone LL, et al. Src-like adaptor protein regulates TCR expression on thymocytes by linking the ubiquitin ligase c-Cbl to the TCR complex. *Nat Immunol*. 2006;7(1):57-66.

177. Senis YA, Tomlinson MG, Garcia A, et al. A comprehensive proteomics and genomics analysis reveals novel transmembrane proteins in human platelets and mouse megakaryocytes including G6b-B, a novel immunoreceptor tyrosine-based inhibitory motif protein. *Mol Cell Proteomics*. 2007;6(3):548-564.

178. Bergmeier W, Rackebrandt K, Schroder W, Zirngibl H, Nieswandt B. Structural and functional characterization of the mouse von Willebrand factor receptor GPIb-IX with novel monoclonal antibodies. *Blood*. 2000;95(3):886-893.

179. Kuijpers MJ, Schulte V, Oury C, et al. Facilitating roles of murine platelet glycoprotein Ib and alphaIIbbeta3 in phosphatidylserine exposure during vWF-collagen-induced thrombus formation. *J Physiol*. 2004;558(Pt 2):403-415.

180. Erpenbeck L, Nieswandt B, Schon M, Pozgajova M, Schon MP. Inhibition of platelet GPIb alpha and promotion of melanoma metastasis. *J Invest Dermatol*. 2010;130(2):576-586.

181. Cueni LN, Chen L, Zhang H, et al. Podoplanin-Fc reduces lymphatic vessel formation in vitro and in vivo and causes disseminated intravascular coagulation when transgenically expressed in the skin. *Blood*. 2010;116(20):4376-4384.

182. Vincent JL, De Backer D. Does disseminated intravascular coagulation lead to multiple organ failure? *Crit Care Clin*. 2005;21(3):469-477.

183. Siedlecki CA, Lestini BJ, Kottke-Marchant KK, Eppell SJ, Wilson DL, Marchant RE. Shear-dependent changes in the three-dimensional structure of human von Willebrand factor. *Blood*. 1996;88(8):2939-2950.

184. Kiefer TL, Becker RC. Inhibitors of platelet adhesion. *Circulation*. 2009;120(24):2488-2495.

185. Takagi J, Springer TA. Integrin activation and structural rearrangement. *Immunol Rev*. 2002;186:141-163.

186. Mocsai A, Abram CL, Jakus Z, Hu Y, Lanier LL, Lowell CA. Integrin signaling in neutrophils and macrophages uses adaptors containing immunoreceptor tyrosine-based activation motifs. *Nat Immunol*. 2006;7(12):1326-1333.

187. Blair P, Flaumenhaft R. Platelet alpha-granules: basic biology and clinical correlates. *Blood Rev*. 2009;23(4):177-189.

188. Gunay-Aygun M, Zivony-Elboum Y, Gumruk F, et al. Gray platelet syndrome: natural history of a large patient cohort and locus assignment to chromosome 3p. *Blood*. 2010;116(23):4990-5001.

189. Gould WR, Simioni P, Silveira JR, Tormene D, Kalafatis M, Tracy PB. Megakaryocytes endocytose and subsequently modify human factor V in vivo to form the entire pool of a unique platelet-derived cofactor. *J Thromb Haemost*. 2005;3(3):450-456.

190. Albers CA, Cvejic A, Favier R, et al. Exome sequencing identifies NBEAL2 as the causative gene for gray platelet syndrome. *Nat Genet*. 2011;43(8):735-737.

191. Gunay-Aygun M, Falik-Zaccai TC, Vilboux T, et al. NBEAL2 is mutated in gray platelet syndrome and is required for biogenesis of platelet alpha-granules. *Nat Genet*. 2011;43(8):732-734.

192. Berger G, Masse JM, Cramer EM. Alpha-granule membrane mirrors the platelet plasma membrane and contains the glycoproteins Ib, IX, and V. *Blood*. 1996;87(4):1385-1395.

6 ANNEX

6.1 Abbreviations

aa	amino acid
AC	adenylyl cyclase
ADAM	a disintegrin andmettalloprotease
ADP	adenosine diphosphate
APS	ammonium peroxodisulphat
aPTT	activated partial thromboplastin time
approx.	approximately
ATP	adenosine trisphosphate
BM	bone marrow
BSA	bovine serum albumin
$[Ca^{2+}]_i$	intracellular calcium concentration
CCCP	cyanide m-chlorophenylhydrazone
CECAM-1	carcinoembryonic antigen cell adhesion molecule-1
CLEC-2	C-type lectin-like receptor 2
cm²	square centimeter
CRD	carbohydrate recognition domain
CRP	collagen-related peptide
CTLD	C-type lectin-like domain
CVX	convulxin
d	days
DAG	diacylglycerol
ddH_2O	double-distilled water
DIC	differential interference contrast
DMEM	Dulbecco/Vogt Modified Eagle's Minimal Essential Medium
DTT	DL-dithiothreitol
E	embryonic day
ECL	enhanced chemiluminescence
ECM	extracellular matrix
EDTA	ethylenediaminetetraacetic acid
ELISA	enzyme-linked immuno absorbance assay
et al.	*et alteri*
F(ab)	fragment antigen-binding
Fc	fragment crystallisable
FcR	Fc receptor
FCS	fetal calf (bovine) serum
FITC	fluorescein isothiocyanate
FRC	Fibroblastic reticular cells
FSC	foreward scatter
GLA	glutaraldehyde
GP	glycoprotein
GPCR	G protein-coupled receptor
GPO	glycine-proline-hydroxyproline
GPS	gray platelet syndrome
Grb-2	growth factor receptor-bound protein-2
GTP	guanosine triphosphate
h	hour(s)
HAT	hypoxanthine-aminopterin-thymidine
HCl	hydrogen chloride
hem	hemi
HEV	high endothelial venules

HGPRT	hypoxanthine-guanine phosphoribosyltransferase
HIV-1	human immunodeficiency virus type 1
HRP	horseradish peroxidase
H_2O	water
IFI	integrated fluorescence intensity
Ig	immunoglobulin
IL	interleukin
IP	immunoprecipitation
IP_3	inositol 1,4,5-triphosphate
ITAM	immunoreceptor tyrosine-based activation motif
ITIM	immunoreceptor tyrosine-based inhibitory motif
IVIS	*in vivo* imaging system
kb	kilo base pair
kDa	kilo Dalton
l	liter
LAT	linker for activation of T-cells
LEC	lymphatic endothelial cells
LN	lymph nodes
LOX-1	lectin-type oxidized low-density lipoprotein receptor-1
LSFM	light sheet fluorescence microscopy
LV	lymphovenouse
LVV	LV valve
M	molar
mAbs	monoclonal antibodies
MFI	mean fluorescence intensity
min	minute(s)
MK	megakaryocyte
ml	milliliter
mm	millimeter
µ	micro
NaCl	sodium chloride
NaOH	sodium hydroxide
n. d.	not determined
NET	neutrophil extracellular traps
NKC	natural killer gene complex
OD	optical density
o/n	overnight
2P-IVM	Two photon-intravital microscopy
PAA	polyacrylamide
PBS	phosphate buffered saline
PCR	polymerase chain reaction
PE	phycoerythrin
PECAM-1	Platelet Endothelial Cell Adhesion Molecule
PEG	polyethylene glycole
PF4	platelet factor 4
PFA	paraformaldehyde
PIG_2	prostacyclin
PIP_2	phosphatidylinositol-4,5-bisphosphate
PI-3-K	phosphoinositide-3-kinase
PKC	proteinkinase C
PL	phospholipase
PM	plasma membrane
PPP	platelet-poor plasma
PRP	platelet-rich plasma
PT	prothrombin time
PVDF	polyvinylidene difluoride

RC	rhodocytin
RhoGEF	Rho-specific guanine nucleotide exchange factor
ROCE	receptor-operated Ca^{2+} entry
rpm	rounds per minute
RT	room temperature
S1P	shingosine-1-phosphate
s	second
SD	standard deviation
SDS	sodium dodecyl sulfate
SDS-PAGE	sodium dodecyl sulfate polyacrylamide gel electrophoresis
SFK	Src family kinase
SH2	Src homology 2 domains
SLAP	Src-like adaptor protein
SLP-76	Src-homology 2 domain-containing leukocyte-specific phosphoprotein of 76 kDa
SOCE	store-operated Ca^{2+} entry
SPIM	selective/ single plane illumination microscopy
SSC	sideward scatter
SYK	spleen tyrosine kinase
TAE	TRIS acetate EDTA buffer
TE	TRIS EDTA buffer
TEM	transmission electron microscopy
TF	tissue factor
TMB	3,3,5,5-tetramethylbenzidine
TRIS	trishydroxymethylaminomethane
TxA_2	thromboxane A_2
U	units
vWF	von Willebrand factor
Wt	wild type
w/o	without
x *g*	acceleration of gravity (9.81 m/ sec²)

6.2 Acknowledgements

The work presented here was accomplished in the group of Prof. Dr. Bernhard Nieswandt at the Department of Experimental Biomedicine, University Hospital and the Rudolf Virchow Center for Experimental Biomedicine, University of Würzburg. During the period of my PhD work (2011-2015), many people helped and supported me. I would like to express my thanks to the following people:

- My supervisor, Prof. Dr. Bernhard Nieswandt, for giving me the opportunity to work in his laboratory, for his constant support, trust, enthusiasm and great scientific ideas during my PhD time. Without this, accomplishing this work would not have been possible. I would also like to thank him for allowing me to present my work at international conferences and symposia, which enabled me getting to know many people in the scientific community and gather experience, which will be of great importance for my future professional life.
- PD Dr. Heike Hermanns for the helpful scientific discussions and fruitful collaboration throughout my PhD and for reviewing my thesis.
- Prof. Dr. Christoph Kleinschnitz for the helpful scientific discussions throughout my PhD period and for reviewing my thesis.
- Prof. Dr. Manfred Gessler for chairing my doctorate procedure and my thesis defense.
- My colleagues and friends David, Judith, Michael, Sarah and Simon for supporting me in good and bad times during my projects and for proof reading my thesis.
- I would like to thank Stefanie for her constant help in resolving technical problems and assistance with all different kind of problems during my projects.
- All present and former members of the group, who have not been mentioned here by name for the enjoyable working atmosphere, the fun and the constant support in the lab. The animal caretakers for running the animals facility and taking care of all our mice and rats.
- All external collaborators for the trustful cooperation and useful advices as well as introducing me into new techniques.
- The Graduate School of Life Sciences (GSLS) for organizing the transferable skills courses, giving me the opportunity to participate in the Mentoring Program and for their financial support, which enabled the attendance of conferences and thereby contributed substantially to my future career.
- Finally, I would like to specially thank and dedicate this thesis to Harald, my family and close friends. Thank you very much for your constant encouragement, everlasting support and patience.

6.3 Affidavit

I hereby confirm that my thesis entitled “Cellular regulation of the hemITAM-coupled platelet receptor C-type lectin-like receptor 2 (CLEC-2): *In vitro* and *in vivo* studies in mice” is the result of my own work. I did not receive any help or support from commercial consultants. All sources and/or materials applied are listed and specified in the thesis.

Furthermore, I confirm that this thesis has not yet been submitted as part of another examination process neither in identical nor in similar form.

Würzburg

Date, Signature

Eidesstattliche Erklärung

Hiermit erkläre ich an Eides statt, die Dissertation “Zelluläre Regulation des hemITAM-gekoppelten Thrombozytenrezeptors *C-type lectin-like receptor 2* (CLEC-2): *In vitro* und *in vivo* Studien in Mäusen” eigenständig, d.h. insbesondere selbständig und ohne Hilfe eines kommerziellen Promotionsberaters, angefertigt und keine anderen als die von mir angegebenen Quellen und Hilfsmittel verwendet zu haben.

Ich erkläre außerdem, dass die Dissertation weder in gleicher noch in ähnlicher Form bereits in einem anderen Prüfungsverfahren vorgelegen hat.

Würzburg

Datum, Unterschrift

6.4 Publications

Articles

Lorenz V, Stegner D, Stritt S, Vögtle T, Kiefer F, Witke W, Schymeinsky J, Watson SP, Walzog B, Nieswandt B. Targeted downregulation of platelet CLEC-2 occurs through Syk-independent internalization. *Blood* 2015, *in press* [epub ahead of print March 20]

Stritt S, Wolf K, **Lorenz V**, Vögtle T, Gupta S, Bösl MR, Nieswandt N. Rap1-GTP interacting adaptor molecule (RIAM) is dispensable for platelet integrin activation and function in mice. *Blood* 2015; 125(2):219-22.

Bender M, May F, **Lorenz V**, Thielmann I, Hagedorn I, Finney BA, Vögtle T, Remer K, Braun A, Bösl MR, Watson SP, Nieswandt B. Combined in vivo depletion of glycoprotein VI and C-type lectin-like receptor 2 severely compromises hemostasis and abrogates arterial thrombosis in mice. *Arterioscler Thromb Vasc Biol* 2013; 33(5):926-34.

Lorenz V, Hessenkemper W, Rödiger J, Kyrylenko S, Kraft F, Baniahmad A. Sodium butyrate induces cellular senescence in neuroblastoma and prostate cancer cells. *Horm Mol Biol Clin Invest* 2011;7(1):265–272.

Oral presentation

Targeted downregulation of CLEC-2 occurs through Src family kinase dependent internalization in mouse platelets. XXVth Congress of the International Society on Thrombosis and Haemostasis (ISTH) and 61th Annual Scientific and Standardization Committee (SSC) Meeting, June 21-24, 2015, Toronto (Canada)
Winner of **Young Investigator's Award** (prize money: CAD 700).

Anti-CLEC-2 antibody-induced receptor regulation in vivo. 9th International Symposium organized by the Students of the Graduate School of Life Sciences, October 14-15, 2014, Würzburg (Germany).

Syk is essential for anti-CLEC-2 antibody-induced thrombocytopenia, but not receptor depletion. XXIVth Congress of the International Society on Thrombosis and Haemostasis (ISTH) and 59th Annual Scientific and Standardization Committee (SSC) Meeting, June 29 to July 4, 2013, Amsterdam (The Netherlands).
Winner of **Young Investigator's Award** (prize money: 500€).

Poster presentation

Phosphorylation of CLEC-2 by Src-family kinases is essential for anti-CLEC-2 antibody-induced receptor internalization. 60th Annual Scientific and Standardization Committee (SSC) Meeting, June 22-26, 2014, Milwaukee (WI, USA).
Winner of **Young Investigator's Award** (prize money: $1000).

Severely defective haemostasis and arterial thrombus formation in GPVI/CLEC-2 double-depletetd mice. 7th International Symposium organized by the Students of the Graduate School of Life Sciences, October 16-17, 2012, Würzburg (Germany).

Severely defective haemostasis and arterial thrombus formation in GPVI/CLEC-2 double-depletetd mice. Joint Symposium of the Collaborative Research Center (SFB) 688, the Rudolf Virchow Center, and the Comprehensive Heart Failure Center Würzburg, June 21-22, 2012 Würzburg (Germany).

INU1 antibody-induced effects on platelet CLEC-2 in vivo. 6th International Symposium organized by the Students of the Graduate School of Liefe Sciences, October 19-20, 2011, Würzburg (Germany).

HDAC Inhibitors Induce Cellular Senescence in Neuroblastoma and Prostate Cancer Cells, 19th Annual conference of the German Society of Human Genetics, Hannover, April 8-10, 2008, Hannover (Germany).